

**ELECTROCHEMICAL DETECTION OF DNA AND
THEIR INTERACTION WITH CHEMICAL
COMPOUNDS**

**A THESIS SUBMITTED TO THE INSTITUTE OF
GRADUATE STUDIES
OF
NEAR EAST UNIVERSITY**

**By
PWADUBASHIYI COSTON PWAVODI**

**In Partial Fulfillment of the Requirements for
the Degree of Doctor of Philosophy
in
Biomedical Engineering**

NICOSIA, 2021

PWADUBASHIYI COSTON PWAVODI

**ELECTROCHEMICAL DETECTION OF DNA AND THEIR
INTERACTION WITH CHEMICAL COMPOUNDS**

**NEU
2021**

**ELECTROCHEMICAL DETECTION OF DNA AND
THEIR INTERACTION WITH CHEMICAL
COMPOUNDS**

**A THESIS SUBMITTED TO THE INSTITUTE OF
GRADUATE STUDIES
OF
NEAR EAST UNIVERSITY**

**By
PWADUBASHIYI COSTON PWAVODI**

**In Partial Fulfillment of the Requirements for
the Degree of Doctor of Philosophy
in
Biomedical Engineering**

NICOSIA, 2021

**Pwadubashiyi Coston PWAVODI: ELECTROCHEMICAL DETECTION OF DNA
AND THEIR INTERACTION WITH CHEMICAL COMPOUNDS**

Approval of Director of Institute of Graduate Studies

Prof. Dr. Hüsnü Can BAŞER

**We certify this thesis is satisfactory for the award of the degree of Doctor of
Philosophy in Biomedical Engineering**

Examining Committee in Charge:

Prof. Dr. Huriye Icil

Committee Chairman, Faculty of Arts and Sciences
Department of Chemistry, EMU

Prof. Dr. Mehmet Ozsoz

Supervisor, Department of Biomedical Engineering,
NEU.

Assist. Prof. Dr. Suleyman Asir

Co-Supervisor, Department of Materials Science and
Nanotechnology Engineering, NEU.

Assoc. Prof. Dr. Aydin Hassani

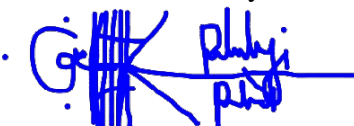
Department of Materials Science and Nanotechnology
Engineering, NEU.

Assist. Prof. Dr. Saltuk Pirgalioglu

Department of Environmental Science, EUL.

I hereby declare that all information in this document has been obtained and presented in accordance with academic rules and ethical conduct. I also declare that, as required by these rules and conduct, I have fully cited and referenced all material and results that are not original to this work.

Name, Last name: Pwadubashiyi Coston Pwavodi

Signature: A handwritten signature in blue ink, appearing to be 'Pwadubashiyi Coston Pwavodi', written over a series of vertical lines.

Date: 22/4/2021

ACKNOWLEDGEMENTS

I want to thank Prof. Dr Mehmet Ozsoz, my inspiring supervisor and Assist. Prof. Dr. Suleyman Asir, my supportive co-supervisor for the constant mentorship, patience, guidance and directives, encouragements, daily inspirations, motivations and presence they gave me throughout the journey of my doctoral studies. I am honoured to have the opportunity to work with all my professors and have them help me reshape my experience in conducting research and even publishing our works. My profound appreciation goes to the supervisory team for their support and guidance throughout my monitoring till the final defence. They are Prof. Dr. Huriye Icil, Assoc. Prof. Dr. Aydin Hassani, and Assist Prof. Dr. Saltuk Pirgalioglu. I appreciate them all for all their contributions to accomplishing my studies.

I want to also show my thankfulness and acknowledgement to Prof. Dr. Ayşe Günay Kibarar, the Head of the Department of Biomedical Engineering, for all your encouragement, support, motherly love and purposeful support. You have indeed been a mother to me in Cyprus and turkey and have shown me the path to selflessness in life. To my course mates, Abdullahi Umar Ibrahim, Zubaida A. Mubarak and Nima Shanma; housemates, Chidi .N. Wilson, Emmanuel O. Adewusi, Ifeanyi Nweke, friends Victor Markus, Friedrich Letong, Kolawole Omole, Olumide Adeniyi, Lorato P. Mphinyane and the list goes on both home and abroad. I will forever remain grateful for your prayers, encouragements and standing by me through it all.

To my father, Mr. Pwavodi S. Matasha and my selfless mother, Mrs. Dorcas T. Pwavodi, thank you for supporting me financially, spiritually and morally and for all your words throughout the journey.

Finally, to my siblings Joshua T. Pwavodi, David T. Pwavodi and Paul A. Mamman, I say a big thank you for all your prayers and support. Thank you all, and I love you all.

To my parents...

ABSTRACT

The Electrochemical DNA Biosensors application in detecting interactions between DNA and other compounds is widely increasing, and the application of electrochemical sensors to detect other compounds in water, food, and the environment. This study aims to fabricate electrochemical DNA biosensors using Pencil Graphite Electrodes (PGEs) and other forms of working electrodes for the detection of double-stranded DNA (dsDNA) and compounds interaction and also the fabrication of electrochemical sensors for the determination of the electrochemical behaviour of compounds using inexpensive materials as working electrodes such as PGEs, carbon paste electrodes (CPEs) and their modified form (MCPE). The characterization techniques adapted for this study for PGEs, CPE, MCPE electrodes, and the solution interface used were differential pulse voltammetry (DPV), electrochemical impedance spectroscopy (EIS), and cyclic voltammetry (CV). Scan rate and pH were the parameters subjected to optimization studies to determine phenolic compounds and the evaluation of the electroactive surface area of the electrodes and also application in real samples. The CV DPV and EIS results using PGEs, demonstrated from the interaction of dsDNA and ADR by adsorption at the electrode surface indicated a decrease in the guanine peak with an increase in ADR concentration. This decrease correlated with the EIS result, which showed decreased charge transfer and solution resistance with an increase in ADR concentration. Limits of detection (LOD) and limits of quantification (LOQ) obtained were 1.393×10^{-6} M, 4.221×10^{-6} M, respectively. The results obtained from the determination of phenolic compounds' electrochemical behaviour show the fabrication of electrochemical sensors in the electrosensitive determination of sinapic acid, syringic acid, and rutin using CPE modified with Fe₃O₄ nanoparticles showed excellent sensitivity, selectivity, repeatability, reproducibility, stability, and low preparation cost. The limits of detection (LOD) obtained were 2.2×10^{-7} M for sinapic acid, 2.6×10^{-7} M for syringic acid, and 0.8×10^{-7} M for rutin, respectively. The fabricated electrochemical sensor was applied to determine phenolic compounds in real red and white wine samples.

Keywords: differential pulse voltammetry; electrochemical impedance spectroscopy; adriamycin; pencil graphite electrodes; cyclic voltammetry; double-stranded DNA.

electrochemical sensor; Fe₃O₄ nanoparticles; carbon paste electrodes; sinapic acid; syringic acid; rutin; voltammetry; electrochemical impedance spectroscopy

ÖZET

DNA ile diğer bileşikler arasındaki etkileşimleri tespit etmede Elektrokimyasal DNA Biyosensörleri uygulaması büyük ölçüde artmaktadır ve su, gıda ve çevredeki diğer bileşikler tespit etmek için elektrokimyasal sensörlerin uygulanması. Bu çalışma, çift sarmallı DNA (dsDNA) ve bileşik etkileşiminin tespiti için Kalem Grafit Elektrotları (PGE'ler) ve diğer çalışma elektrotları kullanarak elektrokimyasal DNA biyosensörleri üretmeyi ve ayrıca PGE'ler, karbon pastası elektrotları (CPE'ler) ve bunların modifiye edilmiş formları (MCPE) gibi çalışma elektrotları olarak ucuz malzemeler kullanan bileşikler. PGE'ler, CPE, MCPE elektrotları için bu çalışma için uyarlanan karakterizasyon teknikleri ve kullanılan çözüm arayüzü, diferansiyel puls voltametri (DPV), elektrokimyasal empedans spektroskopisi (EIS) ve döngüsel voltametri (CV) idi. Tarama hızı ve pH, fenolik bileşiklerin belirlenmesi ve elektrotların elektroaktif yüzey alanının değerlendirilmesi ve ayrıca gerçek numunelerde uygulama için optimizasyon çalışmalarına tabi tutulan parametrelerdir. PGE'leri kullanan CV DPV ve EIS sonuçları, elektrot yüzeyinde adsorpsiyon ile dsDNA ve ADR'nin etkileşiminden ortaya çıkan, ADR konsantrasyonunda bir artış ile guanin zirvesinde bir düşüş olduğunu gösterdi. Bu azalma, ADR konsantrasyonunda bir artışla birlikte azalmış yük transferi ve çözelti direnci gösteren EIS sonucuyla ilişkilidir. Elde edilen saptama sınırları (LOD) ve niceleme sınırları (LOQ) sırasıyla $1.393 \times 10^{-6}M$, $4.221 \times 10^{-6}M$ idi. Fenolik bileşiklerin elektrokimyasal davranışının belirlenmesinden elde edilen sonuçlar, elektrokimyasal sensörlerin Fe₃O₄ nanopartiküller ile modifiye edilmiş CPE kullanılarak sinapik asit, siringik asit ve rutin elektro-hassas tayininde mükemmel hassasiyet, seçicilik, tekrarlanabilirlik, kararlılık gösterdiğini göstermektedir. düşük hazırlık maliyeti. Elde edilen saptama sınırları (LOD) sırasıyla sinapik asit için $2,2 \times 10^{-7} M$, siringik asit için $2,6 \times 10^{-7} M$ ve rutin için $0,8 \times 10^{-7} M$ idi. Gerçek kırmızı ve beyaz şarap örneklerinde fenolik bileşikler belirlemek için fabrikasyon elektrokimyasal sensör uygulandı.

Anahtar Kelimeler: diferansiyel puls voltametri; elektrokimyasal empedans spektroskopisi; adriamisin; kurşun kalem grafit elektrotlar; dönüşümlü voltametri; çift sarmallı DNA.

elektrokimyasal sensör; Fe₃O₄ nanopartiküller; karbon macunu elektrotları; sinapik asit; siringik asit; rutin; voltametri; elektrokimyasal empedans spektroskopisi

TABLE OF CONTENTS

ACKNOWLEDGMENTS	i
ABSTRACT	iii
ÖZET	v
TABLE OF CONTENTS	vii
LIST OF FIGURES	xi
LIST OF TABLES	xvi
LIST OF ABBREVIATIONS	xvii
CHAPTER 1: INTRODUCTION	
1.1 Thesis Problem.....	1
1.2 Aim of Study.....	7
1.3 Limitations of the Study.....	8
CHAPTER 2: LITERATURE REVIEW	
2.1 Electrochemical Sensors.....	9
2.1.1 Potentiometric sensors.....	9
2.1.2 Conductometric and impedimetric sensors.....	10
2.1.3 Voltammetric and amperometric sensors.....	11
2.2. Biosensors.....	12
2.2.1 History of biosensors.....	13
2.2.2 Components of biosensors.....	14
2.2.3 Characteristics of a biosensor.....	15
2.2.4 Advantages of biosensors.....	16
2.2.5 Application of biosensors.....	17
2.2.6 Classification of biosensors.....	18
2.2.7 Challenges of biosensors.....	20
2.3 Electrochemical Biosensors.....	20
2.3.1 Electrochemical DNA biosensors.....	21
2.3.2 Aim of electrochemical DNA biosensors.....	22
2.3.3 The structure of DNA.....	22

2.3.4	Natural electroanalytical characteristics of DNA.....	24
2.3.5	Types of immobilization methodology onto sensor surface.....	25
2.3.5.1	Adsorption method.....	26
2.3.5.2	Covalent binding.....	26
2.4	DNA- Compound Interactions.....	27
2.4.1	Electrostatic interactions.....	27
2.4.2	Groove binding interactions.....	28
2.4.3	External binders.....	28
2.4.4	Metal-Drug complexes.....	29
2.4.5	Intercalation mode.....	29
2.4.6	Interaction in aqueous medium.....	31
2.5	Techniques used to study DNA-Compound Interactions.....	31
2.5.1	Label-free detection based on intrinsic DNA signals (direct detection).....	31
2.5.2	Compound-based detection (indirect redox indicator-based detection).....	32
2.5.3	DNA modified electrode.....	33
2.5.4	Drug-modified electrode.....	34
2.5.5	Interaction in solution phase.....	34
2.5.6	How electrochemical methods work.....	34
2.5.7	Calculations related to DNA-compound interactions.....	35
2.6	Electrochemistry.....	36
2.6.1	Electrochemical cells and reactions.....	36
2.6.2	Faradaic and non-faradaic processes.....	37
2.6.3	Study of electrode reactions.....	41
2.6.3.1	Cyclic voltammetry.....	41
2.6.4	Controlled potential techniques.....	46
2.6.4.1	Chronoamperometry.....	46
2.6.4.2	Pulse voltammetry.....	47
2.6.4.3	Normal pulse voltammetry.....	47
2.6.4.4	Differential pulse voltammetry.....	48
2.6.4.5	Square-wave voltammetry.....	48
2.7	Electrochemical Set-Up.....	49

2.7.1 Solvents and supporting electrolytes.....	50
2.7.2 Working electrodes.....	51
2.7.2.1 Mercury electrodes.....	51
2.7.2.2 Solid electrodes.....	51
2.7.2.3 Carbon electrodes.....	52
2.7.3 Counter electrodes.....	52
2.7.4 Reference electrodes.....	52
CHAPTER 3: MATERIALS AND METHODS	
3.1 Materials and Methods for electrochemical DNA Biosensor.....	54
3.1.1 Chemicals and reagents for DNA biosensor.....	54
3.1.2 Electrochemical set-up	54
3.1.3 Preparation of pencil graphite electrodes.....	54
3.1.4 Immobilization of dsDNA and ADR on the surface of PGEs methods.....	55
3.1.5 Electrochemical detection procedure.....	55
3.2 Materials and Methods for Electrochemical Sensor for Compounds.....	56
3.2.1 Chemicals and reagents.....	56
3.2.2 Instrumentation and methods.....	57
3.2.3 Fabrication of bare CPE and MCPE.....	57
3.2.4 Voltammetric measurements.....	58
3.2.5 Preparation and detection procedure of real samples.....	58
CHAPTER 4: RESULTS AND DISCUSSION	
4.1 Electrochemical Detection of DNA and ADR Interaction.....	60
4.1.1 Electrochemical behaviour of dsDNA and ADR at PGEs surface.....	60
4.1.2 DPV Studies of dsDNA and ADR immobilized on PGEs.....	61
4.1.3 Impedimetric studies of the interaction of dsDNA and ADR.....	62
4.1.4 Scan rate studies of ADR at PGEs surface.....	64
4.1.5 pH studies of ADR at PGEs surface.....	67
4.1.6 Limit of detection and limit of quantification of ADR.....	68
4.2 Electrochemical Detection of Phenolic Compounds at CPE and MCPE.....	69
4.2.1 Electrochemical behaviour of phenolic compounds at CPE and MCPE.....	69
4.2.2 Evaluation of the electroactive surface area.....	72

4.2.3 Effect of pH on the phenolic compounds at CPE and MCPE.....	74
4.2.4 Effect of scan rate on the phenolic compounds at CPE and MCPE.....	77
4.2.5 Characterization of CPE and MCPE using EIS	82
4.2.6 Application of gold screen-printed electrode for rapid test of the phenolic compounds using cyclic voltammetry.....	83
4.2.7 Effect of concentration on the phenolic compounds at CPE/MCPE.....	84
4.2.8 Reproducibility, repeatability and stability.....	86
4.2.9 Selectivity of the electrode.....	89
4.2.10 Simultaneous detection of the phenolic compounds at MCPE.....	90
4.2.11 Application of CPE MCPE on in red and white wine.....	91
CHAPTER 5: CONCLUSION	
5.1 Conclusion.....	94
REFERENCES	96
APPENDICES	109
Appendix I: Voltammetric Procedures using NOVA 2.1.2.....	107
Appendix II: Ethical Approval Document.....	110
Appendix III: Curriculum Vitae.....	111
Appendix IV: Future Works.....	116
Appendix V: Similarity Report.....	117

LIST OF FIGURES

Figure 1.1: Adriamycin Structure.....	3
Figure 1.2: The chemical structures of sinapic acid, syringic acid, and rutin.....	7
Figure 2.1: Potentiometric Sensor (a) inner reference electrode ISE, (b) coated wire ISE.....	10
Figure 2.2: Conductometric sensor Set Up.....	11
Figure 2.3: Voltammetric and amperometric sensor setup (a) voltammetric and (b) amperometric sensors. RE: reference electrode; CE: counter electrode.....	12
Figure 2.4: Typical Biosensor.....	13
Figure 2.5: Components of a Biosensor	15
Figure 2.6: Major areas of application of Biosensors.....	18
Figure 2.7: Classification of Biosensors.....	19
Figure 2.8: Diagram of DNA structure.....	24
Figure 2.9: Grooves of DNA structure.....	25
Figure 2.10: Intercalation Mode.....	30
Figure 2.11: Detection Schemes of Compound –DNA interactions.....	32
Figure 2.12: Electrochemical reactions (a) reduction and (b) oxidation process of a species, A, in solution.....	37
Figure 2.13: (a) Potentials for possible reductions at a platinum electrode, initially at ~ 1 V vs. NHE in a solution of 0.01 M each of Fe ³⁺ , Sn ⁴⁺ , and Ni ²⁺ in 1 M HCL (b) Potentials for possible oxidation reactions at a gold electrode, initially at ~0.1V vs. NHE in a solution of 0.01 M each of Sn ²⁺ and Fe ²⁺ in 1 M HI. (c) Potentials for possible reductions at a mercury electrode in 0.01 M Cr ³⁺ and Zn ²⁺ in 1 M HCL The arrows indicate the directions of potential change.....	39
Figure 2.14: (a) Galvanic and (b) electrolytic cells.....	40
Figure 2.15: Pathway of a general electrode reaction.....	41
Figure 2.16: Potential-time excitation signal in cyclic voltammetric experiment.....	42
Figure 2.17: Typical cyclic voltammogram for a reversible redox process.....	43

Figure 2.18: Cyclic voltammograms for irreversible (curve A) and quasi-reversible (curve B) redox processes.....	44
Figure 2.19: Voltammogram showing increase in cathodic and anodic adsorption process.....	45
Figure 2.20: Chronoamperometric experiment: (a) potential-time waveform; (b) change of concentration profiles with time; (c) the resulting current-time response.....	46
Figure 2.21: Normal-pulse (curve A) and differential-pulse (curve B).....	47
Figure 2.22: Square-wave waveform showing the amplitude, E_{sw} ; step height, DE ; square-wave period, t ; delay time, T_d ; and current measurement times.....	49
Figure 2.23: Schematic of a cell for voltammetric measurements: w.e., working electrode; r.e., reference electrode; c.e., counter electrode	50
Figure 3.1: Experimental Procedure of the electrochemical detection of the interaction between dsDNA and Adriamycin immobilized on Pencil Graphite Electrodes	56
Figure 3.2: Schematic diagram of the phenolic compounds electrochemical sensor preparation.	59
Figure 4.1: Differential pulse voltammograms in pH 4.8, 0.5M acetate buffer solution showing the signal of: (A) 20 ppm, dsDNA only immobilized on bare PGE without interaction with ADR. (B) Adriamycin only with a concentration of $4.6 \times 10^{-4}M$ immobilized on bare PGE without interaction with dsDNA.....	60
Figure 4.2: DPV and the inset error bar plots, shows the different measurements carried out in pH 4.8, 0.5M ABS using PGEs. The labelled results on the voltammogram and the bar plots respectively represent: (a) Bare PGEs, (b) 20 ppm, of dsDNA only immobilized on PGE (c) $4.6 \times 10^{-4}M$ of ADR only immobilized on PGEs. (db) $4.6 \times 10^{-4}M$ of ADR with 20 ppm, dsDNA after interaction immobilized on PGEs (eb) $9.2 \times 10^{-4}M$ of ADR with 20 ppm, of dsDNA after interaction immobilized on PGEs (fb) $1.4 \times 10^{-3}M$ of ADR with 20 ppm, of dsDNA after interaction immobilized on PGEs (gb) $1.8 \times 10^{-3}M$ of ADR with 20 ppm, of dsDNA after interaction immobilized on PGEs.....	62

Figure 4.3: showing the Nyquist diagram for the R_{ct} values in the solution containing 5mM $K_3[Fe(CN)_6]/K_4[Fe(CN)_6]$ (1:1) with 0.5M KCl by using (a) Bare PGEs (b) 20 ppm, dsDNA only immobilized on PGE (c) 4.6×10^{-4} M of ADR only immobilized on PGEs (d) 4.6×10^{-4} M of ADR with 20 ppm, dsDNA after interaction immobilized on PGEs (e) 9.2×10^{-4} M of ADR with 20 ppm, of dsDNA after interaction immobilized on PGEs (f) 1.4×10^{-3} M of ADR with 20 ppm, of dsDNA after interaction immobilized on PGEs (g) 1.8×10^{-3} M of ADR with 20 ppm, of dsDNA after interaction immobilized on PGEs. 64

Figure 4.4: Scan rate study showing cyclic voltammograms of ADR at 9.2×10^{-4} M immobilized on the PGEs at different potential scan rates of (0.02, 0.04, 0.06, 0.08, 0.1, 0.2, 0.25, 0.3, 0.35, 0.4, 0.45)V/s in 0.5M phosphate buffer of pH 4.0. **6B and 6C** Show the influence of the square root of scan rate on the applied peak current in a linear relationship and a logarithm plot of applied anodic peak current versus logarithm of scan rate in a linear relationship respectively..... 66

Figure 4.5: shows Cyclic voltammograms for the pH study and B and C demonstrate error bars charts and linear correlation to validate the effect of changes pH range on the ADR at 9.2×10^{-4} M, immobilized on PGEs with different pH values of 0.5M PBS in pH of 4.0, 4.8, 5.8, 6.0, 7.0 and 8.0 at a scan rate of 0.2V/s..... 68

Figure 4.6: . Showing the calibration curve and error bars charts of different concentrations of the ADR in the range of 9.19×10^{-6} M, 7.36×10^{-6} M, 5.5×10^{-6} M, 3.67×10^{-6} M, and 1.84×10^{-6} M immobilized on the PGEs in 0.5M PBS pH 4.0 used for obtaining the LOD and LOQ..... 69

Figure 4.7: Differential pulse voltammograms (A–C) show the determination of the electrochemical behavior of the selected phenolic compounds of 0.9×10^{-3} M for sinapic, 1.0×10^{-3} M for syringic, and 0.3×10^{-3} M for rutin at carbon paste electrode (CPE) and carbon paste mixture prepared with Fe_3O_4 nanoparticles (MCPE) in 0.5 M ABS with pH 4.8, recorded at 0 V to +1.0 V. The inset cyclic voltammograms (A–C) of the selected phenolic compounds at CPE and MCPE was carried out in 0.5 M acetate buffer solutions (ABS) with pH 4.8 and recorded at a scan rate of 0.2 Vs⁻¹. 71

Figure 4.8: The chemical reaction process showing the oxidation of phenolic compounds having one peak in the reaction path (A) and the oxidation of phenolic compounds having two peaks in the reaction path (B).	72
Figure 4.9: Cyclic voltammogram shows the response of 1 mM K ₄ [Fe (CN) ₆] at the CPE and MCPE at a scan rate of 0.1 V/s.....	73
Figure 4.10: Cyclic voltammograms at (A) CPE and (B) MCPE, respectively in 1 mM K ₄ [Fe(CN) ₆] of 0.1 M KCl by varying scan rates (0.1–0.2 V/s). The corresponding Plots of I_{pa} vs $v^{1/2}$ at (C) CPE and (D) MCPE.....	74
Figure 4.11: Cyclic voltammograms (A–C) show the effect of pH on the electrochemical behavior of the phenolic compounds, in 0.5 M acetate buffer of pH 2.6, 3.8, 4.8, 5.6, 6.5, 7.4, 8.4, and 9.2, at a scan rate of 0.2 V/s with a reversible scanning potential range of –0.4 to 1.0 V. The inset figures show cyclic voltammetry (CV) at CPE.....	75
Figure 4.12: The linear regression plots for both CPE and MCPE to show the effect of pH on the electrochemical behavior of the phenolic compounds, in 0.5 M acetate buffer of pH 2.6, 3.8, 4.8, 5.6, 6.5, 7.4, 8.4 and 9.2, at a scan rate of 0.2 V/s.....	76
Figure 4.13: Cyclic voltammograms showing the electrochemical oxidation and reduction behavior of phenolic compounds at CPE and MCPE in 0.5 M of ABS having pH 4.8 and scan rates of 0.03, 0.06, 0.09, 0.12, 0.15, 0.18, 0.20, 0.25, 0.3, 0.35. and 0.40 V/s, respectively, with a reversible scanning potential range of –0.4 to 1.0 V.	78
Figure 4.14: Linear regression plots of phenolic compounds showing the dependence of redox (anodic and cathodic) peak current I_p on the square root of scan rate $v^{1/2}$ (V/s) ^{1/2} . The plots, represents controlled diffusion at CPE and MCPE in 0.5 M of ABS with pH 4.8, scan rate of 0.03, 0.06, 0.09, 0.12, 0.15, 0.18, 0.20, 0.25, 0.3, 0.35 and 0.40 V/s.....	79
Figure 4.15: Linear regression plots showing the dependence of redox (anodic and cathodic) peak current on scan rate I_p versus scan rate v (V/s) for controlled adsorption The plots, represents controlled adsorption at CPE and MCPE in 0.5 M of ABS with pH 4.8, scan rate	

of 0.03, 0.06, 0.09, 0.12, 0.15, 0.18, 0.20, 0.25, 0.3, 0.35 and 0.40 V/s respectively with a reversible scanning potential range of -0.4 to 1.0 V. 80

Figure 4.16: The linear relationship plots of logarithm of peak current and logarithm of scan rate ($\log I_{pa}$ versus $\log v$) for phenolic compounds. The plots, represents peak current and logarithm of scan rate at CPE and MCPE..... 81

Figure 4.17: Nyquist plots represent the EIS measurement performed in the frequency range of 100 kHz–0.1 Hz, in a redox solution of 5 mM $[\text{Fe}(\text{CN})_6]^{3-/4-}$ containing 1 M KNO_3 using CPE and MCPE for surface characterization. The inset figure is the equivalent circuit showing resistors and capacitor (c). 83

Figure 4.18: Cyclic voltammograms show an overlay of the gold screen-printed electrode with CPE and MCPE of the phenolic compounds rutin and sinapic acids in 0.5 M ABS of pH 4.8 at a scan rate of 0.2 V/s with a reversible scanning potential range of -0.4 to 1.0 V..... 84

Figure 4.19: Differential voltammograms showing the reproducibility and repeatability of MCPE for the determination of the phenolic compounds respectively..... 88

Figure 4.20: A steady amperometric current response for determination of stability of the sensor for phenolic compounds detection in (0.5 M ABS of pH 4.8), for 30 minutes, at MCPE using 0.6V potential. Differential pulse voltammograms shows the determination of 0.9×10^{-3} M for sinapic, 1.0×10^{-3} M for syringic and 0.3×10^{-3} M for rutin respectively in 0.5M ABS pH 4.8 for 1st day and 10th to show stability of the modified electrode. 89

Figure 4.21: Differential pulse voltammogram showing three phenolic compounds' simultaneous determination with 4.5×10^{-3} M for sinapic acid, 5.1×10^{-3} M for syringic acid, and 1.6×10^{-3} M for rutin respectively at MCPE in 0.5 M ABS with pH 4.8, recorded at 0 V to +1.0 V..... 90

Figure 4.22: Cyclic voltammograms and Differential pulse voltammograms showing the determination of red and white wine real samples only using the modified electrode in 0.5M ABS pH 4.8 as supporting electrolyte..... 93

LIST OF TABLES

Table 2.1 Types of Electrochemical Biosensors.....	21
Table 2.2: The electroactivity of DNA bases and their detections conditions.....	25
Table 4.1: Linear regression equation of anodic peak potentials E_{pa} and pH of the phenolic compounds with their slopes respectively reported for cyclic voltammetry method employed in determining the pH on the electrochemical behavior of the phenolic compounds at bare CPE and MCPE.....	77
Table 4.2: Linear regression equations show the dependence of redox peak current I_p on the square root of scan rate $v^{1/2}(V/s)^{1/2}$ for controlled diffusion and dependence of redox peak current I_p on scan rate v (V/s) for controlled adsorption for phenolic compounds at bare CPE and MCPE with their slopes and R-square values.....	80
Table 4.3: Linear regression equation showing the logarithm of anodic peak current and logarithm of scan rate ($\log I_p$ versus $\log v$ (V/s) for the phenolic compounds at CPE and MCPE with their slopes and R-square values.	81
Table 4.4: Limits of detection (LOD) and limit of quantification (LOQ) reported for the differential pulse voltammetry method employed in detecting phenolic compounds compared to other methods used.....	85
Table 4.5: Effect of various interferences on the determination of sinapic, syringic, and rutin.	90
Table 4.6: Results of the determination of phenolic compounds in wine samples (red and white wine) using Fe_3O_4 nanoparticles modified CPE.	91

LIST OF ABBREVIATIONS

ABS:	Acetate Buffer Solution
ADR:	Adriamycin
CE-MS:	Capillary Electrophoresis–Mass Spectrometry
CPE:	Carbon Paste Electrode
CV:	Cyclic Voltammetry
CZE:	Capillary Zone Electrophoresis
DME:	Dropping Mercury Electrode
DMF:	Dimethylformamide
DMSO:	Dimethylsulfoxide
DNA:	Deoxyribonucleic acid
DPV:	Differential Pulse Voltammetry
dsDNA:	Double-stranded deoxyribonucleic acid
EIS:	Electrochemical impedance spectroscopy
FET:	Field-Effect Transistor
FID:	Flame ionization detector
GCE:	Glassy Carbon Electrode
GRC:	Graphite Reinforcement Carbon
HDME:	Hanging Mercury Drop Electrode
IPE:	Ideal Polarized Electrode
IUPAC:	International Union of Pure and Applied Chemistry

LC-MS:	Liquid chromatography-mass spectrometry
LOD:	Limit of Detection
LOQ:	Limit of Quantification
MDB:	Meldola's blue
MEMS:	Microelectromechanical systems
MIPs:	Molecularly Imprinted Polymers
mL:	Millilitre
NPs:	Nanoparticles
PGEs:	Pencil Graphite Electrodes
PPM:	Parts Per Million
SPEs:	Screen Printed Electrodes
SPR:	Surface Plasmon Resonance
SQWV:	Square Wave Voltammetry
ssDNA:	Single-stranded deoxyribonucleic acid
UV:	Ultra Violet

CHAPTER 1

INTRODUCTION

1.1 Thesis Problem

Nucleic acids have been integrated with transducers electrochemically, to fabricate new kind of biosensors that are used for detection of affinities of molecular interactions that occur between double-strand deoxyribonucleic acid (dsDNA) with other compounds such as pollutants or drugs. This detection also helps in screening these compounds as they interact with the dsDNA (McGown et al., 1995). The small molecules of the anticancer drug or other compounds bind to the negatively charged nucleic acid sugar phosphate structure of the DNA through electrostatic interactions and they bind to the major and minor grooves of the of the double stranded DNA through the process of intercalation which occurs between the small molecules and the stacked DNA base pairs (Chu et al., 1999). Varieties of techniques electrochemically have been used for the detection of interactions between DNA and the anticancer drugs (Fritzsche et al., 1993; Kurucsev & Kubista, 1992; Lown et al., 1984; Nunn et al., 1991). Plambeck & William Lown, (1984) used an electrochemical method to describe the reaction process of both free and drugs bound intercalatively by using the mercury drop electrode method. Fojta et al. (Fojta et al., 1996), in their work, stated that the conformational changes that happen to DNA are as a result of the interaction of the DNA with anticancer agents which are intercalators. Teijero et al., (Teijeiro et al., 1995) did a quantitative analysis and studied anthramycin employing the method of differential pulse polarography, an aqueous buffered solution using the Hanging Mercury Drop Electrode. They reported that from the interaction of anthramycin with native DNA, covalent adducts were observed. Erdem et al. (Erdem et al., 1999) used a Carbon Paste Electrode (CPE) modified with DNA and also used CV and DPV (Purushothama et al., 2018) for studying the interaction between Epirubicin (EPR) with dsDNA and also single strand DNA (ssDNA).

Electrochemical DNA biosensors possess the potential high sensitivity and rapidity in genetic detection analysis. These advantages and many others overcome the limitation in the use DNA microarrays. Some of the disadvantages of using the Electrochemical DNA biosensors include: a) Production of microchip integrated with nucleic acids through microelectronics incorporation, b) Automation of the detection steps of the electrochemical

DNA biosensor in detail and c) Application these biosensors to carry out signal transduction analysis directly in order to avoid processes of statistical analysis and image processing. DNA biosensors can be applied in several fields such as; medical diagnosis, environmental monitoring, pharmaceutical screenings, food analyses and molecular diagnostics. These biosensors have several advantages compared to other traditional methods of hybridization detection such as the optical transducers used in fibre optics, reflection contrast interference contrast microscopy, surface Plasmon resonance, Raman spectroscopy and other spectroscopy techniques (Cagnin et al., 2009).

Adriamycin (ADR) (Figure 1.1) is an antibiotic that belongs to the anthracycline family and has a wide area of applications chemotherapeutically and in its anti-neoplastic action. The antitumor characteristics of the drug have been recognized for a long time of about 30 years (Di, A. M., Gaetani, M., & Scarpinato, 1969; Perry, 1996), up till now it's mode of action is yet to be fully understood in in-vivo (Kiyomiya et al., 2001). The understanding and explanation of anticancer activities and its mode of action are still essential because it will aid in achieving the goal of improving its administration; experimental evidence reported, showed that ADR promotes oxidative damage to the DNA in cancerous cells by generating reactive oxygen species (Kiyomiya et al., 2001; Kostoryz & Yourtee, 2001; Minotti, 1999; Zhou et al., 2001). The product from the guanine oxidation of the DNA is seen to be strongly mutagenic and contributes to the dysfunctionality of cells (S. S. David & Williams, 1998). X-ray crystallography was used as evidence in 1972 and other methods to show that ADR and other analogous of anthracycline family interacts intercalatively with the DNA (Berg et al., 1981; Frederick et al., 1990; Lipscomb et al., 1994; Perry, 1996; Pigram, W. J., W. Fuller, 1972; Zunino et al., 1977). When ADR intercalates with dsDNA, the rings shown on B and C of the ADR is the region that intercalates with the DNA base pairs (Cullinane & Phillips, 1990; Frederick et al., 1990; Lipscomb et al., 1994; Wang et al., 1998). The amino sugar portion of the ADR and its carbonyl side chain which links to A remains inside the double helix minor groove of the of the DNA. The ring D extends into the double helix major groove side of the DNA (Cullinane & Phillips, 1990; Pigram, W. J., W. Fuller, 1972; Wang et al., 1998). The amino sugar, that is the positively charged part of the amino group function by interacting with the phosphate backbone of the DNA and is essential in the binding affinities and intercalation with the dsDNA (Berg et al., 1981).

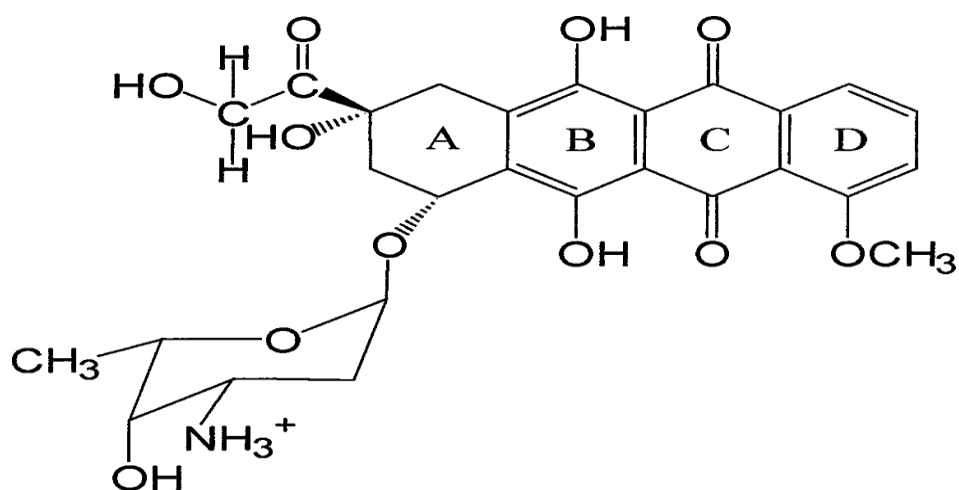


Figure 1.1: Adriamycin Structure

Graphite possesses both the property of metals and non-metals making it useful as an electrode material (Chehreh Chelgani et al., 2016). Pencils consist of graphite powder made out of 4% of graphite in the world mixed with inorganic resin, matrix of clay and cellulose (Alipour et al., 2013). The application of graphite reinforcement carbon (GRC) was first reported by Aoki et al., where they used mechanical pencil leads in voltammetry as electrodes. The commercial availability of GRC is large and used as disposable sensors because of its low content of impurities from heavy metals and high quality (Aoki et al., 1989). Pencil Graphite Electrodes (PGEs) have gained large applicability in the recent years with so many researches and analysis of organic and inorganic compounds reported by different researchers around the world. They are used, because they possess electrochemical and also economical characteristics. The PGEs are used from pencil graphite leads which are commercially available, cheap, easily disposable, ease of use and reduces time consumption when cleaning surfaces of solid electrodes during measurements. PGEs compared to other electrodes, have lower currents when used, they are highly sensitive, support adsorption easily, have good reproducibility of results, and their surfaces can be modified easily and pre-treated or activated. Several Voltammetric methods can be applied using the PGEs (David et al., 2017).

The EIS has been used to investigate the bulk and interfacial electrical properties of systems. The method showed to be a technique that is excellent and can be used for the analysis of quantitative parameters of different electrochemical processes. EIS provides a result to show

the region where interfacial properties change after the biorecognition reactions and events occur on the modified surfaces (Maalouf et al., 2007). The electrochemical reactions which are known as electron transfers occur on the surfaces of the electrodes and these reactions involve the resistance of the electrolyte, the electroactive species been adsorped, charged transfers, and mass transfers occurring through diffusion of the bulk solution to the surface of electrode (Wang, 2006). Randles-Ersher equivalent circuit model is the most favourite model that is used for electrical circuits to represent electrochemical reactions. The model consists of electrolyte resistance which is also the solution resistance (R_s), Warburg impedance (W), charge transfer (R_{ct}), mass transfer resistance (R_{mt}), and double-layer capacitance (C_{dl}), (Yuan et al., 2009).

Phenolic compounds contain a broad class of flavonoids and non-flavonoids phenols, which occur naturally as secondary metabolites throughout the plant kingdom (Figure 1.2). They spread widely into several taxonomic groups and play structural and protective functions in plants (Fukuji et al., 2010; Ramirez-Lopez et al., 2014). Flavonoids and phenolic acids contain at least one aromatic ring that has one or more hydroxyl groups attached to it. They have a range of structures, and they can be classified based on the number and arrangement of carbon atoms in their structures. Flavonoids are classified into flavones, isoflavones, flavan-3-ols, anthocyanidins, flavonols, flavanones and others, while the non-flavonoids are classified into stilbenes, phenolic acids, hydroxybenzoic acids, hydroxycinnamic acids and other. These phenolic acids are generally conjugated to organic acids and sugars (Gutiérrez-Grijalva et al., 2018). These phenolic compounds are used in food processing due to their properties associated with color, flavors, preservatives, and antioxidants that improve human health (Robbins, 2003). Phenolic compounds have a ubiquitous presence of different proportions in plant-based foods. Daily consumption of products such as fruits, wines, vegetables, grains, teas, spices, and coffees improves human health. They improve human health through their radical scavenging activities, which provide an anticancer effect against atherosclerosis, inflammatory diseases, and other oxidative damage diseases and control oxidation in the human body (Dobes et al., 2013; Gabriella et al., 2012; Robbins, 2003; Tian et al., 2009; Tomac et al., 2020). These phenolic compounds undergo electrochemical oxidation at modified electrodes through the following basic principles: (1) Phenols oxidize to phenoxy radicals in one-proton, one-electron irreversible step. (2) The anodic oxidation

of phenolics is determined by the stability of the produced phenoxy radical. (3) The formed phenoxy radicals that are unstable co-exist in three resonant configurations, the ortho and para-phenoxy radicals. They have a spin density that is large and a stability that undergoes secondary chemical reaction hydroxylation. (4) When an extra electroactive –OH group is added at the ortho and para points, the process controls the production of two number of electrons and protons in a pH-dependent reversible process, which has higher stability and acts at a less potential than that of the meta-di-phenol or mono-phenol. (5) The substituents that are non-electroactive that are present produce small oxidation peak potentials shift while a larger shift is observed when substituents at the para and ortho-positions are linked. (6) Substituents that have their electrons removed have a higher anodic peak potential shift, while substituents that are electron donor make oxidation process easy. (7) The electrochemical oxidation process involves protons participation; the higher the pH values, the simpler the electron loss (Chiorcea-Paquim et al., 2020; Robbins, 2003). Other researchers have published works on rutin (Apetrei & Apetrei, 2018; D’Souza et al., 2019; da Silva & da Cunha Areias, 2020; Karabiberoğlu & Dursun, 2018; Sheng et al., 2020; Yan et al., 2016), but less or no work is reported on sinapic acid (Sousa et al., 2004) and syringic acid. These phenolic acids contain oxidizable phenolic substituents on the aromatic ring or reducible olefinic bond, which is why their voltammetric determination (Janeiro et al., 2007; Sousa et al., 2004). Different methodologies have been used for the analysis of phenolic compounds from different origins, which includes high-performance liquid chromatography (HPLC) in reversed-phase under UV detection, liquid chromatography with mass spectrometry (LC-MS) via electrospray ionization (ESI), gas chromatography (GC) with flame ionization (FID) and MS detection, capillary zone electrophoresis (CZE) under UV direct detection, and capillary electrophoresis coupled to mass spectrometry (CE-MS) (Cao et al., 2004; Fukuji et al., 2010; Gabriella et al., 2012; Yıldırım et al., 2017). The techniques mentioned above used for phenolic compounds determination are sensitive and selective; however, they present some disadvantages. They include a large amount of sample needed for analysis, complex procedures for sample determination, time-consuming procedures, and the pretreatment process for the sample is unfriendly. In comparison to the above traditional instrumentation, electrochemical methods have the advantage of high sensitivity, selectivity, ease of use of instruments, low cost of preparation, and simple and rapid detection of a low

amount of sample (David et al., 2016; Dobes et al., 2013; Karabiberoğlu & Dursun, 2018; Yan et al., 2016).

Modified electrodes in electrochemical analysis for sensitive and selective detection of compounds have been widely used (Tashkhourian & Nami-Ana, 2015). CPE has many advantages over other solid electrodes, which include their biocompatibility with test samples, a fast and straightforward method of preparation from cheap materials. They possess a reproducible and renewable surface, which presents low residual current during analysis. CPE also has low production cost, porous surfaces, and can be used for miniaturization in electrodes for electrochemical sensors (Arduini et al., 2010; Tashkhourian & Nami-Ana, 2015). However, MCPE with nanomaterials has recently shown a substantial increase in the electrochemical properties of the analyzed compounds. The main advantages of using MCPE with nanoparticles over macro electrodes or unmodified CPE are effective surface area, increased sensitivity and selectivity, and effective mass transport by mediating electron-transfer between electroactive species during reactions in solution (Chikere et al., 2020).

Nanoparticles are in small sizes, ranging from 1–100 nm, and they possess chemically, physically, and electronically unique properties that make them different from those of bulk materials. These different properties allow them to be utilized in various analytical methods, where they are employed to fabricate novel and improved sensing devices such as in electroanalytical sensors. Nanoparticles have been widely used to modify electrodes used in sensitive and selective detection of biological compounds in analytical methods. The application of nanostructured materials to these electrodes indicated considerable improvements in the electrochemical behavior of compounds because of their high effective surface area, catalytic effect, and mass transport (Abdi et al., 2020; Tashkhourian et al., 2013). Fe₃O₄ nanoparticle belongs to the class of nanoparticles, and they are used for modifying electrodes because of their excellent electrochemical properties (Abdi et al., 2020). They are used to modify the working electrode to enhance detection limit, provide large electroactive surface area, catalytic effect, high electromagnetic activity, attractive electron transport, sensitivity, and chemical stability (Sanchayanukun & Muncharoen, 2020). The Fe₃O₄ nanoparticles also offer a conductivity effect, making it suitable for enhancing the electron transfer between analytes and electrodes. Fe₃O₄ nanoparticles have

significant application areas in biomaterials, bioseparation, biomedical and bioengineering, and food analysis (Xu et al., 2014).

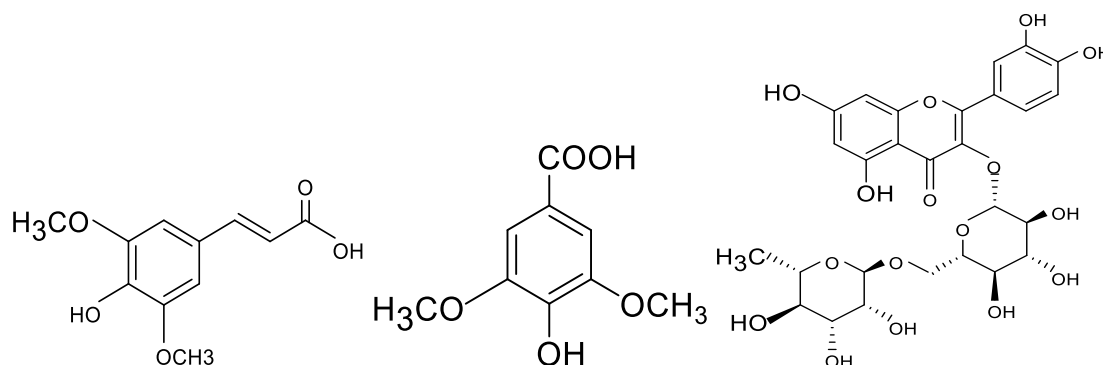


Figure 1.2: The chemical structures of sinapic acid, syringic acid, and rutin, accordingly.

1.2. Aim of Study

This study aimed at using voltammetric and impedimetric technique in the detection of dsDNA of fish sperm and an anti-cancer drug ADR interaction using pencil graphite electrodes (Figure 1.1). There are few works on electrochemical DNA biosensors for detection of interaction between dsDNA and Adriamycin of atleast 10years ago. There is no or few presented reports on the impedimetric technique on dsDNA and ADR using the pencil graphite electrodes. This study provides additional report on the impedimetric analysis of dsDNA-ADR, added to voltammetric techniques such as differential pulse voltammetry using pencil graphite electrodes.

This research also aims to study the electrochemical behavior of various phenolic compounds (Figure 1.2) by fabricating an electrochemical sensor using carbon paste electrodes modified with Fe₃O₄ nanoparticles. This study reports on using Fe₃O₄ nanoparticles to modify carbon paste electrodes for the electrochemical determination of sinapic acid, syringic acid, and rutin based on our careful check of works reported on the detection of these phenolic compounds. CV, DPV, and EIS analyses were performed as characterization studies for CPE, MCPE, and the solution interface. Scan rate and pH studies were performed as optimization studies. A rapid validation test was carried out using gold screen-printed electrodes, and the result was compared to CPE and MCPE. The

electrochemical sensor was applied in real samples of red and white wine to determine the presence of phenolic compounds.

1.3 Limitation of the Study

The first major challenge with our study is the interferences of substances in real samples that are complex because the biosensors been fabricated are for detection of DNA interaction with compounds and detection of pure substances. The electrochemical biosensors generally require improvements with a current technology that is user friendly and possess all the characteristics of a biosensor. There is a major challenge also in the commercialization and clinical awareness of the fabricated biosensors. The electrochemical sensors needs to be developed into high-throughput point of care devices but for it to work, a huge amount of money needs to be inversed for mass production of the sensors and its commercialization. There is a limitation of temperature dependent where high temperature or low temperature can affect the study. There is error caused by logarithmic response of the device. There is also a limitation on the characteristic of selectivity.

CHAPTER 2

LITERATURE REVIEW

2.1 Electrochemical Sensors

Electrochemical sensors can be defined as devices that provide details and data about reactions between chemical species. Chemical energy in the system is transduced between the selective chemical layer, the recognition element, and the electrochemical transducer. A chemical sensor is an analytical tool used first to detect analytes of importance, which is determined by the selective recognition elements of the electrochemical sensors. The electrochemical sensors are easily miniaturised and incorporated into systems. These features have made these sensors attractive in the present day. Electrochemical sensors have different types that can be classified based on the magnitude of electricity applied to them for transduction to occur. There are potentiometric, conductometric, impedimetric, voltammetric, or amperometric reactions (Janata, 2009). Sensors are devices used to detect physical stimuli that include heat, light, pressures movements and sounds. They are transmitted as an electrical impulse that resulted from the detection to measure the change (Janata, 2009). Electrochemical sensors are a class of sensors that have transducing elements as electrodes employed in the presence of analytes for the detection of substances. They use several features to detect various parameters, which are physical, chemical, biological in the environment, health industry, and applied in machines such as automobiles, phones, and aeroplanes. Electrochemical sensors in recent times have been manufactured into smaller sensors that possess higher sensitivity, selectivity with low cost of production and maintenance (Antuña-Jiménez et al., 2012).

2.1.1 Potentiometric Sensors

Potentiometric sensors are the most important types of electrochemical sensors with the lowest cost available today (Figure 2.1). They are fabricated using a selectively permeable membrane for a particular ion, which develops the potential of the membrane in contact with the solution having the analyte ion. Ion-selective electrodes (ISEs) are the electrodes, which build up with the membranes used for the sensors. The interaction between the analyte ion

and the selective membrane used produces a particular change in the potential across the samples' interface and the membrane phase, which depends on the activity of the target ion present inside the solution. Molecularly imprinted polymers (MIPs) are the type of agents that can satisfy the requirements to act as receptors for these sensors (Antuña-Jiménez et al., 2012; Brett & Oliveira-Brett, 2011).

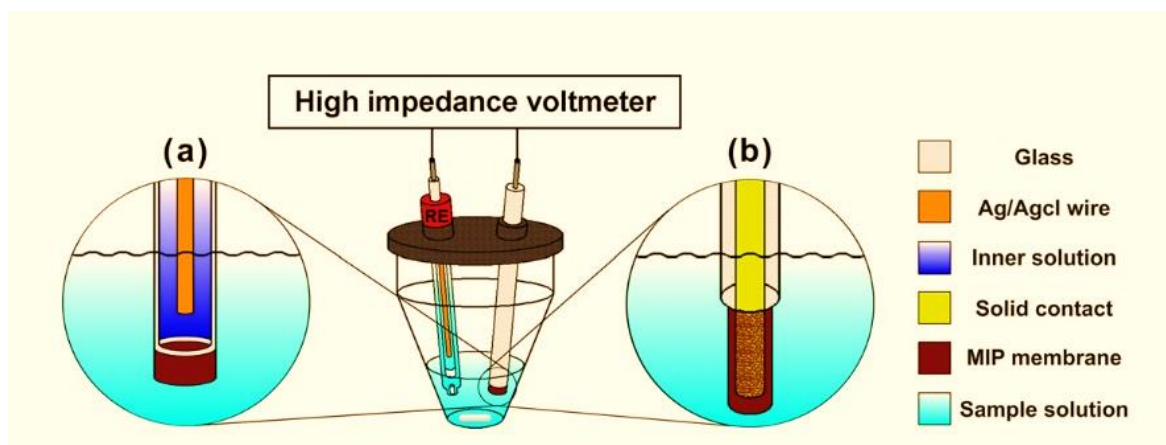


Figure 2.1. Potentiometric Sensor with (a) an inner reference electrode ISE, (b) coated-wire ISE.

2.1.2 Conductometric and Impedimetric Sensors

Conductometric and impedimetric sensors are non-selective; they become selective when coupled to a selective recognition element such as the MIPs, making the sensors selective. The measurements performed using these sensors (Figure 2.2) are done by applying an alternating voltage between two electrodes. The conductometric devices have two electrodes. The impedimetric devices have one reference electrode, while the response obtained is from the alternating current. Two electrode systems are sufficient for these kinds of sensors. However, a potentiostat with three-electrode systems is frequently used for impedimetric measurements (Antuña-Jiménez et al., 2012; Brett & Oliveira-Brett, 2011).

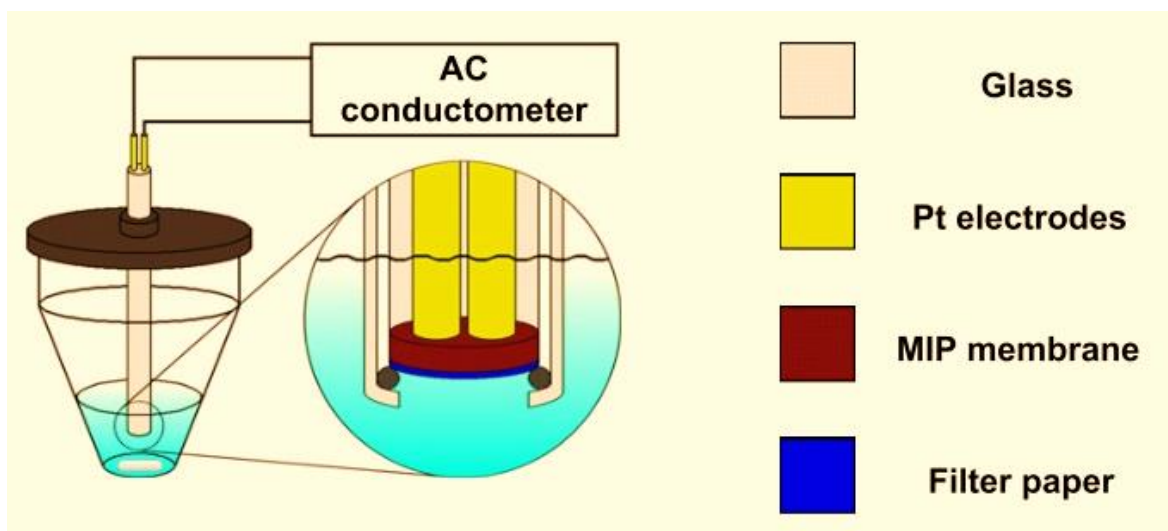


Figure 2.2. Conductometric sensor Set Up

2.1.3 Voltammetric and Amperometric Sensors

This group of electrochemical sensors involves measuring current flow as the primary transducing activity and belongs to the group of coupled devices with faradaic features. The measurements taken for these sensors are performed by applying a fixed and variable potential in the amperometric and voltammetric three-electrode electrochemical system. These types of sensors (Figure 2.3) require the presence of electroactive species in the electrolyte solution for measurements to be performed (Antuña-Jiménez et al., 2012). This type of electrochemical sensors indicates the recording of current-voltage as a potentiostat or galvanostat measures the current to be a function of the potential applied. These sensors have three-electrode in their system: the working, reference, and counter electrodes. In a two-electrode system, the reference electrode can also serve as a counter electrode when the currents are very small. These electrochemical sensors have lower detection limits than the potentiometric sensors and can detect more than the electroactive species. There is no need to separate the electroactive species in solution and their detection using these sensors (Brett & Oliveira-Brett, 2011).

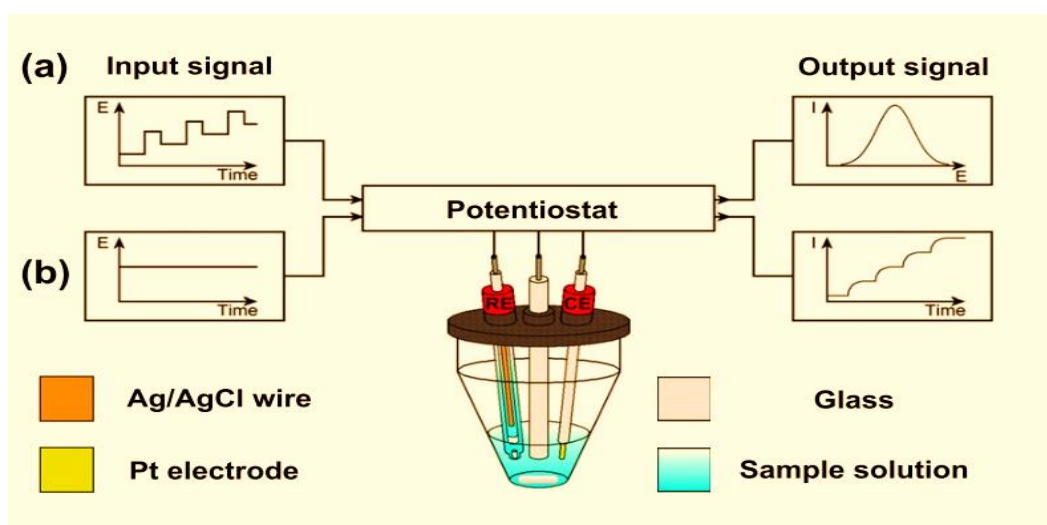


Figure 2.3. Voltammetric and amperometric sensor setup (a) voltammetric and (b) amperometric sensors. RE: reference electrode; CE: counter electrode.

2.2 Biosensors

The International Union of Pure and Applied Chemistry (IUPAC) defined biosensor to be a device that uses biochemical reactions or biological response that are specific with immunosystems, organelles, isolated enzymes, whole cells, and tissues mediate between these reactions. They are used for detecting compounds that are chemical through quantifiable signals that are electrical, optical and thermal (Lowe, 1984); The typical biosensor (Figure 2.4) has the following:

- (a) The bioreceptors act to bind to specific analytes.
- (b) The interface where the particular biological reaction occurs and produces a signal sensed by the transducer.
- (c) The signal sensed by the transducer is converted into an electrical signal, which is then amplified and then detected by a circuit, which is later shown through a display interface. (Baryeh et al., 2017; Bhalla et al., 2016; Gan, T., Shi, Z., Sun, J., & Liu, 2014; Serra, 2010; Zeng & Xiao, 2017).

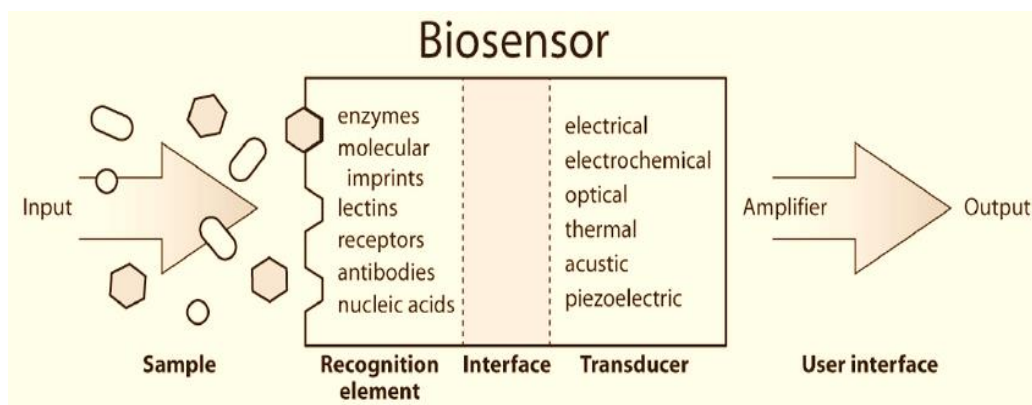


Figure 2.4. Typical Biosensor

2.2.1 The History of Biosensors

Biosensors have an early history traced to the demonstration of acids in a liquid by M. Cremer in 1906, who stated that the concentration is proportional to the potential generated between the fluid and the glass membrane. In 1909, Soren Peder Lauritz Sorensen introduced hydrogen ion concentration (pH) with an electrode for pH measurements while W. S Hughes in 1922 invented it. Griffin and Nelson reported the enzyme invertase's immobilisation between 1909 and 1922 using charcoal and aluminium hydroxide. In 1956, Leland C. Clark invented the first biosensor to use for oxygen detection, called the Clark electrode. Since then, he has been called the father of biosensors. In 1962, he later invented the Amperometric enzyme electrode, which was then followed by Guilbault and Montalvo Jr's invention to detect urea in 1969. The Yellow Spring Instruments (YSI) in 1975 developed the first commercial biosensor. The area of the biosensor has made remarkable progress after the development of the I-STAT sensor. The area of biosensors forms a platform that connects different fields of (physics, chemistry and biology) and technology both in micro and nano levels where they are applied in different fields. Today, over 84000 reports indexed in the web of science about biosensors from 2005 till the present (Bhalla et al., 2016; Evtugyn, 2014).

2.2.2 Components of Biosensor

The biosensor is a device with several components (Figure 2.5), which majorly includes the following;

1. **Analyte:** This is defined as a substance needed to be detected by the biosensor.
2. **Bioreceptor:** This is a substance or molecule that recognises the analyte of interest, such as enzymes, deoxyribonucleic acid (DNA), antibodies, and aptamers as bioreceptors.
3. **Biorecognition:** This is the process of producing signals in the form of pH, charge, heat, light, mass and pressure e.t.c when the bioreceptors interacts with the analyte. This process occurs when a bioreceptors attaches a counter part molecule by a complementary shape of the molecule due to non-covalent interactions.
4. **Transducer:** This is a part of the biosensor (a sensor, electrode) that deals with converting one form of energy into another. These transducers produce electrical or optical signals, and they represent the amount of the analyte that interacted with the bioreceptors.
5. **Electronics:** This can be defined as part of a biosensor that takes the signal converted, process it, and sends it for display. The electronics consist of circuits that function to amplify and convert the signals from analogue forms into digital forms measured and quantified.
6. **Display:** This component of the biosensor consists of the interpretation system, which is either a liquid crystal display or can use a printer to generate curves and numbers easily understandable (Bhalla et al., 2016; Evtugyn, 2014).

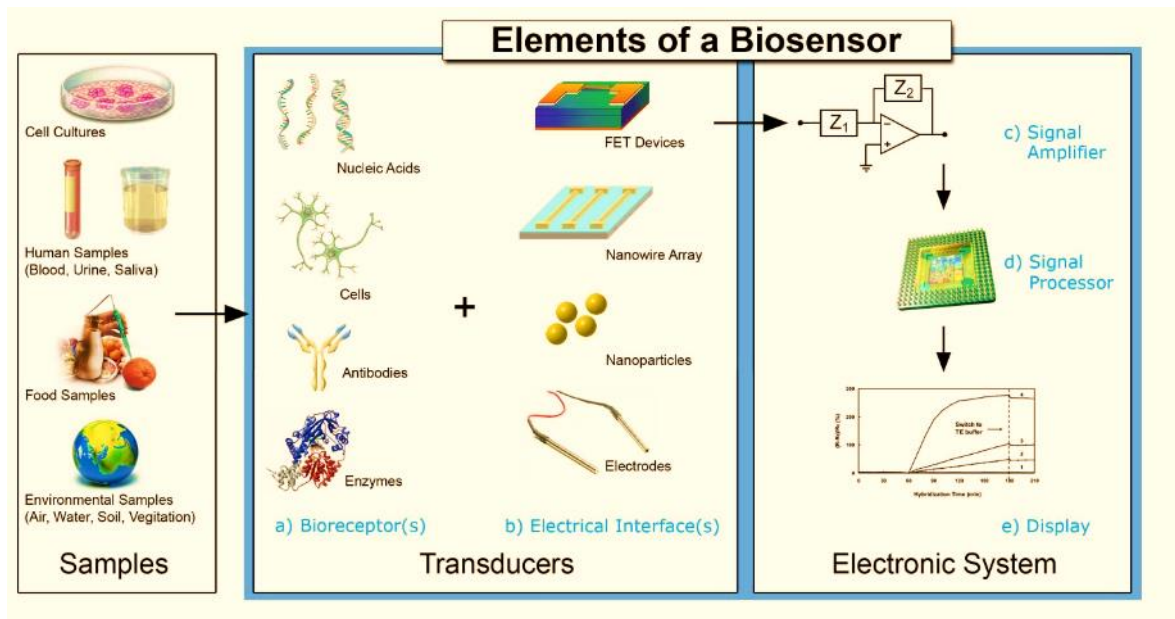


Figure 2.5. Components of a Biosensor

2.2.3 Characteristics of a Biosensor

1. **Selectivity:** This is the most sensitive part of the biosensor. The bioreceptors detect an analyte of interest in the sample of mixtures and other components. The example is seen in antigen and antibody interaction detection. This characteristic is the main consideration for a biosensor.
2. **Reproducibility:** The ability of the biosensor to produce similar responses when an experiment or analysis is duplicated. The transducer of the biosensor and its electronic part is responsible for the accuracy and precision of the biosensor's reproducibility. The ability of the biosensor to produce results that are alike every time its measures a sample is called precision. The ability of the biosensor to produce a mean value result that is close to the value of the sample when it was measured more than once is called accuracy. The ability of the biosensor to have reproducible results makes it highly reliable. It increases its robustness when it comes to interferences by other samples.
3. **Stability:** A shift or changes in the output signals of the biosensor can be affected by ambient disturbances when measurements are taken, which affects the precision and

accuracy of the biosensor. This feature can make the biosensor have a long incubation period and continuous monitoring during measurements. The response of the transducers of the biosensor can be sensitive to temperature and other disturbances such as degradation of the bioreceptors, the affinity of the bioreceptors, which may affect the biosensor's stability. The biosensor needs to be tuned to ensure the stability of the biosensor is unaffected by any disturbances.

4. **Sensitivity of biosensor:** This feature of the biosensor determines the analyte of interest that can be detected at a minimum concentration. It is also called the limit of detection of the biosensor. For biosensors to be used in medical and environmental monitoring, they have to measure analytes in ng/ml or fg/ml concentrations to confirm their presence in samples.
5. **Linearity of biosensor:** This feature of the biosensor determines the accuracy of the response that has been measured on a straight line. Linearity is obtained from a series set of analyte measurements with different concentrations. Mathematically it is represented using linear equation ($y = mc$), c is the concentration of the analyte, m is the sensitivity of the biosensor and y is the output of the signal. The biosensor's linearity and the resolution can be related, which is the smallest change observed in the concentration of the analytes that brings a change to the biosensor. A resolution of the biosensor is needed because the analyte concentration is measured over a wide working range. The linear range is associated with the biosensor's linearity, which responds to the analytes concentration's linear changes.
6. The fabricated biosensor should be portable, cheap, and global in every environment (Bhalla et al., 2016; Gan et al., 2014).

2.2.4 The advantages of Biosensors

1. **Real-Time or Rapid Analysis:** The Biosensors are employed to immediately detect analytes and offer rapid or real-time information during analysis. This information is used to check for corrective measures before the products analysed are processed further for use.
2. **The Point of Care devices:** The Biosensors are fabricated for diagnostic testings, which forms the platform for molecular analysis or experiments.

3. **Continuous Flow Analysis:** This offers an advantage for the biosensor to allow them to be used for bulk liquid analysis. The liquids are injected into the biosensor's flow cell or column that allows for continuous monitoring of the analytes as they bind to the sensor, enhancing the efficiency of the analytes.
4. **Miniaturization:** Biosensors have the advantage of being miniaturized into other equipment where they are used in different applications and fields, either *in vivo* or *in vitro* detection.
5. **Control and Automation:** This is the ability of the biosensors to be integrated into online platforms to provide real-time monitoring during analysis that gives information about multiple parameters during a process for better control and automation (Zeng & Xiao, 2017).

2.2.5 Application of Biosensors

Biosensors can be used in different applications to improve the standard of life. They can detect diseases, food analysis, drug discovery, environmental monitoring and defence. The biosensors major application is in detecting biomolecules that serve as indicators of diseases or targets for a drug. Electrochemical biosensors are used as a clinical tool to detect biomarkers for protein cancer. The electrochemical biosensors can detect Food quality, food safety, traceability, and nutritional value. They are also used in the monitoring of environmental pollution. Some biosensors are used for short term monitoring which is rapid and easily disposable. In contrast, some are used for long term monitoring which takes few hours to several days. They are also used to detect biological and chemical agents that are toxic; they are also used in artificial implantable devices, prosthetics, and sewage epidemiology (Bhalla et al., 2016) (Figure 2.6).

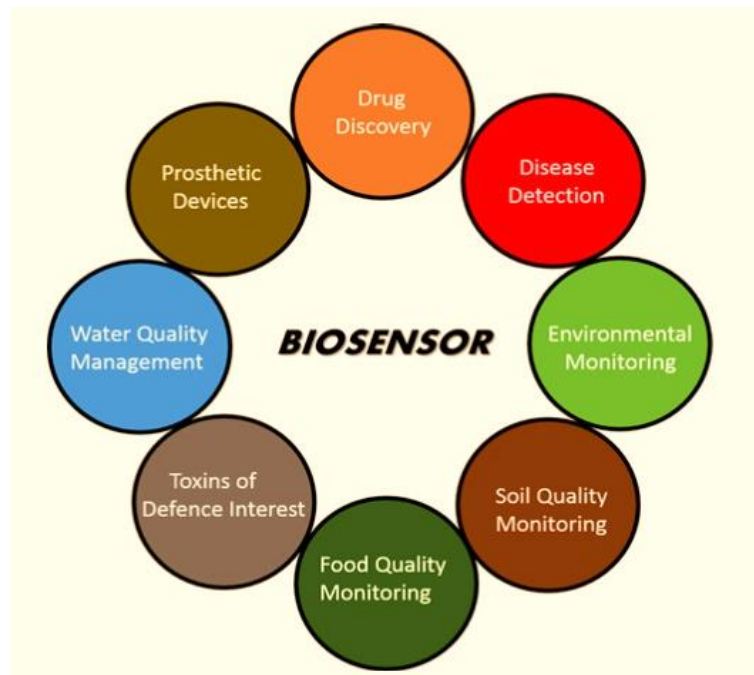


Figure 2.6. Major areas of application of Biosensors

2.2.6 Classification of Biosensors

The biosensors are divided into direct recognition and indirect recognition sensors (Figure 2.7).

1. The direct recognition sensors measure biological agents directly. The indirect ones depend on secondary elements like fluorescent tags or enzymes. There are several types in each group of biosensors, which are optical, electrochemical, mechanical transducers. The choice of a biosensor depends on several factors such as the area used, the type of molecule incorporated, its sensitivity, its cost, rapid detection time and the number of channels measured (Zeng & Xiao, 2017).

The Direct Label-Free Detection Biosensors: These sensors have a platform where biological molecules interact directly and are measured in real-time. They use non-catalytic ligands like antibodies and cell receptors to measure direct physical changes, including mechanical, electrical and optical. They are activated by the interaction of biological molecules, which do not require additional labelled molecules for detection. The most common types of these sensors are optical biosensors, including resonant mirror sensors and surface plasmon resonance (SPR) sensors. They use evanescent

waves produced when a focused beam of light on a surface yields total reflection. The non-optical direct detection sensors have the quartz resonator transducer, which measures the resonant frequency of an oscillating piezoelectric crystal when it changes. This function is used when an analyte binds to the surface of the crystal, such as in microelectrochemical systems (MEMS) and field-effect transistor (FET) biosensors (Zeng & Xiao, 2017).

Indirect Label-Based Detection Biosensors: These sensors use secondary elements and catalytic elements such as enzymes to function during measurements. The enzymes are tagged fluorescently to antibodies, which enhances the detection ability of the sensor.

2. Indirect detection biosensors: These types of sensors measure the oxidation and reduction of compounds on the secondary ligand. Electrochemical transducers are types of sensors used for direct detection biosensors to detect ions in a solution due to changes in electric current when an analyte is oxidized or reduced. Indirect detection of biosensors can also be combined with direct detection biosensors to increase their sensitivity or validate their results (Zeng & Xiao, 2017).

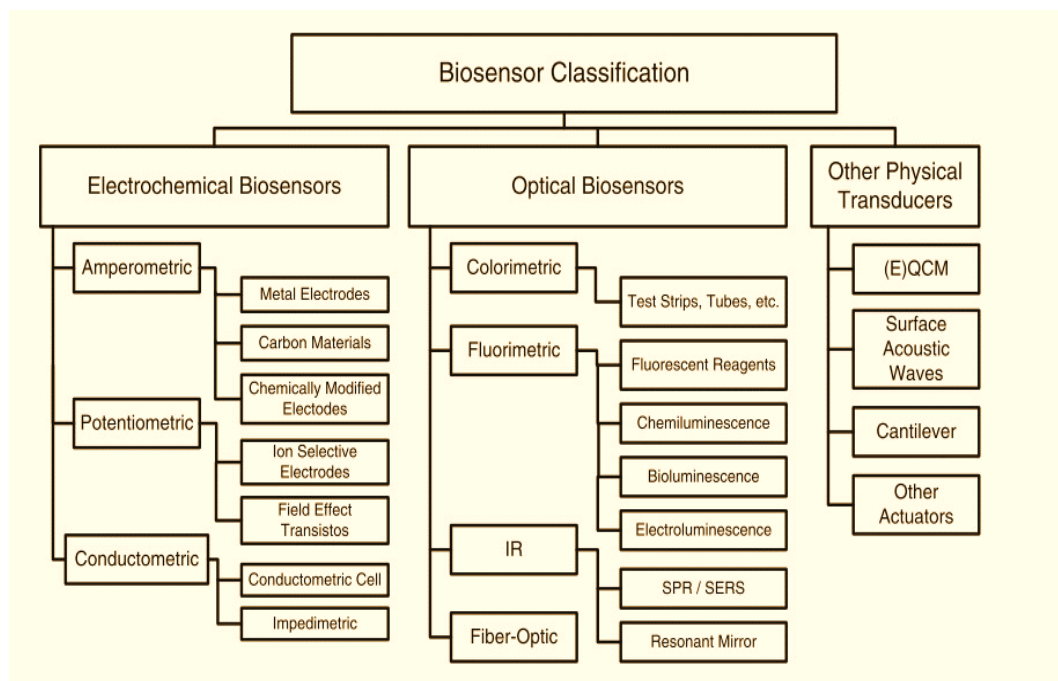


Figure 2.7. Classification of Biosensors

2.2.7 Challenges with Biosensors

The development of Biosensors has improved over the 50 years. There has been tremendous progress and contributions in the academic field, too, over the last 10 years. Few of these biosensors have been used globally with success rates. The biosensors that have been commercially used successfully are the electrochemical glucose biosensors and the biosensors for lateral flow pregnancy tests. Several factors limit the manufacture of biosensors for commercial use because of the difficulties of translating academic scientific research into prototypes by industries to be used commercially. The difficulty of scientists who have a background in biosensors to engage with other scientists from other disciplines such as engineering fabricate biosensors. There is difficulty finding agencies that will fund the academic research peer-reviewed and proposed for commercial production. There is also scientific politics that cause conflicts of interest. The biosensors research should aim at fabricating biosensor devices that can be used for testing and measurements. Commercially producing a biosensor takes a long time from the proof of concept shown in academic research. Other issues that affect the biosensors are finding the market that is interested in the consumption of biosensor. The performance test of the biosensor for a long time is highly recommended, and its storage for about six months is the minimum time required for commercial applications. Great interest is generated between academia and engineering scientists to overcome such challenges, and more commercial biosensors are developed (Bhalla et al., 2016).

2.3 Electrochemical Biosensors

Electrochemical biosensors are the type of biosensors, which detects analytes of interest using electrochemical transducers. Electrochemical transducers are chemically modified electrodes and are used as electrode conducting, semi-conducting or ionic conducting materials. The different types of electrochemical biosensors (Table 2.1) are based on their transducers (Dudok de Wit, 1987).

Table 2.1 Types of Electrochemical Biosensors

Measurement type	Transducer	Transducer analyte
1. Potentiometric	Ion-selective electrode (ISE); glass electrode; gas electrode; metal electrode	K^+ , Cl^- , Ca^{2+} , F^- H^+ , Na^+ ...; CO_2 , NH_3 ; redox species
2. Amperometric	Metal or carbon electrode; chemically modified electrodes (CME)	O_2 , sugars, alcohols ...; sugars, alcohols, phenols, oligonucleotides ...
3. Conductometric, impedimetric	Interdigitated electrodes; metal electrode	Urea, charged species, oligonucleotides ...
4. Ion charge or field effect	Ion-sensitive field-effect transistor (ISFET); enzyme FET (ENFET)	H^+ , K^+ ...

The electrochemical biosensors use principles that depend on the consumption of the chemical species generated in the interaction of the biologically active substance and a substrate in a reaction. The transducer of the electrochemical biosensor measures the signals observed from the chemical or biological reaction. The differences in the types of electrochemical biosensors detectors are based on their working principles to measure biochemical reactions in solution. The design of an electrochemical biosensor has advantages based on its fast response, how simple they are, low cost of production compared to piezoelectric, calorimetric and optical biosensors, which are suitable to detect substrate based on their material, size and geometry (Dudok de Wit, 1987).

2.3.1 Electrochemical DNA Biosensors

The electrochemical DNA biosensor is a device that incorporates nucleic acid or uses DNA as a biological recognition element to function as the physicochemical transducer, which detects the signal. This transducer is an electrode that is chemically modified by nucleic acid, leading to DNA testing during analysis to detect the decrease in guanine signal from the voltammogram (Labuda, 2012).

2.3.2 Aim of Electrochemical DNA Biosensor

Clark and Lyons designed and invented the first electrochemical DNA biosensor in 1962, which was based on monitoring the hybridization of DNA to detect genetic diseases or to detect the amount of hazardous compounds. They interact with the DNA by causing damage to it. Genosensors are examples of electrochemical DNA biosensors used to detect and determine DNA sequences based on the principle of hybridization of the DNA sequences or the interactions between compounds and DNA. Knowledge and understanding of the DNA structure and all its possible binding sites will help design electrochemical DNA biosensors (Ozkan-Ariksoysal et al., 2012).

2.3.3 The DNA structure

DNA is the most important biological target used for electrochemical DNA biosensors analysis of compounds that pose a hazard to the DNA. Different molecules are found to bind to the DNA. Their interaction with the DNA and the damage they cause to the DNA damage leads to their electrochemical detection. The DNA has binding sites, which encourages binding these molecules to the DNA. The DNA molecules are localized in the chromosomes of eukaryotic cells as large polymers and have a backbone of sugars and phosphates residues. They contain five-carbon sugar (Figure 2.8) called deoxyribose sugars linked by a covalent bond to the phosphodiester bridge. The nitrogenous base is covalently bonded to carbon one or one prime of the sugar, and they are the Cytosine (C), Guanine (G), Thymine (T) and Adenine (A). These bases are classified broadly into purines and pyrimidines. Guanine and Adenine belong to the purine group, which atoms of carbon and nitrogen carrying have two heterocyclic rings. The Thymine and Cytosine belong to the pyrimidine group and possess a single ring. The base and the sugar contain nucleoside where the phosphate group attaches to it to form a nucleotide. The phosphate groups contain negative charges. The different bonds that contribute to the stability of the DNA are the strong covalent bonds and non-covalent bonds, which are the ionic bonds, hydrophobic forces, hydrogen bonds, and Van der Waals forces. The covalent bonds are stronger than the non-covalent bonds. However, the strength of the non-covalent bonds increases in aqueous media due to the formation of the hydrogen bonds between the oxygen atom that is partially negative and the hydrogen

atom of water that is partially positive. These bonds can be broken reversibly by heating them, and the covalent bonds cannot be easily broken by heat. All these interactions taking place molecularly in the living cells play an important role in their biological function. These same molecular behaviour and interactions are the basis for the development of biosensor devices. The duplex structure of the DNA gives it stability, and the hydrogen bonds between the bases also protect the DNA. The hydrogen bonds can be found within the bases of DNA or RNA. Planar compounds have aromatic rings that help them bind to the DNA through intercalation, which occurs between the adjacent base pairs of the DNA or the hydrogen bonds between the base pairs (Ozkan-Ariksoysal et al., 2012).

Living cells have DNAs, and most of the DNAs in the cells have B-DNA. However, DNAs possess various helical structures, which are A-DNA or Z-DNA. The helices of the A and B forms of the DNAs are both right-handed and are in the clockwise direction. Their turns contain eleven base pairs for the (A form) and ten base pairs for the (B form) of the DNA. The left-handed helices have twelve base pairs per turn in the Z-DNA form (Ozkan-Ariksoysal et al., 2012). The distance between each turn of the helix is called a pitch, and it is 3.4nm long, where each 1pitch (3.4nm) = length of minor groove + length of major groove. The dsDNA has an antiparallel nature due to the double strands linking 3' carbon to 5' carbon atom in the opposite direction. Watson and Crick model for the complementary rule for bases states that the composition of the DNA bases shows that the total amount of Guanine = total amount of Cytosine and the same with a total amount of Adenine = total amount of Thymine (Ozkan-Ariksoysal et al., 2012).

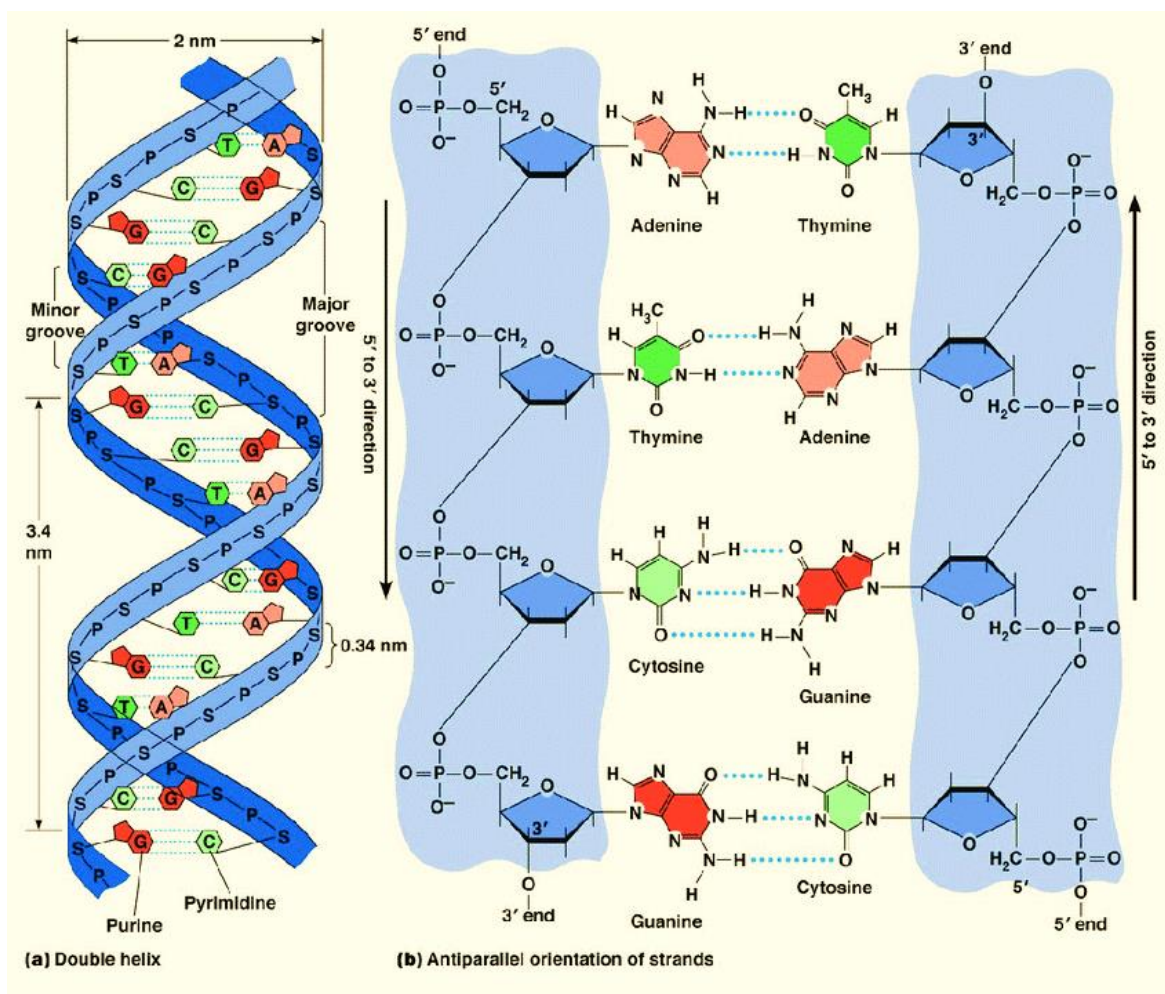


Figure 2.8. Diagram of DNA structure

2.3.4 Natural Electroanalytical Characteristics of DNA

The DNA bases have electroactive properties, which makes them able to undergo oxidation and reduction (Figure 2.9). In contrast, the sugar and phosphate components of the DNA components are electro-inactive. This electroactivity of the purines and the pyrimidines were discovered in 1958 by Emil Palecek. Different works have been reported on the oxidation and reduction of A, G and C. The reduction of the DNA signals of A and C at mercury were also reported. DNA determination at the surface of carbon-based electrodes has also been reported. However, they are less sensitive to changes in the structure of DNA. Some were used to detect G and A while others C and A (Table 2.2). In the last decade, different voltammetric approaches have been employed. They were sensitive to both single-stranded

DNA and double-stranded DNA at the surface of electrodes compared to the analysis of DNA at mercury electrodes surface (Ozkan-Ariksoysal et al., 2012).

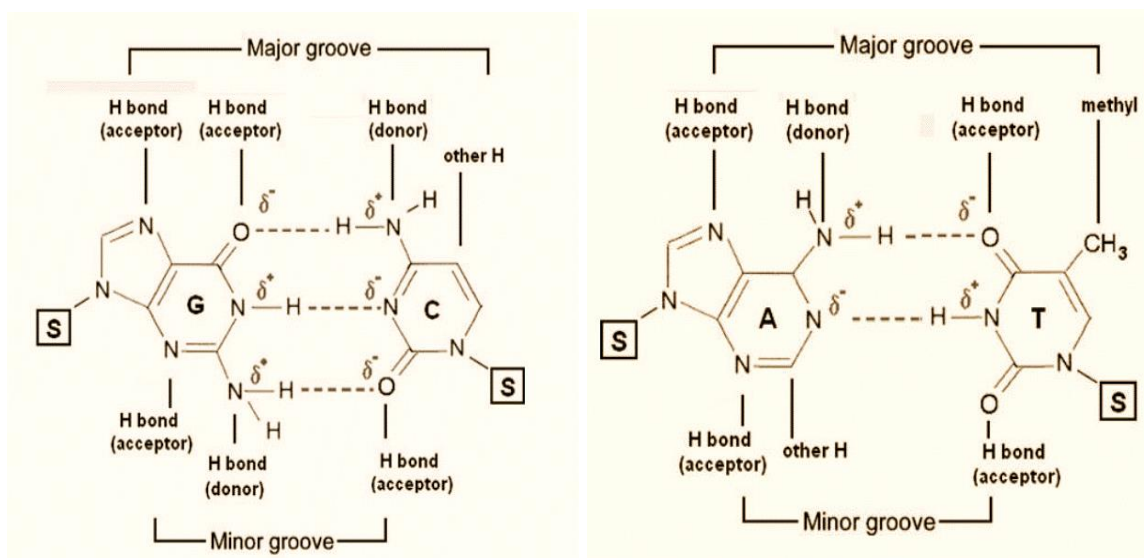


Figure 2.9. Grooves of DNA structure

Table 2.2 The electroactivity of DNA bases and their detections conditions

Method	Base	Ox/red	Electrode	Peak Potential (V) vs. SCE	pH
DPV	G	Ox	carbon	+1.0	4.8
DPV	G	Ox	carbon	+0.8, +0.9	7.4
CV	G	Ox for reduced product	HMDE	-0.3	
DPP	A	Red	DME	-1.5	Acid/neutral
DPV	A	Ox	carbon	+1.2	4.8
DPP	C	Red	HMDE	-1.5	Acid/neutral

2.3.5 Types of DNA Immobilization Methodologies onto Sensor Surfaces

The early applications of electrochemical DNA biosensors are in the solution phase. In the last ten years, researchers have focused on using synthetic short DNA fragments that have known sequences related to viruses and bacteria. They used them on the sensor's surface by

utilizing their sensitivity to detect the target analyte of DNA. A typical sequence of DNA used as a probe for detecting its complementary target sequence is about 15 to 25 base pairs long. The biosensor can also detect other DNA products like the calf fish sperm DNA, calf thymus DNA. The damage to dsDNA has been employed for many sensor applications; it is based on the electrochemical signal observed from the guanine base of the nucleic acids. The steps of immobilizing DNA are important in determining the performance of electrochemical genosensor; this is sensitive for interactions between DNA-compounds or DNA-DNA (Ozkan-Ariksoysal et al., 2012).

2.3.5.1 Adsorption Method

The adsorption method is the easiest immobilization method for DNA or probes onto transducers of carbon origin. Also, it operates for both the application of controlled potential or the wet adsorption method, which does not need applied potential. The adsorption immobilization method does not have time-consuming experimental steps. It does not need special reagents and uses less expensive labelled nucleic acids. In this method, DNA can be bound weakly to the surface of the transducers and can be removed when rinsed because they are non-covalently bound (Ozkan-Ariksoysal et al., 2012).

2.3.5.2 Covalent Binding to Activated and Non-activated Surfaces

The covalent binding of the DNA to electrode surfaces is irreversible, leading to the complete inhibition of DNA function and cell death. Covalent binders have an advantage by conferring high binding strength and can cause damage to the DNA backbone, which affects the process of transcription and replication. The covalent binding method to DNA is divided into three modes: replacing the bases, alkylation of the bases, and then inter and intra DNA strand cross-linking. The most common anticancer drug used as a covalent binder is cisplatin; other anticancer drugs are Mitomycin C, Anthramycin and alkylating agents like the temozolomide, chlorambucil and nimustine (Aleksić & Kapetanović, 2014).

2.4 DNA-Compound Interactions

The identification of the DNA-Compound interactions involves several methods. However, voltammetric methods are also used to identify where the DNA strand was damaged and broken. It also determines the compounds that bind electro-actively to the DNA, either through a covalent or non-covalent bond. There has been an extensive study of DNA-compound interactions in the past 30 years, which has attracted attention because of its important role in the living organisms towards achieving analysis that is inexpensive and rapid in molecular biology. The characteristics of electrochemical DNA biosensors have been utilized in this scientific area, with different voltammetric methods developed to determine the interactions (Ozkan-Ariksoysal et al., 2012).

The Non-covalent bonds between drugs and DNA are more desirable to the covalent bonds. They are reversible, which is important in drug metabolism and its potentially toxic effects. The interaction of DNA to other compounds by covalent bonds can modify the DNA structure, its conformation, torsional tension, interrupt protein – DNA interaction, and potentially lead to breakage and damage of the DNA strands. Molecular recognition is the principle by which DNA chemistry operates, where molecules recognize other molecules selectively. They do this through hydrogen bonding, electrostatic interaction, and van der Waals forces interaction. The compounds that interact non-covalently with the DNA are classified as intercalating agents, cross-linking agents, external binders, minor and major groove binders (Aleksić & Kapetanović, 2014).

2.4.1 Electrostatic Interactions

Metal ions interact with the DNA through electrostatic bonds called external associations that are non-specific. Compounds can bind covalently or non-covalently to the phosphate backbone that is negatively charged or interact with the parts of the bases that donates an electron. The strength of these interactions is affected by the charge of the compounds, total size of the ions, hydrophilic and hydrophobic structure which affects the DNA double structure by causing damage to it (Aleksić & Kapetanović, 2014; Ozkan-Ariksoysal et al., 2012).

2.4.2 Groove Binding Interactions

The DNA structure has minor grooves, which are the attractive sites for binding small, flat and positively charged molecules that are flexible and electrostatic; these are the metal complexes. The compound mitramycin binds to the bases of the minor grooves through hydrogen bonding and electrostatic interactions between minor grooves bases and phosphate groups. Compounds that bind to the minor grooves possess special chemical structures, which contain aromatic heterocycles linked by amide or vinyl groups, which have positively charged points. This results in steric hindrances that make only part of the metal complexes bound to the minor grooves. When the compounds finally binds to the DNA, van der Waals forces enables the newly formed structure to be held in a stable position. However, the DNA is not affected significantly when these compounds bind to the minor grooves. Cis-platins are small compounds that bind to the major grooves of DNA through hydrogen bonding. The compound was used to detect damage that occurs in the DNA. It bounds covalently to the purine bases of the DNA, on the N7 of the guanine base and the major groove side. Other small compounds that bind to the major groove side of the DNA are methyl green, antitumor agents like the acridine carboxamide skeleton, aminoglycoside antibiotics tobramycin, pluramycins, aflatoxins, azinomycins (Aleksić & Kapetanović, 2014; Ozkan-Ariksoysal et al., 2012).

2.4.3 External Binders

The type of binding found between these molecules and the DNA is electrostatic. The DNA phosphate backbone serves as a position where some ligands can form stacking non-specific interactions. The ligands self-associate through forming higher order aggregates that stack on the anionic DNA backbone, which happens to minimize charge-charge repulsion between the ligand molecules. Some metal complexes use the process of external binding to interact with the DNA as seen in $[\text{Ru}(\text{bpy})_3]^{2+}$ as the luminescence is enhanced through the complex as it binds to the DNA strongly binding using ionic strength. Other examples of such binders are the Mg^{2+} (Aleksić & Kapetanović, 2014).

2.4.4 Metal-Drug Complexes

DNA has served as an important target for metal complexes. The transition metals complexes use covalent and non-covalent bonds to bind to DNA. The ligand of the metal complex, through covalent bonding, replaces the nitrogen base of DNA. While the interactions that occur through non-covalent bonding to the DNA include intercalation, electrostatic interactions and groove binding of the metal complexes along outside of DNA helix and along the major and minor groove. Some of the complexes that react with DNA are the quinolone antibiotics, and do they provide three binding sites which are distinctive for the interaction quinolone metal complexes; these sites are the groove binding sites, electrostatic binding that occurs on the phosphate groups and the intercalation interaction (Aleksić & Kapetanović, 2014)

2.4.5 Intercalation Mode

Intercalators are molecules that stack perpendicularly to the backbone of the DNA without forming covalent bonds and do not break up the hydrogen bonds between the DNA bases (Figure 2.10). The description of the term intercalation was reported in 1982, where it was observed that intercalators have a high affinity to dsDNA. They are located between the bases pairs because they have planar aromatic rings, as in antibiotics like daunomycin which damages the deoxyribose phosphate structures. Intercalators are molecules that are stabilized by π -bonds within the bases; they cause stabilization, lengthening, stiffening and unwinding of the double helix structure of the DNA. They have constants that bind to DNA. When they have interacted with the double structure of the DNA, they cause a change in the DNA form, which produces favourable free energy from the complex formation. The number of aromatic moieties determines whether intercalators are either mono or bi-functional. Examples of mono-intercalators are the acridine derivatives like aminacrine, proflavine, acriflavine, ethacridine, and other substances like ADR daunomycin have six-membered rings and are attached to positions seven and nine. Bis-intercalators such as Echinomycin exhibit two intercalative interactions by covalent bonding between the DNA and the aromatic rings of the molecule. Other mediators of electrochemical hybridization used as

intercalators are the Meldola's blue (MDB) and Reid et al. reported on its intercalation mechanism (Ozkan-Ariksoysal et al., 2012).

The general phenomenon involved in intercalating agents has to do with the aromatic part of a drug molecule that positions within the base pairs of the DNA through hydrophobic interactions. These interactions favour the hydrophobic and aromatic side chains within the aromatic environment of the base pairs of DNA. These agents cause strong structural changes to the DNA molecule and increase the distance between the adjacent base pairs. The fitting of intercalators between base pairs is dependent on the DNA being able to open a space between the base pairs. The intercalation process causes the sugar-phosphate backbone to unwind the double helix structure, thus causing conformational changes to the DNA. The stacking interactions between the intercalating molecule and the bases are the major factors that stabilize the formed complex. Bi-functional intercalators interact with the DNA molecule first through intramolecular cross-linking when aromatic moieties intercalate with the same DNA molecule. They interact with two separate DNA molecules through intermolecular cross-linking. Other intercalators, called multi-intercalators, contain three or more rings as they bind to the DNA. This feature causes their binding constants to be high, and their therapeutic activity increased (Aleksić & Kapetanović, 2014).

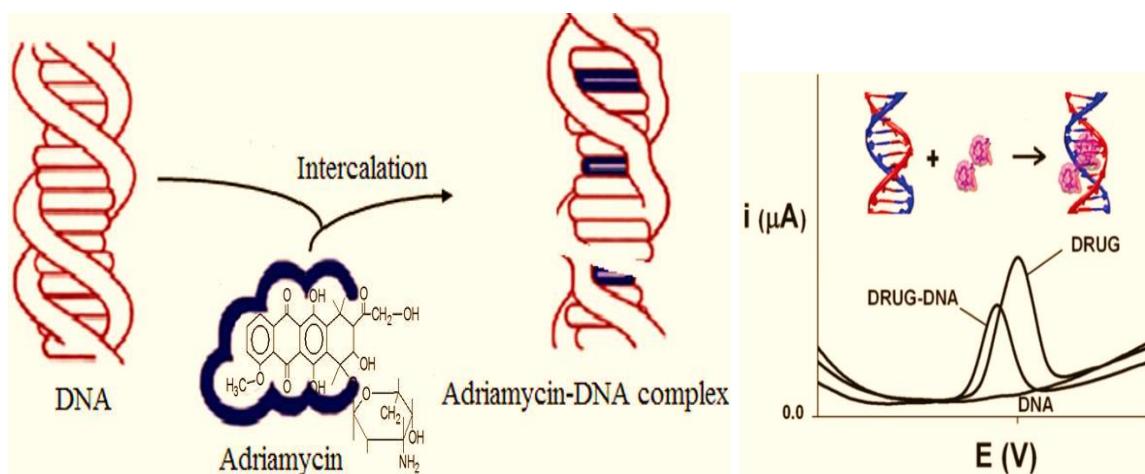


Figure 2.10. Intercalation Mode

2.4.6 Interaction in aqueous medium

The DNA is poly-anion inside an aqueous solution; this feature allows it to attract charged counter ions such as the Na^+ , Ca^{2+} or Mg^{2+} . These counter ions are associated with drug molecules because of the charge they possess. The ions on the drug molecules lie close to the charged groups of the molecule and are solvated partially. When the interaction process is initiated and the binding occurs, the solvent from the DNA and the drugs are displaced. This will result in the DNA's charges being compensated partially. The drug is fully solvated as the counter ions are released into the bulk solvent. The process of hydration and dehydration interaction also occurs during drug-solvent interaction and DNA-solvent interaction. The double helix structure of the DNA assumes a stable form when it complexes with other intercalating compounds. This indicates a reduction in the heat of denaturation compared to the DNA that has not interacted with any compound. There is no covalent bond in this interaction because the interaction involved is through an equilibrium process. The constants in the process, which are the free and bound part of the drug, can be measured (Aleksić & Kapetanović, 2014).

2.5 The Techniques used to study the interactions between Compounds and DNA

The interaction of the mechanism between compounds and DNA can be detected inside the solution or at the surface of the sensor (Figure 2.11) when there is an affinity of the compound to the DNA when oxidation and reduction occurs or when there is an intrinsic oxidation signal of the bases of guanine and adenine.

2.5.1 Label-free detection of DNA based on intrinsic signals (direct detection)

The changes that occur to DNA caused by chemicals or their metabolites are important for carcinogenic processes. Mutations and carcinogenesis are first induced by the interaction of the carcinogens, chemicals, and drugs metabolized with the cellular DNA. When the DNA is damaged, it can cause genetic mutations, affecting many functions in the living organism. This knowledge leads to the detection and quantification of the interaction between the

compound, DNA and its adducts which have major significance in cancer research (Ozkan-Ariksoysal et al., 2012).

During the detection, the increase or decrease in the guanine signal after oxidation helps in the monitoring of the interactions occurring between the DNA-molecule electrochemically, which gives an idea about the damage caused to the DNA. When the peak is formed newly from the voltammogram, it shows that an adduct has been formed. Synthetic polynucleotides sequences of the guanine and adenine bases are employed to show how DNA undergoes interaction with a compound. The study of the interactions between the compound and DNA is suggested under three assumptions: (a) The guanine peak height decreases due to the oxidizable groups of the guanine being covered during the DNA-molecule interaction. (b) The guanine bases might be damaged due to the compound bound to the DNA. (c) The compound and the DNA interaction result in the charge transfer of the DNA properties changing, which could decrease the guanine signal at the surface of the electrodes (Ozkan-Ariksoysal et al., 2012).

Electrochemical detection schemes for compound-DNA interactions

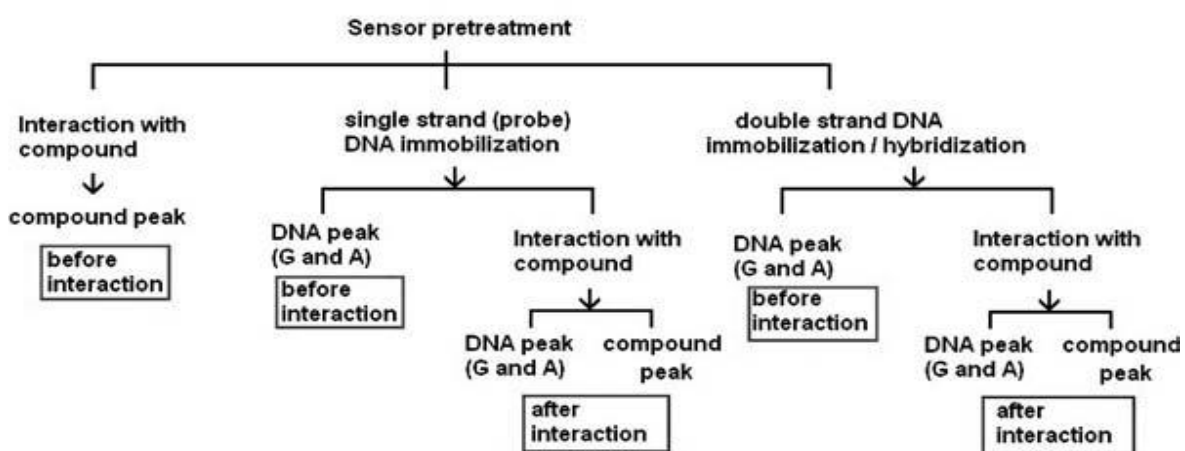


Figure 2.11 shows the detection of interactions between Compound and the DNA

2.5.2 The detection of compound-based reaction

The detection of the electrochemical interaction between chemicals and DNA begins with identifying the potentials in the reduction and oxidation reaction of the compounds using the cyclic voltammetry procedure. This is generally applied when obtaining the peaks of both

DNA and the compound. The guanine base has a redox potential of +1.0 V. Also, sometimes it does not lie at the same peak position in the voltammogram. The best way to make evaluations for such interactions is to measure the signals of both the bare and DNA-modified compounds at the surface of the electrode. In other applications of the detection of compound-DNA interactions (Figure 2.11), the compound molecules can serve as indicators of DNA hybridization because of the different behaviours of the dsDNA and ssDNA in their binding to the molecules. This understanding offers the basis for the new drugs and DNA sensors to be developed, which can later be converted into microchip devices. Some indicators contain electroactive compounds used in electrochemical DNA biosensor; these compounds are methylene blue (MB), ferrocenylnaphthalene diimide, and other metal complexes, which are osmium, cobalt phenanthroline, and ruthenium. There are other reports where electroactive intercalators are covalently bound to the DNA to detect different kinds of single-base nucleotide changes. There are redox-active markers of DNA which include tris-bipyridine complexes of osmium or ruthenium, ferrocene, amino tags and nitro-phenyl tags, which were applied for the detection of SNPs. The covalent or non-covalent binding labels have been utilized on DNA using carbon-based transducers (Ozkan-Ariksoysal et al., 2012).

2.5.3 DNA modified electrode

The fabrication of electrochemical DNA biosensors monitors the interactions between drugs and DNA and the immobilization of the DNA on the electrode surface. The sensors are used for accessing DNA to drugs in solution and can influence the affinity of drug binding. The process of DNA immobilization onto the electrode surface is through a covalent bond, electrostatic interaction or trapping the molecules inside the polymer's layer. The DNA is located at the surface of the electrode, where it is accessible to the binding molecule, which is the target in the solution. The covalent binding of the DNA to the electrode surface makes the DNA easily detected by the drug compounds inside the solution. The guanine and adenine bases oxidation can change when the DNA binds to the drugs. The DNA immobilized throughout a polymer is less easily accessible in solution. When the interaction happens, the guanine and adenine bases are drawn to the surface of the electrode for electron transfer to occur (Ozkan-Ariksoysal et al., 2012; Rauf et al., 2005).

2.5.4 Drug-modified electrode

In this method, the drug is immobilized onto the electrode's surface, after which the drug signals are then measured, observed changes from the interaction of the drug with the DNA are also measured. This is observed in the interaction between adriamycin and DNA (Ozkan-Ariksoysal et al., 2012; Rauf et al., 2005).

2.5.5 Interaction in Solution Phase

The drug and the DNA are placed in the same solution and given some time for interaction. The signals of the drug and DNA are then monitored and compared with the signals of the DNA alone and the drug alone in the solution. Epirubicin in the solution phase was determined by a glassy carbon electrode using a single sweep cyclic voltammetry (Ozkan-Ariksoysal et al., 2012; Rauf et al., 2005).

The working principle of electrochemical methods : Electrochemical methods can understand the mechanism behind anticancer drug interaction with DNA. This depends mainly on the electrochemical behaviour of the anticancer drug, whether in the presence or absence of the DNA. Different kinds of electrode materials are used to investigate the interaction between DNA and anticancer drugs. These are carbon paste electrode, hanging mercury drop electrode (HDME), gold electrodes, pencil graphite electrodes (PGE), glassy carbon electrode (GCE) and screen -printed electrodes (SPEs). In the electrochemical procedures, there are three kinds of electrode system used: the working electrode, a reference electrode (Ag/AgCl or saturated calomel electrode) and auxiliary electrode (Pt wire). Different electrochemical techniques are applied to detect anticancer-DNA interactions and electrochemical methods: CV, SQWV, DPV and chronoamperometry. While the mechanism of interaction between the DNA and the compounds can be done in the solution phase, DNA modified electrode or drug modified electrode (Rauf et al., 2005).

2.5.7 Calculations about Compound-DNA Interactions

There are different approaches used to investigate the mechanism that occurs through the interaction of a compound with DNA. These are approaches that can be used for practical applications in measuring the guanine signal and the compound signal. The changes occurring in the guanine peaks are generally used for the calculations of the electrochemical DNA biosensors because the guanine base of the DNA is the base that is easily oxidized to the other bases. They are also used for analysis as one of the major criteria for detecting DNA-drug interactions during voltammetry. The current ratio of the guanine (S%) is used to evaluate the decrease observed in the guanine signal when DNA interacts with other compounds through the equation:

$$S\% = (S_s/S_b) \times 100 \quad 2.1$$

S_s represents the signal ratio of guanine peak height after interaction with a compound. S_b represents the magnitude of the guanine signal after the interaction with the buffer used to prepare the compound.

The DPV signal obtained from the oxidized guanine is 100% when a compound is absent. Suppose the value obtained after the interaction of a compound with the DNA is $S > 85\%$. In that case, the molecule that the DNA interacted with is nontoxic; if the value obtained for S% is between 50 and 85, then the compound is toxic moderately. However, when the value obtained for S% is $S < 50\%$, then the compound obtained is termed toxic. To determine the idea behind the interaction mechanism that occurred between DNA and a compound, the partition coefficient value needs to be considered. The calculation of the partition coefficient is taken from the bare electrodes, modified probe and hybrid probe using current signals with the given equation:

$$\text{Partition coefficient} = \text{Compound}_{\text{bound}}/\text{Compound}_{\text{free}} = |(i_{\text{bound}} - i_{\text{free}})/i_{\text{free}}| \quad 2.2$$

Here i_{free} represents the peak height of a compound at the bare electrode. i_{bound} represents the peak current of an oxidized compound obtained from a modified probe (ssDNA) or modified electrodes having the hybrid (dsDNA). Suppose there is a higher value obtained from the calculation of the transducer modified with ssDNA more than than the one modified

with dsDNA. In that case, this shows that the molecule has a high affinity to the structure of ssDNA. In other words, the compound partitions more into the ssDNA microenvironment than the one of dsDNA as a result of these calculations (Ozkan-Ariksoysal et al., 2012).

2.6 Electrochemistry

The field of electrochemistry is a branch of chemistry concerned with the interrelation of electrical and chemical effects. This field deals with the chemical changes caused by the passage of electric current and the production of electrical energy resulting from chemical reactions. The field of electrochemistry covers a huge array of different processes, which are electrophoresis and corrosion, devices such as the fuel cells, electrochromic displays, batteries, electroanalytical sensors, and technologies such as the electroplating of metals and the production of aluminium and chlorine on a large scale (Allen & Larry 2001).

2.6.1 Electrochemical Cells and Reactions

The electrochemical systems involve the processes and factors which affect the charges across the chemical phases within the system. They include the electronic conductor, the electrode, and an ionic conductor, the electrolyte. Charges are transported through the electrode by the movement of the electrons (movement of ions) in the electrolyte phase (Figure 2.12). The materials typically used for electrodes are solid metals such as the platinum and gold, liquid metals such as the mercury and amalgams. Carbon is graphite, semiconductors such as indium-tin-oxide and silicon. The electrolytes that are used frequently in liquid solutions containing ionic species such as the H^+ , Na^+ , and Cl^- are either in water or non-aqueous solvent. The resistance of the electrolyte or solvent that is to be used must be low, which means conductive for the electrochemical use needed. Other less conventional electrolytes are infused with salts such as the $NaCl-KCl$ and ionic conductive polymers such as the nation, polyethylene oxide- $LiClO_4$. There are solid electrolytes such as sodium β -alumina where the charges are carried by mobile sodium ions which move between the aluminium oxide sheets. These systems generally have two electrodes separated by at least one electrolyte phase. They can be measured with a voltmeter that has a high impedance and measured in volts (V) (where $1\text{ V} = 1\text{ joule/coulomb (J/C)}$). This is the measured energy needed between electrodes to move a charge. (Allen & Larry 2001).

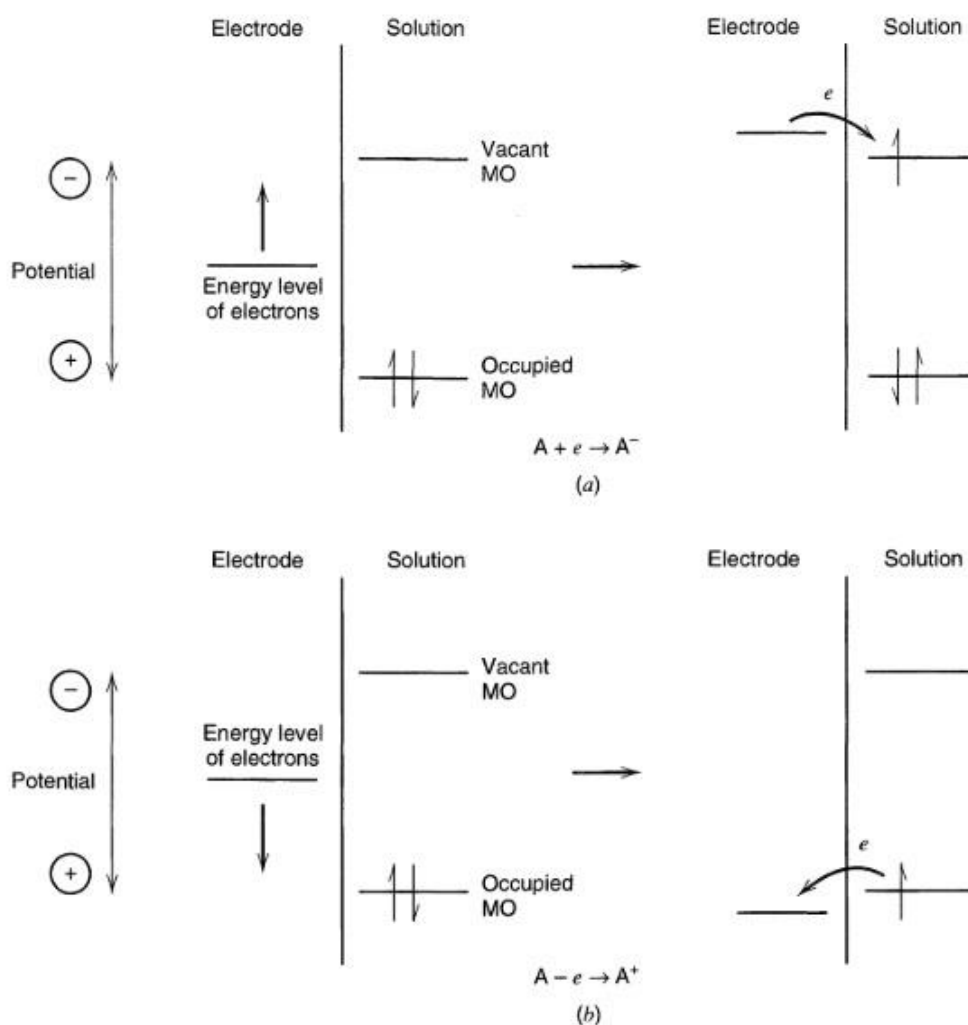


Figure 2.12. Showing reduction and oxidation process of species of electrochemical reactions, A, in solution.

2.6.2 The Processes of Faradaic and Non-faradaic Reactions

Two processes occur at the electrodes. The first occurs by transferring charges across the electrode interface to the solution (Figure 2.13). The transfer of electrons causes oxidation and reduction in an electrochemical process. The reactions are controlled by Faradaic Law, which can be defined as the amount of chemical reaction caused by the flow of current, which is proportional to the amount of electricity passed through the system, called the Faradaic processes. The faradaic processes occur at the electrodes, named charge transfer electrodes. Certain conditions show a range of potential in an interface of electrode and solution. In this reaction, charge transfer reactions are absent because the reactions are

unfavourable thermodynamically or kinetically. The adsorption processes and desorption occurs at the electrode-solution interface, changing as the potential or solution composition changes. These processes that occur are called the non-faradaic processes. Even though charges are not transferred across the interface, external currents can flow when the potential is applied to the electrode area or the solution composition changes. Faradaic and non-Faradaic processes occur when the reactions take place. The faradaic processes are usually the point of interest in the investigation of an electrode reaction, except in studies in the electrode-solution interface, the effects of the non-faradaic processes can be taken into account using electrochemical data to obtain information about the charge transfer and associated reactions (Allen & Larry 2001).

Non-faradaic Processes and the nature of the electrode-solution interface: The electrode at which there is no charge occurring at the metal-solution interface, regardless of its potential by an outside voltage, is called an ideal polarized electrode (IPE). There is no real electrode that can behave as an IPE over the whole potential range available in a solution. In contrast, some of the electrode – solutions systems can approach ideal polarizability over a limited range. An example of IPE is a mercury electrode in contact with a deaerated potassium chloride solution that approaches an IPE behaviour over a potential range of about 2V wide. The behaviour of the electrode-solution interface acts as same as that of the capacitor since the charge cannot cross the IPE interface. A capacitor can be defined as an electrical circuit element composed of two sheets of metal separated by a dielectric material. This is defined by an equation which is:

$$I=CE \qquad \qquad \qquad 2.3$$

where q is the charge stored on the capacitor (in coulombs, C), E is the potential across the capacitor (in volts, V), and C is the capacitance (in farads, F). A continuous accumulation of charge on the metals as potential is applied until q is satisfied in the equation. During the charging process, there is a flow of current. The charge on the capacitor contains electrons in excess on one plate and lacks electrons on the opposite plate (Allen, & Larry, 2001).

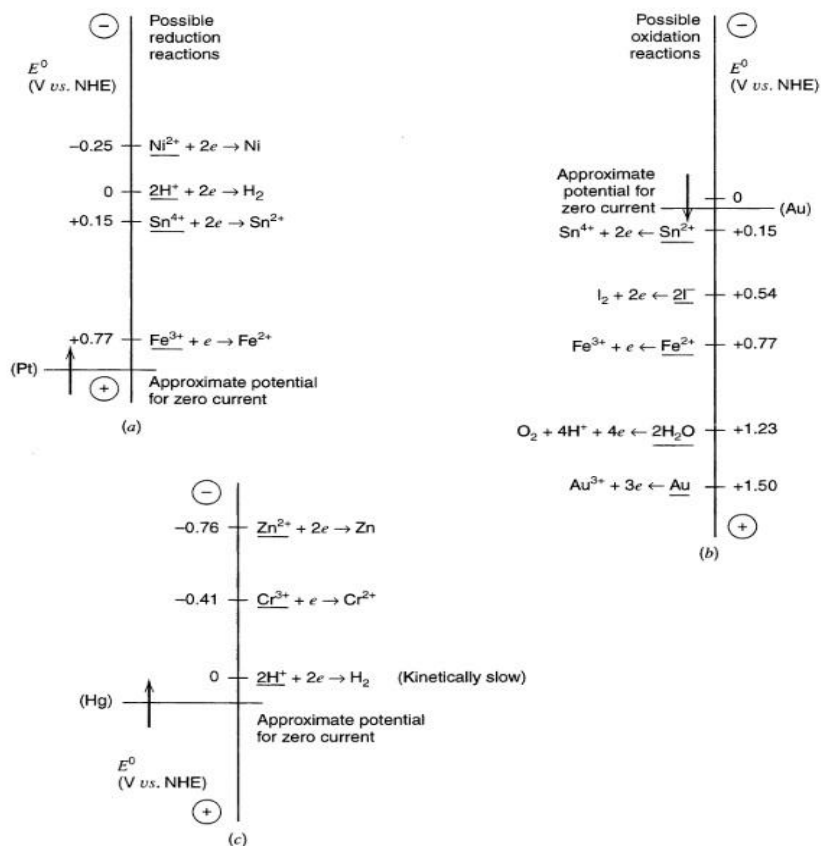


Figure 2.13. Shows the possible potentials that can be reduced at the platinum electrode, at 1 V vs NHE in a solution of 0.01 M which contains Fe³⁺, Sn⁴⁺, and Ni²⁺ in 1 M HCl. It also shows the possible potentials that can be oxidized at the gold electrode at 0.1V vs NHE in a solution of 0.01 M which contains Sn²⁺ and Fe²⁺ in 1 M HI, and finally, possible potentials that can be reduced at mercury electrode in 0.01 M Cr³⁺ and Zn²⁺ in 1 M HCl.

Faradaic Processes and the factors that affect rates of reactions at the electrode: The electrochemical cells found in which faradaic currents are flowing are divided into galvanic or electrolytic cells (Figure 2.14). The galvanic cells are cells in which reactions spontaneously occur at the electrodes when connected by a conductor externally. They are mostly used in the conversion of chemical energy into electrical energy. Commercially they are used primarily as non-rechargeable cells such as in Leclanche Zn-MnO₂ cells and secondarily as rechargeable cells such as in Pb-PbO₂ storage battery and fuel cells such as in H₂-O₂ cells. Electrolytic cells are the type of cells in which the reactions that occur in

them are affected by the imposition of an external voltage greater than the open circuit potential of the cells. These cells are used for carrying out chemical reactions by expending electrical energy. The term electrolysis is defined as the chemical changes that occur during faradaic processes at the surface of the electrode that is in contact with the electrolytes. The electrode on which reductions occur is called the cathode. The electrode on which oxidations occur is called the anode. The current where the electrons cross from the electrode interface to the species in the solution is called the cathodic current. The current flow from solution species into the electrode is called the anodic current. The cathode is negative, and the anode positive in an electrolytic cell. In the galvanic cell, the cathode is positive. The anode is negative (Allen & Larry 2001).

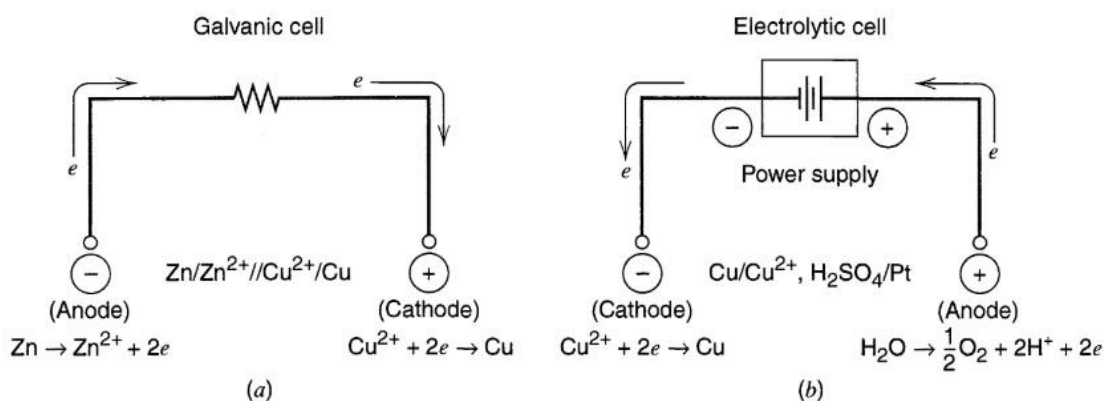


Figure 2.14. shows a Galvanic and electrolytic cell.

Factors that affect reaction rates and current at the electrode surface: The overall electrode reaction, $O + ne \rightleftharpoons R$, is composed of a series of steps (Figure 2.15) that cause the conversion of the dissolved oxidized species, O, to a reduced form, R, also in solution. The processes involved are:

1. The process of mass transfer: The transfer of O from the bulk solution to the surface of the electrode.
2. There is electron transfer at the electrode surface.
3. There are chemical reactions that follow electron transfer, which can be homogeneous or heterogeneous.
4. Other surface reactions occur, such as adsorption, desorption, or crystallization. The rate of the constants for some of the processes that occur is potential dependent. The simplest

reactions that occur only involve the mass transfer of the reactant to the electrode, while heterogeneous electron transfer involves non-adsorbed species and mass transfer of the product to the bulk solution (Allen & Larry 2001).

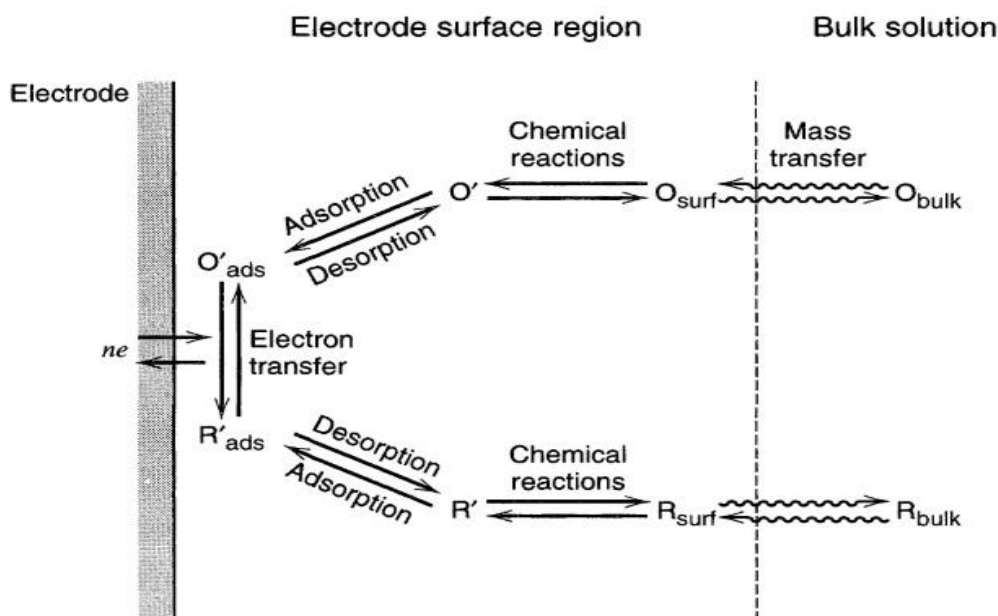


Figure 2.15. Pathway of a general electrode reaction

2.6.3 The Study of reactions at the electrode surface

2.6.3.1 Cyclic Voltammetry

The CV technique is the most used technique for determining qualitative information about electrochemical reactions (Figure 2.16). This method provides information about the thermodynamics of the redox processes on the kinetics of heterogeneous electron-transfer reactions and information on coupled chemical reactions or adsorption processes. The method offers rapid analysis and determination of the redox potentials of the electroactive species. Also, it offers a convenient way of evaluating the effect of media on the redox process. The method involves applying a linear potential to a stationary working electrode in an unstirred solution using a triangular waveform. The potentiostat used for measuring the current is from the applied potential during a potential sweep. The measurement results

are shown on a plot called cyclic voltammogram, where the current is plotted against potential (Wang, 2001).

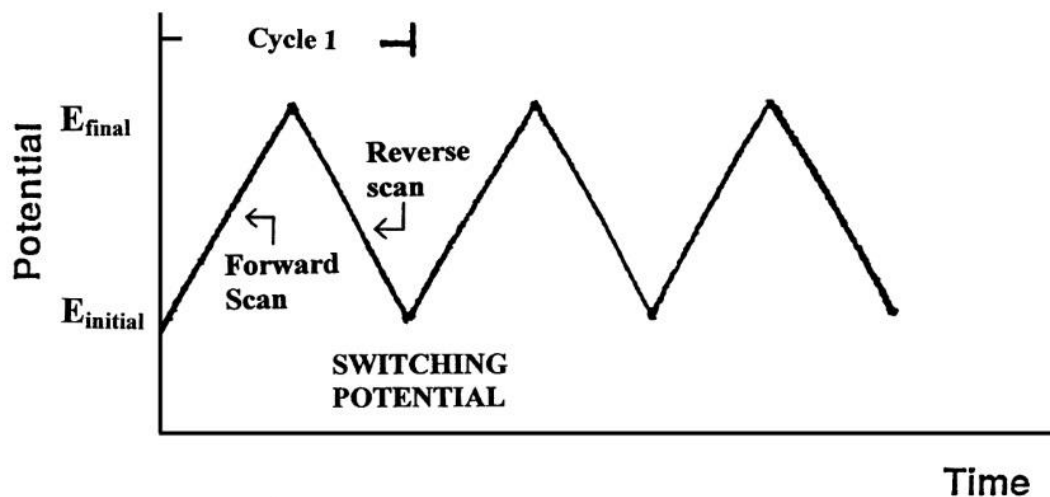


Figure 2.16. Shows the cyclic voltammetry with potential plotted against time

The expected response of a reversible redox couple during a single potential cycle is assumed that only the oxidized form O is present initially. Thus, a negative-going potential scan is chosen for the first half-cycle, starting from a value where no reduction occurs. As the applied potential approaches the characteristic E^0 for the redox process, a cathodic current increases until a peak is reached. After traversing the potential region in which the reduction process occurs (at least 90mV beyond the peak), the direction of the potential sweep is reversed (Figure 2.17). The reverse scan shows R molecules (generated in the forward half cycle and accumulated near the surface) reoxidized back to O and an anodic peak results. The characteristic peaks in the cyclic voltammogram are caused by the diffusion layer formation near the electrode surface. These can best be understood by carefully examining the concentration-distance profiles during the potential sweep. Four observable characteristics are seen from the cyclic voltammogram: two peaks and two potentials. These parameters were developed for diagnostics when cyclic voltammograms are analyzed (Wang, 2001).

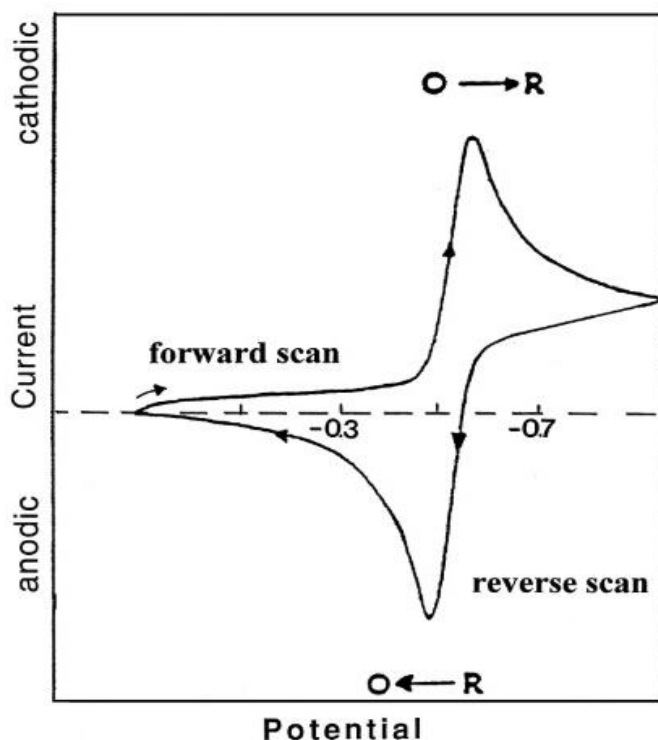


Figure 2.17. Typical cyclic voltammogram for a reversible redox process

Reversible Systems: The peak current observed for a reversible couple reaction at 25°C is given by the Randles Sevcik equation:

$$i_p = (2.69 \times 10^5) n^{3/2} A C D^{1/2} v^{1/2} \quad 2.4$$

where n represents electron number, A is the area of the electrode (in cm^2), C represents the concentration (in mol cm^{-3}), D represents the coefficient of diffusion (in $\text{cm}^2 \text{s}^{-1}$), and v is the square root of scan rate (in V s^{-1}). The current measured is directly proportional to the scan rate's concentration and square root (Figure 2.18). The ratio of the reverse to forward peak currents is the unity for a simple reverse couple. The peak ratio can be affected by chemical reactions coupled with the redox process. The measurements of the peak currents can be taken when the baseline current that precedes is drawn. The peaks position seen on the potential axis is related to the redox potential in a reaction (Wang, 2001). The potential that represents a reversible couple reaction can be seen in the centre of $E_{p,a}$ and $E_{p,c}$:

$$E^\circ = \frac{E_{p,a} + E_{p,c}}{2} \quad 2.5$$

The peak potentials separated in a reversible reaction is given by

$$\Delta E_p = E_{p,a} - E_{p,c} = \frac{0.059}{n} \text{ V} \quad 2.6$$

The half-peak potential ($E_{p/2}$, where the current is half of the peak current) to the polarographic half-wave potential, $E_{1/2}$:

$$E_{p/2} = E_{1/2} \pm \frac{0.028}{n} \text{ V} \quad 2.7$$

Irreversible and Quasi-Reversible Systems For irreversible processes: These processes are characterized by reduced size and widely separated individual peaks with sluggish electron exchange. The irreversible systems have a total characteristic of a shift in the peak potential alongside the scan rate.

$$E_p = E^\circ - \frac{RT}{\alpha n_a F} \left[0.78 - \ln \frac{k^\circ}{D^{1/2}} + \ln \left(\frac{\alpha n_a F v}{RT} \right)^{1/2} \right] \quad 2.8$$

where α represents transfer coefficient, αn represents the number of electrons involved in the charge transfer (Figure 2.18). E_p is found at higher potentials than E° , and the over-potential is related to k° and α . The peak potential and the half-peak potential (at 25°C) will differ by $48/\alpha n$ mV. Hence, the voltammogram becomes more drawn-out as αn decreases (Wang, 2001).

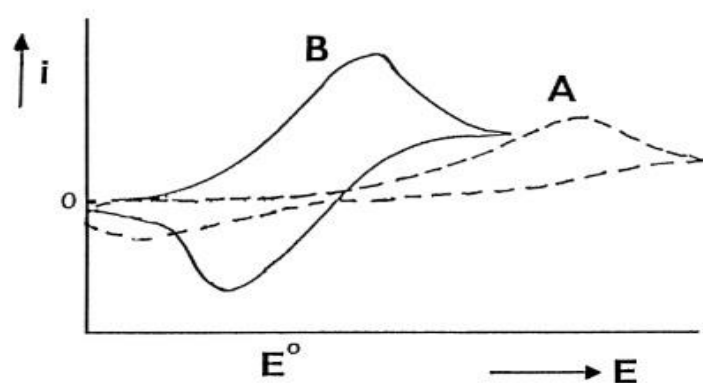


Figure 2.18. shows cyclic voltammograms of irreversible and quasi-reversible redox reactions in curve A and B.

The study of Adsorption reactions at electrodes surface: The cyclic voltammetry method is used to determine the electrochemical behaviour of electroactive compounds. The reactant and product can be both involved in the process of adsorption and desorption. This behaviour can be observed in the studies of numerous organic compounds and metal complexes. Adsorptive accumulation at the surface of the electrode is indicated by a gradual increase in the cathodic and anodic peak currents. (Figure 2.19). The peak separation is also smaller than in the reactions that occur in the solution phase. When non-reacting species are connected to the surface of the electrode, there is a manifestation of CV peaks that are symmetrical and peaks that are half the width. This behaviour is termed the Nernstian behaviour. The peak current is directly proportional to the surface coverage (Γ) and the potential scan rate. Nernstian behaviour of diffusing species yields a $v^{1/2}$ dependence. The ideal behaviour is approached for relatively slow scan rates. An adsorbed layer shows no intermolecular interactions and fast electron transfers. The peak area at saturation (i.e., the quantity of charge consumed during the reduction or adsorption of the adsorbed layer) can be used to calculate the surface coverage (Wang, 2001):

$$Q = nF\Gamma$$

2.9

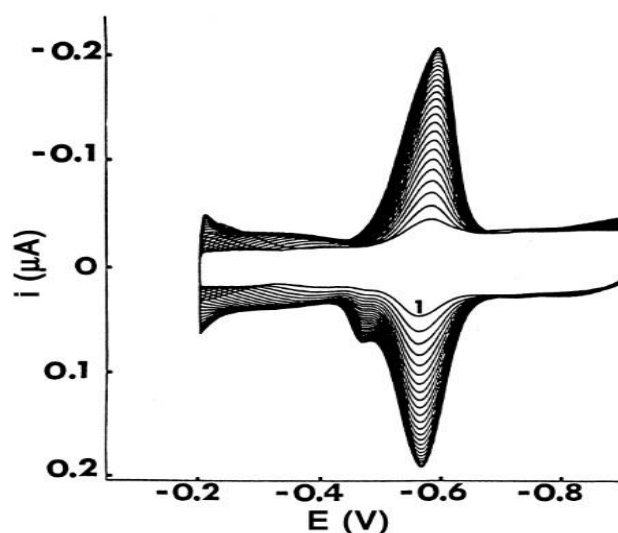


Figure 2.19. Voltammogram showing increase in the cathodic and anodic adsorption process

2.6.4 Controlled Potential Techniques

2.6.4.1 Chronoamperometry

This method shows how the working electrode's potential is stepped down from a value where there is no faradaic reaction to a value at which the electroactive species on the surface of the electrodes is effectively zero. In this method, an immovable electrode and an unstirred solution are used, after which a current against time dependence is monitored as a result. Mass transport in this condition is strictly diffusion. The current plot against the time curve reacts to the change in the concentration gradient found in the vicinity of the surface. This involves the gradual expansion of the diffusion layer associated with the depletion of the reactant and hence decreased the slope of the concentration profile as time progresses. The current decays with time at the electrode surface.

$$i(t) = \frac{nFACD^{1/2}}{\pi^{1/2} t^{1/2}} = kt^{-1/2} \quad 2.10$$

The chronoamperometry procedure is often employed to measure the diffusion coefficient of the electroactive species in the reaction of the working electrode surface area (Figure 2.20). The method can be applied when pulses of potential are repetitively applied to the working electrode at fixed time intervals. It can also be used to study the reactions on the electrode surface (Wang, 2001).

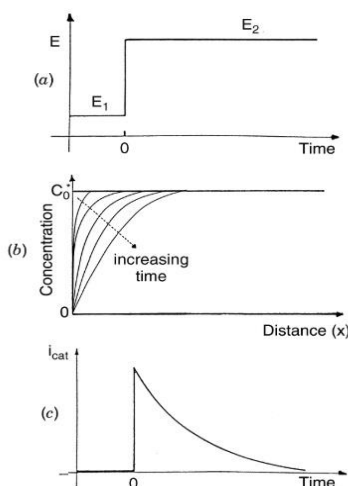


Figure 2.20. shows chronoamperometry representing potential-time waveform, change of concentration profiles with time and the resulting current-time response in a,b and c.

2.6.4.2 Pulse Voltammetry

Barker and Jenkin first reported the method of pulse voltammetry. The method aimed to lower the detection limits of the concentration of species during voltammetric measurements. The pulse voltammetry method permits the quantification of the concentration of species as low as 10^{-8}M by increasing the ratio between the currents of faradaic and non-faradaic processes (Wang, 2001).

2.6.4.3 Normal-Pulse Voltammetry

This method consists of series of pulses that have increasing amplitude potentials that are applied after a successive drop is completed at a time that is preselected near the end of each life that is dropping. A constant potential is maintained between the pulses at the surface of the electrode; at this potential, the analyte undergoes no reaction. The measurements show a linear increase in amplitude with each drop (Figure 2.21). The current to be measured is done 40 minutes after the pulse is applied; at this time, the contribution of the charging current is nearly zero. The voltammogram obtained from this method is sigmoidal and has a limiting current (Wang, 2001).

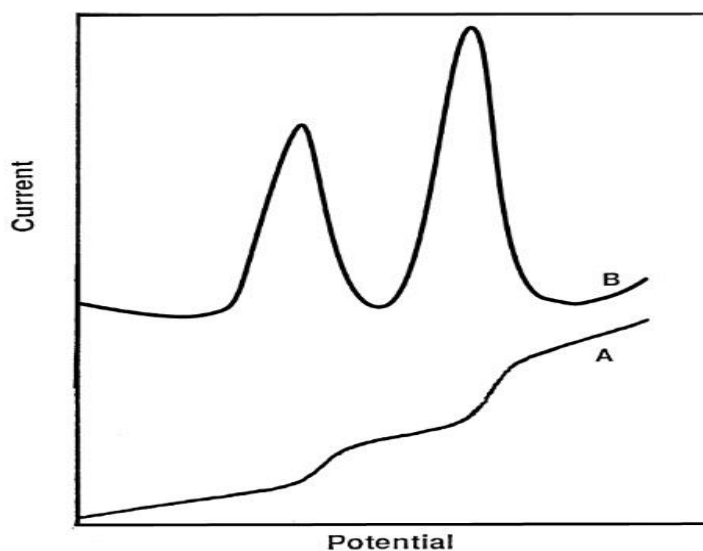


Figure 2.21. Shows cyclic voltammograms of a normal-pulse and differential-pulse in curve A and B.

2.6.4.4 Differential Pulse Voltammetry

This technique is used for measuring trace levels of organic and inorganic species. The magnitude of pulses superimposed in this method is on a linear potential applied to the working electrode at a time just before the end of the drop. The current is sampled twice, just before applying the pulse and again late in the pulse life when the charging current has decayed. In this method, the voltammogram plot consists of the current against the applied potential (Figure 2.21). Measurements in DPV can be taken at a concentration level of 10^{-8} M, about 1mgL^{-1} . The peak shaped response observed in differential pulse measurements results in improved resolution between two species with similar redox potentials. The peaks measured are separated by 50mV and depend not only on the peak potentials but also on the widths of the peak. The width of the peak is related to electron stoichiometry. Irreversible redox reactions result in peak currents that are lower and broader than peak currents, which shows reversible systems. The DPV method offers information about how the analyte appears in its chemical form, such as in its oxidation states or complexation (Wang, 2001).

2.6.4.5 The Square-Wave Voltammetry

The square wave technique is a large amplitude differential technique with a symmetrical square waveform that is superimposed on a base staircase potential applied to the working electrode. The current observed is sampled twice during each square wave cycle, with one at the end of the forward pulse and another once at the end of the reverse pulse. The reverse pulse causes the reverse reaction of the pulse since the square wave modulation of the amplitude is large, and their difference is plotted against the base staircase potential. The produced voltammogram (Figure 2.22) is symmetrical. It shows a half-wave potential where the peak current is directly proportional to the concentration. This method has excellent sensitivity, resulting in the net current being larger than the forward or reverse parts. The sensitivity of this method is higher than DPP, in which the reverse current is not used. The method can detect as low as 1×10^{-8} M of the concentration of the species. When the square-wave is compared to differential pulse voltammetry for reversible and irreversible reactions, square wave currents are 4 and 3.3 times higher than the differential pulse response. The major advantage of this method is its speed (Wang, 2001).

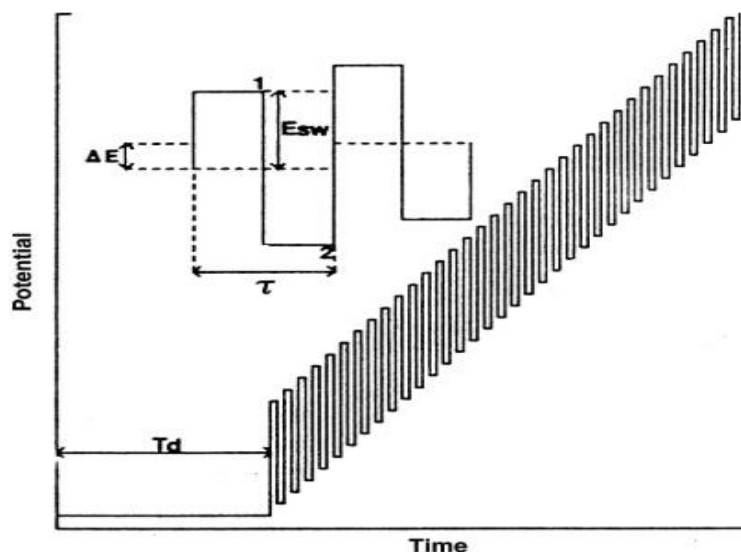


Figure 2.22. Shows square-wave form representing the amplitude, E_{sw} ; step height, ΔE ; square-wave period, τ ; delay time, T_d ; and current measurement times.

2.7 Electrochemical Set-up

There are three electrodes utilized during controlled experiments when potentials are applied. The beaker used as a cell is usually in a volume of 5 to 50 mL and has the WE, the RE and the AE inside the solution (Figure 2.23). The working electrode is the electrode on which the reaction of interest occurs. The reference electrode provides a stable and reproducible potential and is independent of the sample composition against which the potential of the working electrode is compared. The Ag/AgCl or Hg/Hg₂Cl₂ are the commonly used reference electrodes. For the solution to be prevented from contamination, the reference electrode has to be insulated from the sample through an intermediate bridge. Conducting materials like platinum wire and graphite rod are employed as auxiliary electrodes in the electrochemical cell (Wang, 2001).

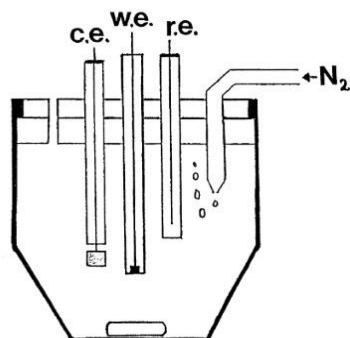


Figure 2.23. Shows an electrochemical cell used for voltammetric analysis having WE, RE and AE.

2.7.1 The supporting Electrolytes or solvents used in an electrochemical cell

The electrochemical measurements are carried out in mediums that consist of solvents containing supporting electrolytes. The kind of solvent used for electrochemical reactions is primarily selected based on the solubility of analytes, their redox activities and their properties that include electrical conductivity, chemical reactivities and electrochemical activities. The solvent used for electrochemical processes should not react with the analyte of interest. Over a wide potential range, it should not undergo any electrochemical reaction. Many other solvents are used aside from water. These solvents are nonaqueous and are acetonitrile, dimethylformamide (DMF), methanol, dimethyl sulfoxide (DMSO), or propylene carbonate. Sometimes solvents can be mixed and used for specific applications. Most times, double distilled water is adequate for most works in aqueous media, while triple distilled water is used for trace stripping analysis. The resistance of a solution can be decreased in a controlled experiment by supporting electrolytes. The electrolytes can also be used to eliminate the effect of electromigration and constantly maintain ionic strength. The electrolyte solution may be a buffer, mineral acid or inorganic salt. Sodium hydroxide, hydrochloric acid, ammonium chloride, potassium nitrate or chloride are widely used when water is used as a solvent. The composition of a buffer solution usually affects the measurements taken during a voltammetric analysis. They are used when pH control is needed. Some of the ones used are acetate buffer, phosphate buffer or citrate buffer.). The

concentration of the electrolyte range is between 0.1 to 1.0M, which means that the electroactive species are in a large excess of concentration (Wang, 2001).

2.7.2 Working Electrodes

The material used as a working electrode affects the voltammetric procedure performance. The electrodes used must be able to have a reproducible response and also have high signal noise characteristics. The selection of the materials used as working electrodes is based on the behaviour of the target analyte in a redox reaction and the background current, which can be measured over the potential region. Other characteristics of the materials are cost, electrical conductivity, mechanical properties, surface reproducibility, availability and toxicity. The working electrodes used popularly are carbon, nickel, gold, mercury, silver, copper and platinum (Smith & Stevenson, 2007; Wang, 2001; Westbroek, 2005).

2.7.2.1 Mercury Electrodes

These electrodes are highly attractive because they have high hydrogen overvoltage that greatly extends the cathodic potential window and possesses a highly reproducible, readily renewable and smooth surface. The disadvantages of using the mercury electrodes are that it is toxic and has a limited anodic range. Different types of mercury electrodes are frequently used; they are dropping mercury electrode (DME) and hanging mercury drop electrode (HMDE), and mercury film electrode (MFE). The type used mostly in polarography is the DME and for electrocapillary studies. The HDME is used mainly for stripping analysis and cyclic voltammetry (Smith & Stevenson, 2007; Wang, 2001; Westbroek, 2005).

2.7.2.2 Solid Electrodes

The materials used for such electrodes are carbon, platinum, and gold. However, copper, silver and nickel can also be used for applications. The importance of using such electrodes is their response to the electrode's surface. They require pretreatment and polishing when used to obtain reproducible results. The mechanical polishing method for a smooth finish and potential cycling is commonly used for metal electrodes. At the same time, chemical,

electrochemical or thermal surface procedures are added for activating carbon-based electrodes (Smith & Stevenson, 2007; Wang, 2001; Westbroek, 2005).

2.7.2.3 Carbon Electrodes

Carbon electrodes are the type of solid electrodes used in electroanalysis because of their low background noise, rich surface chemistry, low cost, chemical inertness, suitability for sensing and detecting applications. The rates of electron transfer observed at carbon surfaces are often slower than those observed at metal electrodes. The carbon electrodes share the basic structure of a six-membered aromatic ring of an sp^2 bonding. They differ in the relative density of the edge and basal planes at their surfaces. The most used carbon materials are carbon paste, glassy carbon, carbon fibre, screen printed carbon strips, carbon films and carbon composites such as graphite-epoxy, wax-impregnated graphite and kelgraf (Smith & Stevenson, 2007; Wang, 2001; Westbroek, 2005).

2.7.3 Counter Electrodes

The counter electrode in an electrochemical reaction helps understand the half-reaction in the working electrode. The surface of the electrode must be at least ten times larger than that of the working electrode. Half of the reaction taking place on the working electrode is the slowest. The properties of the counter electrode determine the characteristics of the electrical current that has been measured. That is why electrodes with the larger surface electrode are used to prevent the problem. However, the reaction on the counter electrode is also slow but faster than that of the working electrode. The counter electrode must be a good conductor. The positioning of the counter electrode against the working electrode in an electrochemical setup is very important (Westbroek, 2005).

2.7.4 Silver/Silver Chloride Electrode

The electrolyte solution used for the reference electrode provides the reference electrodes with a constant potential. It serves as the electrolytic bridge of the solution containing the analyte. The electrolyte solution used for the salt bridge is selected not to influence the measurement. The reference electrolyte solution and the analyte solution must tolerate the

electrolyte solution in the salt bridge. The most important electrolytes for salt bridges are potassium nitrate, potassium chloride, sodium sulphate or ammonium nitrate solutions (Smith & Stevenson, 2007).

The refilling of the Reference Electrode' Solution

The electrolyte of reference electrodes needs to be changed with a new solution after some time because of the diffusion between the half - cell and the main cell when the electrolyte undergoes reaction. The two factors needed are the new solution which must have the right composition and concentration, and air bubbles must be removed from the tubes. The reference electrode must be done carefully, and no air bubbles should be present in the system (Smith & Stevenson, 2007).

CHAPTER 3

MATERIALS AND METHODS

3.1 Materials and Methods for electrochemical DNA Biosensor

3.1.1 Chemicals and Reagents

The dsDNA of fish sperm or synthetic sequences of DNA used for the study were bought from Sigma. A stock solution of 1000 ppm, (5mg/5ml) of the dsDNA was made with an acetate buffer solution (ABS) of 0.5M at a pH of 4.8 mixed with 20mM NaCl. Potassium Phosphate Buffer solutions (PBS) were prepared into different pH values from 4.0 to 8.0 respectively, with a concentration of 0.5 M at 25°C. They were prepared standardly from a volume of 0.5M K_2HPO_4 as millilitre (mL) and volume of 0.5M KH_2PO_4 millilitre (mL). The ADR stock solution of 1000 ppm, (5mg/5ml) was prepared with ultra-pure water and then diluted into different concentrations, which were used as the working solutions (Figure 3.1).

3.1.2 Electrochemical Set-up

Voltammetric and impedimetric measurements were carried out using the AUTOLAB-PGSTAT204 and software called Nova 2.1.2. The AUTOLAB was connected to a three-electrode system which was used to carry out the analysis. These are the auxiliary electrode which is a platinum wire, $Ag/AgCl/3MKCl$ used as the reference electrode and PGEs for the working electrode.

3.1.3 Preparation of Pencil Graphite Electrodes

The Pencil leads that were used are the Ultra-Polymer TOMBOW 0.5HB obtained from a local stationery store in Turkey. They were carefully cut into two halves of 3.5cm and used as the PGEs, and the pencil leads were then marked with a white marker, leaving at least 1.5cm as the electrode surface to be used as the transducer. The PGEs were then pre-treated, and the surface cleaned and activated by applying 1.4 volts (V) as potential using chronoamperometry for 30seconds. The process was repeated for all the PGEs to avoid impurities and noise in the results of the analysis.

3.1.4 Immobilizations of dsDNA and ADR on the surface of the Pencil Graphite Electrodes

The PGEs were inserted into vial tubes containing 200 μL of the dsDNA of fish sperm, prepared as the working solution with a concentration of 20 ppm. The immobilization time for the dsDNA on the PGEs was 30 minutes and was done for all the PGEs used for the work. Passive adsorption method was employed in the immobilization of dsDNA on the electrode surface of PGEs.

Serial dilutions of ADR with different concentrations were made from the stock solution and used as the working solutions. After the immobilisation of the dsDNA on the PGEs, the PGEs modified with the dsDNA were then removed and inserted into the vial tubes containing 200 μL of ADR and allowed for 30mins for immobilization to occur. The PGEs were then rinsed in ABS of 0.5 M at pH 4.8 for 3seconds to remove unbound dsDNA and ADR.

For the pH study, we made a working solution of ADR 9.2×10^{-4} M in a 5 ml beaker from the ADR stock solution. The working solution was used for immobilization on the PGEs for 30mins after which the PGEs were rinsed in a buffer solution for 2 seconds then analyzed in the respective different phosphate buffer solutions.

3.1.5 Electrochemical detection Procedure

The experiments were all repeated at least three times, with 5 PGEs for each concentration or group. After which their average values were taken and presented in the result section. In all the repeated rounds, new pre-treated PGEs were used for the interaction of the dsDNA with ADR. DPV measurements were done in ABS of 0.5 M at pH 4.8 (Figure 3.1). The measurements were taken using the conditions; the scanning potential applied +0.15 to +1.4 V and the applied scan rate was 0.010071 V/s. There was no oxidation signal observed for blank in ABS.

The measurements for the EIS were then taken using a solution of 2.5 mM concentration of $\text{K} [\text{Fe} (\text{CN})_6]^{3-/4-}$ using a ratio of (1:1), prepared in 0.1 M KCl. The range for the frequency used for the measurement was from $1\text{E} + 05$ Hz to 0.1 Hz and a potential of +0.23 V was applied. The amplitude applied is $0.01V_{\text{RMS}}$. The values for charge transfer resistance (R_{ct}),

which corresponded with the semicircle diameter of Nyquist diagram, were calculated from the fit and simulation in the Nova 2.1.2 using the AUTOLAB-PGSTAT204.

For the pH study of the ADR alone, CV and DPV analyses were used in different respective prepared 0.5 M PBS at pH 4.0 to 8.0. Peak currents for each of the measurements were recorded after the analysis. The range for the scan rates that were used was (0.02, 0.04, 0.06, 0.08, 0.1, 0.2, 0.25, 0.3, 0.35, 0.4, 0.45) V/s.

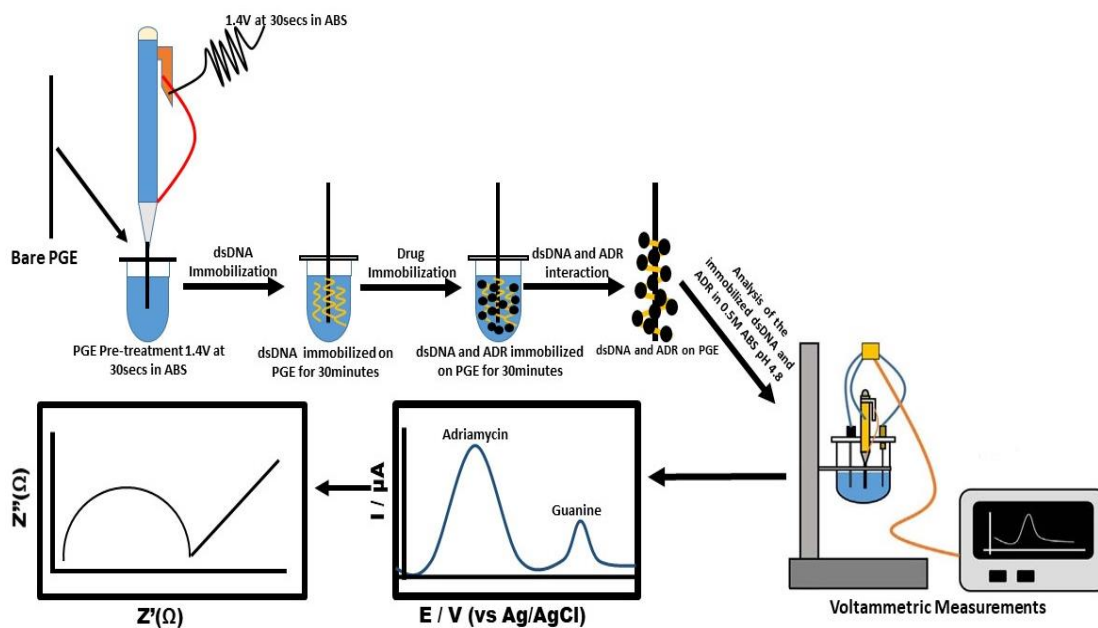


Figure 3.1: Experimental Procedure of the electrochemical detection of the interaction between dsDNA and Adriamycin immobilized on Pencil Graphite Electrodes

3.2 Materials and Methods for electrochemical sensor for detection of compound

3.2.1 Chemicals and Reagents

The powdered phenolic compounds (sinapic acid, syringic acid, and rutin), paraffin oil, and carbon powder were all procured commercially from Sigma-Aldrich, Istanbul, Turkey. Fe₃O₄ nanoparticles powder was purchased commercially from Sigma-Aldrich, Istanbul, Turkey. They have a particle size of 50–100 nm, scanning electron microscopy (SEM) for surface characterization; Brunauer–Emmett–Teller (BET) surface area analysis is 6–8 m²/g, melting point of 1538 °C, titration by Na₂S₂O₃, % of Fe is 71.5%, an appearance of black

color, powder form and spherical shape, the density of 4.8–5.1 g/mL at 25 °C, a bulk density of 0.84 g/mL, the purity determined using trace metal analysis is 97% (≤ 35000.0 ppm), a quality level of 100, Inductively coupled plasma (ICP) major analysis confirms iron component. All reagents were of analytical standards and used as obtained (Figure 3.2). The pH value of the acetate buffer solutions (ABS) used for the study is 0.5 M, ABS pH 4.8. The stock solutions of the phenolic compounds were prepared with ultra-pure water at a concentration of 1000 ppm (4.5×10^{-3} M for sinapic, 5.1×10^{-3} M for syringic, and 1.6×10^{-3} M for rutin). The stock solution was then diluted into standard concentrations of 200 ppm (0.9×10^{-3} M for sinapic acid, 1.0×10^{-3} M for syringic acid, and 0.3×10^{-3} M for rutin), which were used as working solutions. The wine samples used for the analysis were commercial brands of wine (Angola kavaklidere—dry white wine— and dikmen kavaklidere—dry red wine) purchased from a market.

3.2.2 Instrumentation and Methods

All the voltammetric measurements were performed using the potentiostat–galvanostat AUTOLAB-PGSTAT204, Metrohm, Utrecht, The Netherlands) and operated with Nova 2.1.2 software. The potentiostat–galvanostat was connected to a three-electrode system cell, a carbon paste electrode, and Fe₃O₄ nanoparticles modified carbon paste electrode as working electrodes. Ag/AgCl/3 M KCl was used as a reference electrode and a platinum wire as an auxiliary electrode in a 10mL cell containing 0.5 M ABS pH 4.8 as supporting electrolyte. The pH measurements were all carried out with an edge H12002 pH meter (Hanna Instruments).

3.2.3 Fabrication of Bare CPE and MCPE

The ratios of carbon powder to paraffin oil (binder) were compared for best results using the ratios 70:30 and 60:40 (wt/wt %), respectively, and 60:40 ratio was taken as the optimized proportion for the study. The carbon paste mixture, as the control (CPE), was prepared by hand, mixing 60 mg of carbon powder with 40 mg of paraffin oil to obtain a homogeneous mixture of 60 vs. 40 mg. The carbon paste mixture prepared with Fe₃O₄ nanoparticles (MCPE) contained 60.0 mg carbon powder, 30.0 mg of paraffin oil, and 10.0 mg of Fe₃O₄ powder in a ratio of 60:30:10 (wt/wt/wt %) (Chikere et al., 2020). The homogenous pastes

were packed to fill two different 4 mm diameter cavity of Teflon tubes, one for the CPE and the other for the MCPE. A copper wire for conductivity was connected to the end of the electrodes (Teflon tubes). The surfaces of the electrodes were polished by smoothening them with a smooth paper to obtain a smooth and crack-free surface. After each analysis, new electrode surfaces were prepared by inserting the paste into the Teflon tubes and their surfaces polished. This process was repeated (Figure 3.2) throughout the experiments before each new measurement.

3.2.4 Voltammetric Measurements

The voltammetric techniques used for the study were CV and DPV. The measurements of these analytes at the electrode surfaces were carried out in ABS 0.5 M, pH 4.8. The scan rate study was done using CV, by varying the applied scan rates at a range of 0.03, 0.06, 0.09, 0.12, 0.15, 0.18, 0.20, 0.25, 0.3, 0.35, and 0.40 V/s. The pH study was done using CV by varying the pH values at a range of 2.6, 3.8, 4.8, 5.6, 6.5, 7.4, 8.4, and 9.2 pH, respectively, using a scan rate of 0.2 V/s. The DPV analysis was done from 0.0 V to 1.0 V. EIS measurements were performed in the frequency range of 100 kHz–0.1 Hz, in a redox solution of 5 mM $[\text{Fe}(\text{CN})_6]^{3-/4-}$ containing 1 M KNO_3 . At CPE and MCPE; the electroactive surface area of CPE and MCPE was determined in 1 mM $\text{K}_4[\text{Fe}(\text{CN})_6]$, which was used as an electrochemical redox probe in 0.1 M KCl . The same condition was used for the scan rate study by varying the scan rates from 0.1, 0.12, 0.14, 0.16, 0.18, and 0.2 V/s, employing the Randles–Sevcik equation.

3.2.5 Preparation and Detection Procedure of Real Samples (Red and White Wine)

DPV technique was used to analyze phenolic compounds' content in spiked samples of the red and white wine samples. The voltammograms produced were recorded using a method of standard addition of serial dilutions of known volumes and concentrations of the phenolic compounds (sinapic acid, syringic acid, and rutin). A volume of 1 mL of the wine samples only was inserted into a 10 mL beaker and was completed with ABS of (0.5 M, pH 4.8) to a volume of 10 mL. Aliquots of the standard phenolic compounds from (0.03×10^{-3} – 0.05×10^{-3} M) were then added to the 10 mL beakers having 1 mL of the wine samples and completed to 10 mL with ABS. After which, they were stirred for two minutes with a

magnetic stirrer. Measurements from the DPV analysis were recorded from each beaker that contains the wine and aliquots of the standard phenolic compounds (Chikere et al., 2020).

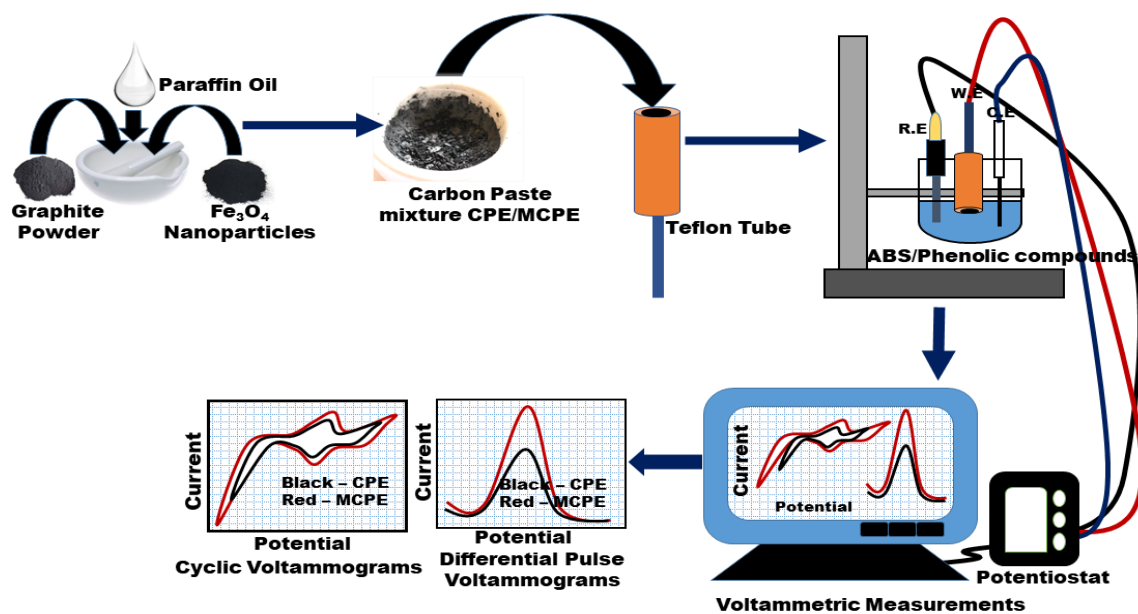


Figure 3.2: Schematic diagram of the phenolic compounds electrochemical sensor preparation.

CHAPTER 4

RESULTS AND DISCUSSIONS

4. Results and Discussion

4.1 Electrochemical Detection of DNA and ADR interaction

4.1.1 Electrochemical behaviour of dsDNA and ADR alone at PGEs surface

The dsDNA concentration used for the study of interaction between dsDNA and ADR is 20 ppm. At this concentration, the dsDNA was analysed alone and the guanine oxidation signal measured was at a potential of 1.0 V-1.1 V after DPV was applied in ABS (Figure 4.1) (Erdem et al., 2012; Topkaya et al., 2018; Topkaya & Cetin, 2019; Zhao et al., 2007). This oxidation potential for guanine was observed repeatedly in all the results obtained from the interaction study of dsDNA and ADR. The guanine signal was used as a marker for the interaction study because it is easily more oxidizable and the most electro-active DNA base among the other bases of the dsDNA helix. The behaviour of Adriamycin alone at 4.6×10^{-4} M concentration was also studied using DPV measurements in ABS. The oxidation potential of ADR after applying a positive potential was obtained at 0.55 V-0.60 V (Oliveira-Brett et al., 2002).

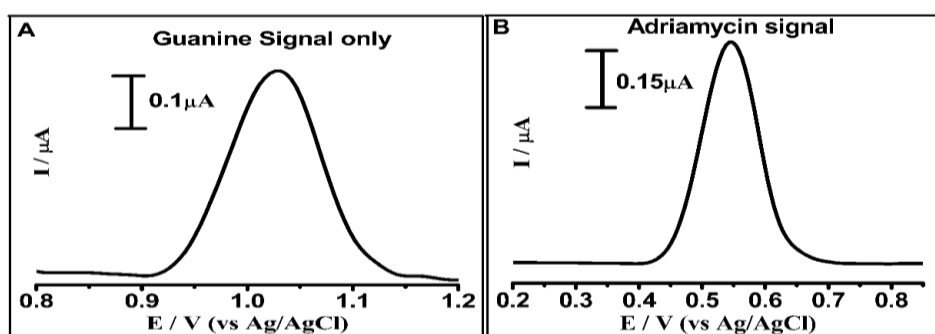


Figure 4.1. Differential pulse voltammograms in pH 4.8, 0.5M acetate buffer solution showing the signal of: **(A)** 20 ppm, dsDNA only immobilized on bare PGE without interaction with ADR. **(B)** Adriamycin only with a concentration of 4.6×10^{-4} M immobilized on bare PGE without interaction with dsDNA.

4.1.2 Differential Pulse Voltammetric Studies of dsDNA and ADR immobilized on PGEs

The interaction of dsDNA and ADR, indicates the effect of increase in concentration of ADR on dsDNA using PGEs after DPV measurements were taken (Figure 4.2). As the concentration of ADR is increased from $4.6 \times 10^{-4} \text{M}$, $9.2 \times 10^{-4} \text{M}$, $1.4 \times 10^{-3} \text{M}$ and $1.8 \times 10^{-3} \text{M}$ as they interact with 20 ppm of the dsDNA respectively, the peak height of the ADR signal is seen to increase progressively. This increase in the concentration of the ADR affects the peak height of the guanine signal, causing it to decrease also progressively in the interaction. This can be attributed to the 3 assumptions which are (a) The ADR bounded to the bases of dsDNA, hence resulting in the oxidizable groups of electroactive DNA bases to be shielded. This is as a result of the drug confining to the surface and interacting with dsDNA especially in higher concentrations (Erdem et al., 2012), (b) The decrease in the dsDNA guanine signals, can also be an indication of the intercalation activity of the ADR as a planar compound into the dsDNA (Erdem et al., 2009). This can be explained from the ADR structure from figure 1 showing how the drug interacts with the double helix of the DNA through intercalation. The ring B and C intercalate between the DNA bases while the carbonyl side chain and the aminosugar linked to ring A interacts with the minor groove of the DNA's double helix. Then ring D protrudes and interacts with the major groove of the double helix of the DNA (Cullinane & Phillips, 1990; Pigram, W. J., W. Fuller, 1972; Wang et al., 1998) and the aminosugar which are positively charged, interacts with the phosphate backbone of the dsDNA (Berg et al., 1981). (c) A change in the charge transfer properties of DNA as a result of its interaction with the drug (Erdem et al., 2009; Wong & Gooding, 2007), could lead to the decrease of guanine signal oxidised at PGEs surface. It is also observed that as the concentration of the drug increases, the oxidation peak position of ADR became broader, being greater than that obtained for ADR alone.

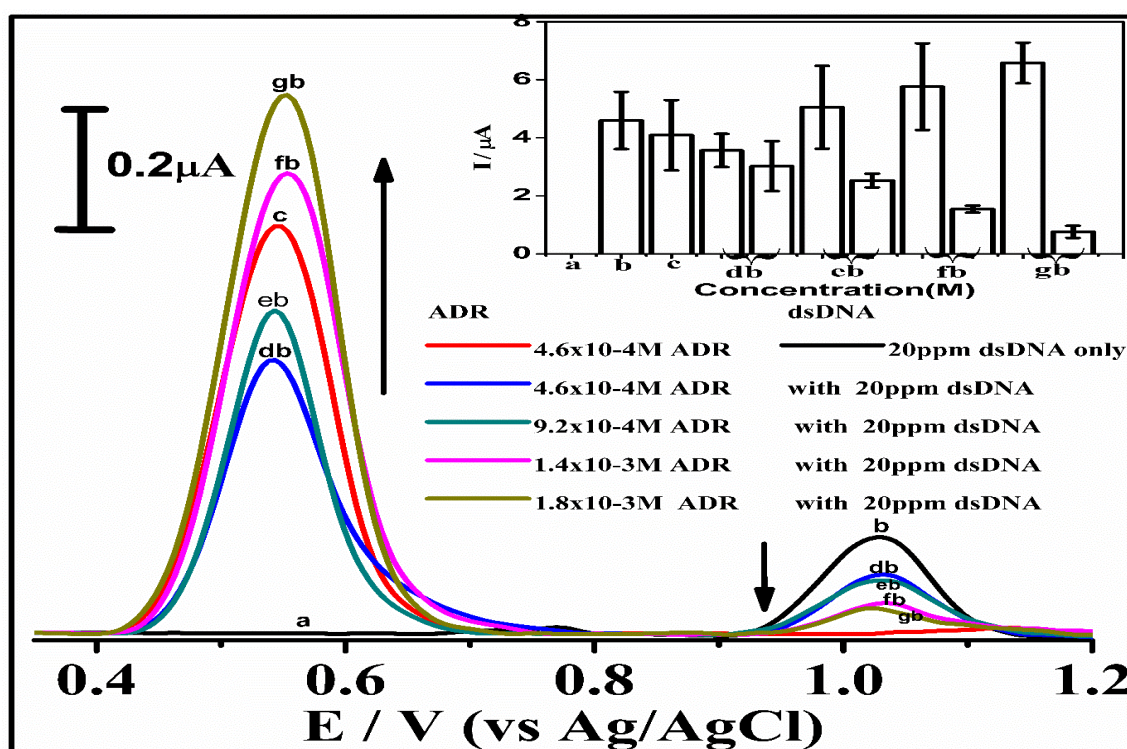
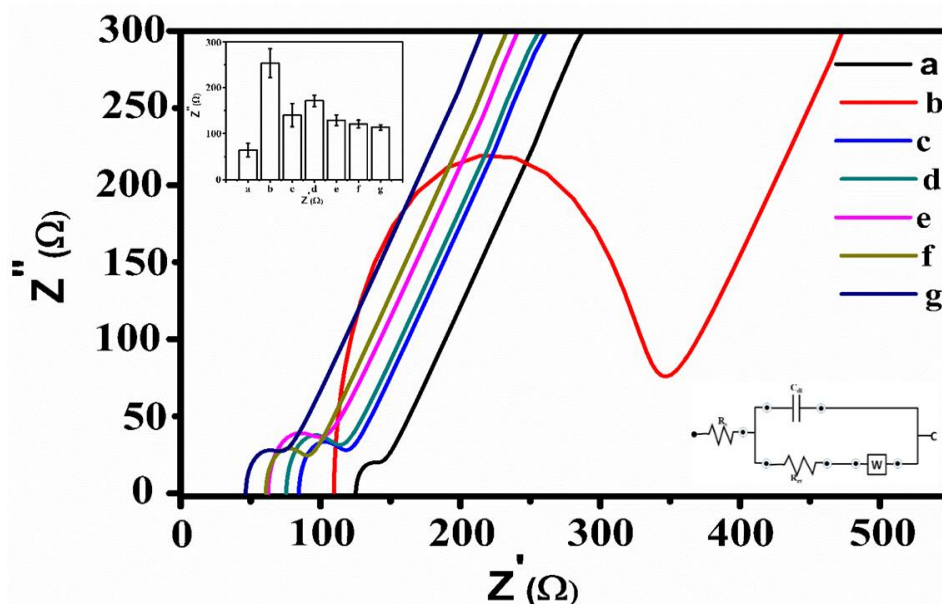


Figure 4.2: DPV and the inset error bar plots, shows the different measurements carried out in pH 4.8, 0.5M ABS using PGEs. The labelled results on the voltammogram and the bar plots respectively represent: (a) Bare PGEs, (b) 20 ppm, of dsDNA only immobilized on PGE (c) 4.6×10^{-4} M of ADR only immobilized on PGEs. (db) 4.6×10^{-4} M of ADR with 20 ppm, dsDNA after interaction immobilized on PGEs (eb) 9.2×10^{-4} M of ADR with 20 ppm, of dsDNA after interaction immobilized on PGEs (fb) 1.4×10^{-3} M of ADR with 20 ppm, of dsDNA after interaction immobilized on PGEs (gb) 1.8×10^{-3} M of ADR with 20 ppm, of dsDNA after interaction immobilized on PGEs.

4.1.3 Impedimetric studies of the interaction of dsDNA and ADR

The impedimetric spectrum obtained (Figure 4.3) using the EIS measurement of the bare PGEs and the modified PGEs with 20 ppm dsDNA alone, 4.6×10^{-4} M ADR alone and different concentrations (4.6×10^{-4} M, 9.2×10^{-4} M, 1.4×10^{-3} M and 1.8×10^{-3} M) of ADR with 20 ppm dsDNA in the presence of $[\text{Fe}(\text{CN})_6]^{3-/4-}$ solution. The bare PGE 'a' showed an almost straight line, indicating a diffusional limited occurring electrochemical process. Following the immobilization and adsorption of dsDNA and ADR on the electrode surface,

the diameters of the semicircles of ‘c-g’ in the figure decreased gradually, aside ‘b’ for dsDNA alone. The highest R_{ct} value obtained from the semicircle ‘b’ for dsDNA alone, showed that dsDNA successfully adsorbed to the surface of PGEs and demonstrates that the dsDNA slowed down the rate of electron transfer in the reaction process, as a result of electrostatic repulsion between the negatively charged phosphate backbone of dsDNA and redox couple $[\text{Fe}(\text{CN})_6]^{3-/4-}$ solution. The voltammetric measurements represented with the bar plots (inset Figure 4.3) were integrated with EIS results for the characterisation of dsDNA/ADR onto the electrode surface. The impedance measurement showed a progressive decrease in R_{ct} values with increase in the concentration of ADR. This decrease in the R_{ct} values from the semicircles can be attributed to the intercalation effect of ADR on the dsDNA, as there is a compensation of the negative charges of the solution with the positive charges on the ADR. This interaction also tries to explain the concept of conductivity of the solution, where an increase in ADR concentration leads to increase in solution conductivity, and a decrease in solution resistance (R_s). The values of charge-transfer resistance (R_{ct}) from the Nyquist diagram, decreased gradually with the deposition of increased concentration of ADR with 20 ppm dsDNA on the electrode surface where R_{ct} ‘b’ $>$ R_{ct} ‘a’ $>$ R_{ct} ‘c’ $>$ R_{ct} ‘d’ $>$ R_{ct} ‘e’ $>$ R_{ct} ‘f’ $>$ R_{ct} ‘g’. It is also noticeable that solution resistance (R_s) measurement also decreased progressively where R_s ‘a’ $>$ R_s ‘b’ $>$ R_s ‘c’ $>$ R_s ‘d’ $>$ R_s ‘e’ $>$ R_s ‘f’ $>$ ‘g’ (Canavar et al., 2011; Eksin et al., 2013, 2015; Ozkan et al., 2004; Rountree et al., 2018). The circuit model figure inside the Nyquist diagram, is the equivalent measurement of impedance where C_{dl} is the space charge capacitance at the electrode-electrolyte interface: R_s is the solution resistance, W is the Warburg impedance which is a result of mass transfer to the electrode surface and R_{ct} is the charge transfer resistance at the electrode- electrolyte interface (Erdem et al., 2012).



Figures 4.3: showing the Nyquist diagram for the R_{ct} values in the solution containing 5mM $K_3[Fe(CN)_6]/K_4[Fe(CN)_6]$ (1:1) with 0.5M KCl by using (a) Bare PGEs (b) 20 ppm, dsDNA only immobilized on PGE (c) $4.6 \times 10^{-4}M$ of ADR only immobilized on PGEs (d) $4.6 \times 10^{-4}M$ of ADR with 20 ppm, dsDNA after interaction immobilized on PGEs (e) $9.2 \times 10^{-4}M$ of ADR with 20 ppm, of dsDNA after interaction immobilized on PGEs (f) $1.4 \times 10^{-3}M$ of ADR with 20 ppm, of dsDNA after interaction immobilized on PGEs (g) $1.8 \times 10^{-3}M$ of ADR with 20 ppm, of dsDNA after interaction immobilized on PGEs.

4.1.4 Scan Rate Studies of ADR at PGEs surface

The Cyclic voltammograms (Figure 4.4), indicated the behavior of Adriamycin immobilized on the PGEs. This study was carried out to investigate the redox reaction that occurred kinetically between ADR immobilized on the surface of PGEs / electrolytic solution, and to confirm whether diffusion is the only controlling factor for mass transport in the redox process or not. The oxidation and reduction peak of ADR on the cyclic voltammograms occurred at a peak position of 0.75V and 0.45V respectively. As the scan rate potential applied is increased, the oxidation and reduction peak signals also increases gradually. The linear correlation of this redox reaction and the effect of this direct proportionality of

increase in scan rates, indicates that there is a decrease in the size of diffusion layer on the electrode surface and the effect is seen in higher peak currents of the cyclic voltammograms (Rountree et al., 2018). Another importance of this study is in providing the suitable scan rate that could be used for the pH study which is 0.2V/s. At this scan rate, the peak current is at an average between the other scan rates applied from 0.02-0.45V/s (Antonio et al., 2013). The peak currents measured at this range, are seen to be directly proportional to the square root of the scan rate ($v^{1/2}$), indicating that the determining step by step reaction to the surface of the PGE is mass transport. This confirms that it is a freely diffusing reaction at the electrode surface, where the peak-to-peak separation observed were stable and also reproducible after different potential cycles. The redox reaction process is an electrochemically quasi-reversible electron transfer process (Antonio et al., 2013; Nandibewoor, 2015).

Randles Sevcik Equation:
$$I_p = 0.4463nFAC \left(\frac{nFvD}{RT}\right)^{1/2} \quad 4.1$$

The result of the linear relationship from the applied scan rates (0.02-0.45 Vs⁻¹) using cyclic voltammetry, demonstrated that the square root of scan rates have effect on the peak currents, which is a typical description of a diffusion controlled reaction process (Nandibewoor, 2015), and this can expressed in the equation.

$$I_p (\mu A) = 11.82v (V/s) - 0.39, r = 0.99 \quad 4.2$$

The logarithm plot of anodic peak current and scan rate showed a linear relationship having a slope of 0.57. This value is theoretically within the expected range of 0.5 for a purely diffused controlled current. The result further confirms the redox reaction to be diffusion controlled, where the electro-active species of ADR in the bulk solution diffuses to the electrode surface (Nandibewoor, 2015). This can be expressed also in the equation:

$$\text{Log } I_p (\mu A) = 0.57 \log v (V/s) - 0.63, r = 0.98 \quad 4.3$$

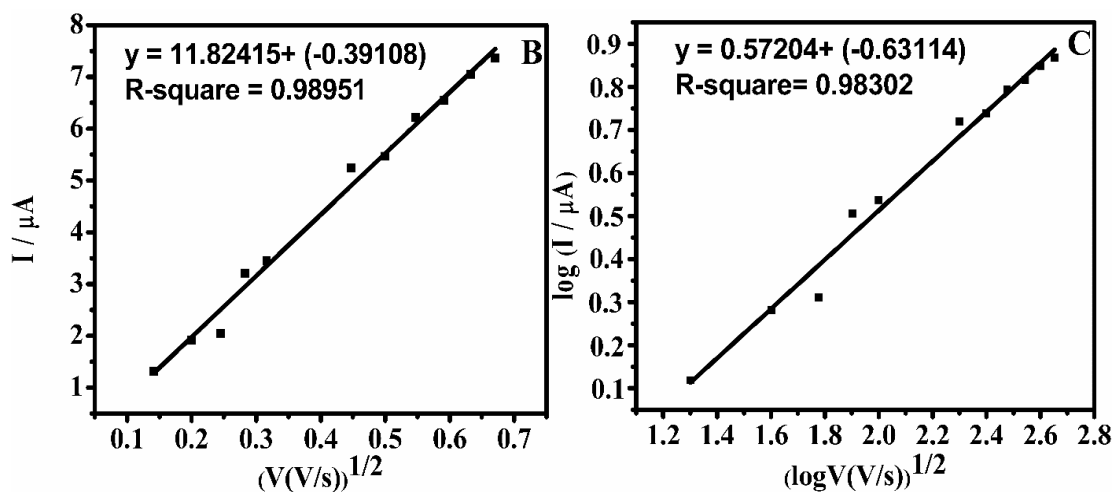
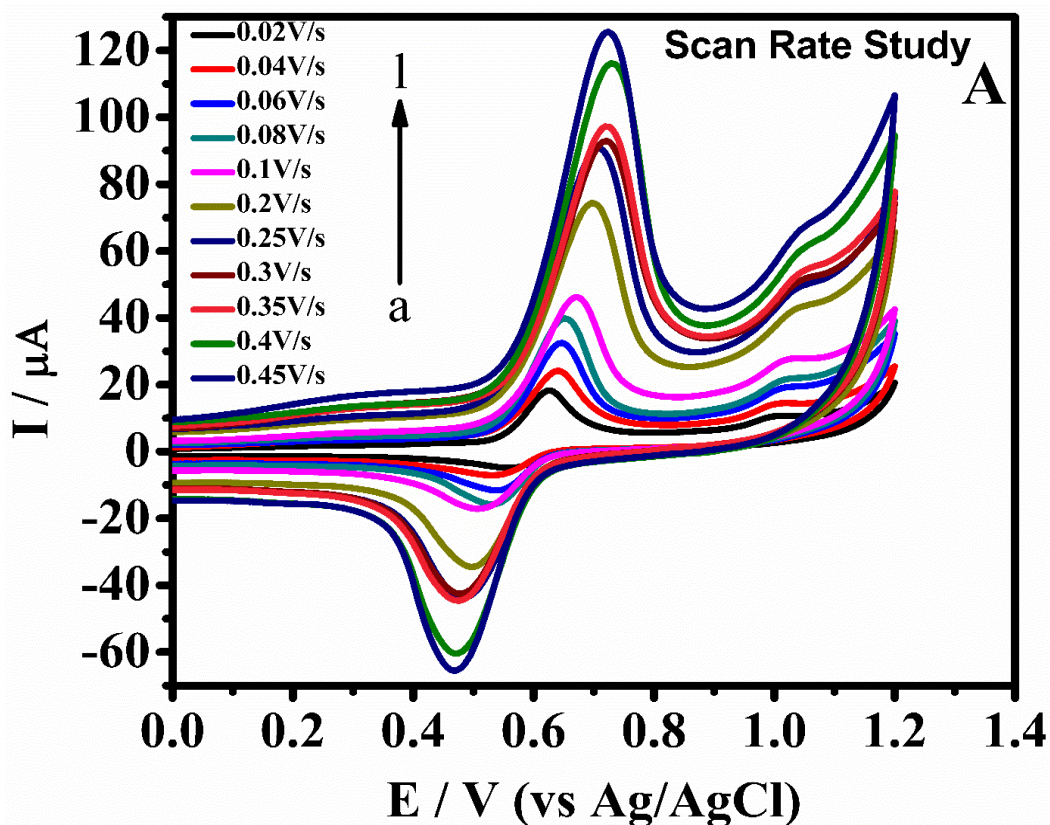
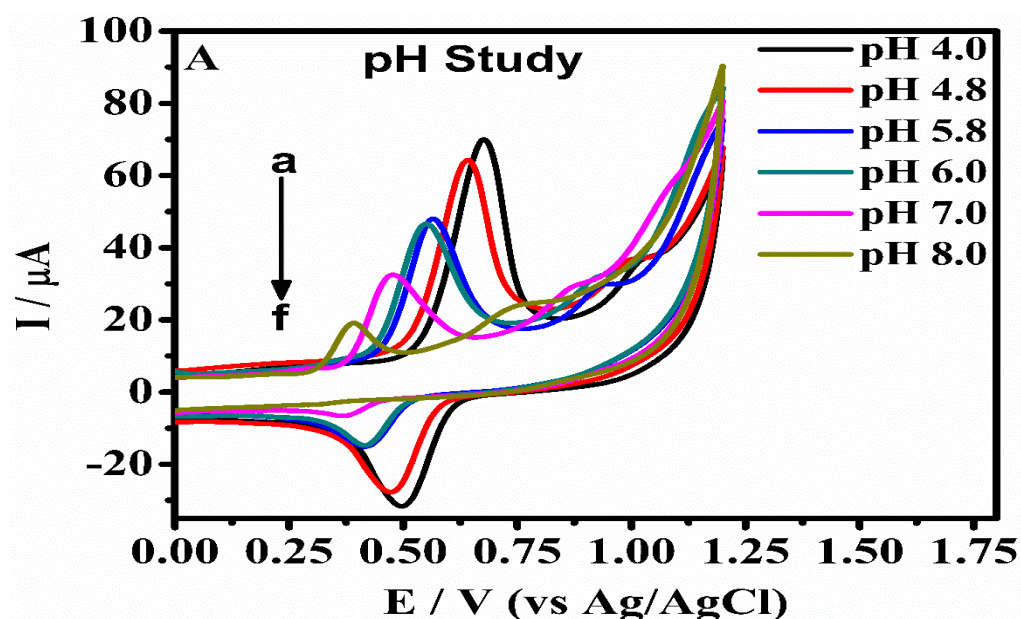


Figure 4.4. Scan rate study showing cyclic voltammograms of ADR at 9.2×10^{-4} M immobilized on the PGEs at different potential scan rates of (0.02, 0.04, 0.06, 0.08, 0.1, 0.2, 0.25, 0.3, 0.35, 0.4, 0.45)V/s in 0.5M phosphate buffer of pH 4.0. The influence of the square root of scan rate on the applied peak current in a linear relationship B and C and a logarithm plot of applied anodic peak current versus logarithm of scan rate in a linear relationship respectively.

4.1.5 pH studies of ADR at PGEs surface

The effect of pH on peak potential and peak current was investigated for ADR immobilised on the PGEs in 0.5M PBS. The varying pH values for the study, are within the range of 4.0, 4.8, 5.8, 6.0, 7.0 and 8.0 respectively. The shift in the peak potential (Figure 4.5) from 0.67V-0.39V, shows that the study was strongly pH-dependent and adsorption on the electrode surface occurred. The peak current is maximum at pH of 4.0, and decreases gradually as the pH values increases to pH 8.0. This correlation is also demonstrated from the error bar plots and the linear correlation for the pH study (Figure 4.5B and C). This decrease in the peak height, is as a result of increase in pH values which indicates that the thickness of diffusion layer to the electrode surface is decreased and adsorption to the electrode surface is also reduced. At pH 8.0, there is a decrease of the peak current of the ADR, this is due to the effect of electrostatic repulsion of the negatively charged ions thus restricting the electrochemical process between electrode surface and electrolyte solution. (Antonio et al., 2013).



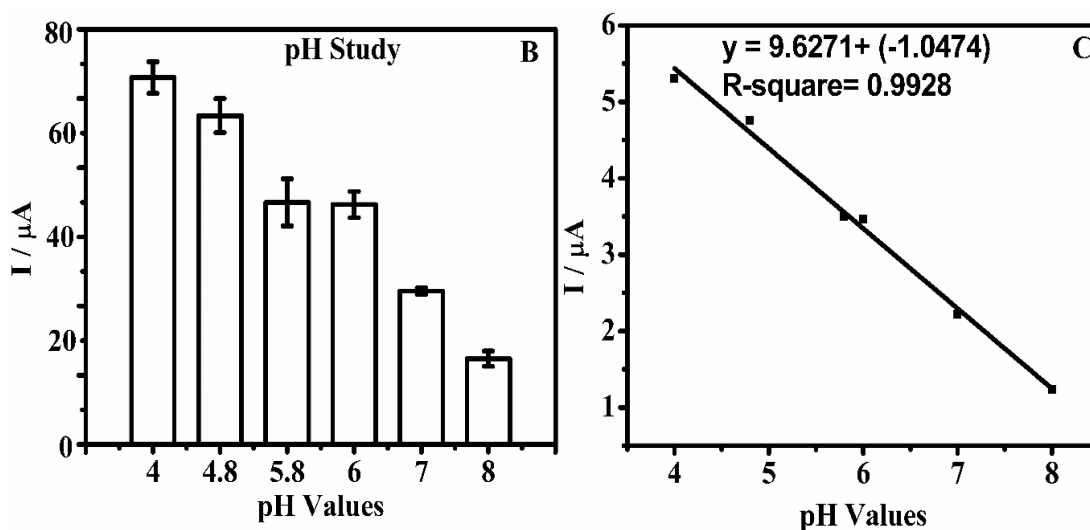


Figure 4.5: shows Cyclic voltammograms for the pH study and B and C demonstrate error bars charts and linear correlation to validate the effect of changes pH range on the ADR at $9.2 \times 10^{-4}\text{M}$, immobilized on PGEs with different pH values of 0.5M PBS in pH of 4.0, 4.8, 5.8, 6.0, 7.0 and 8.0 at a scan rate of 0.2V/s.

4.1.6 Limit of detection (LOD) and Limit of quantification (LOQ) of Adriamycin

The DPV method was used for the investigation the LOD and LOQ of ADR in 0.5M PBS pH 4.0. (Figure 4.6) demonstrates the result of the analysis on error bar plots and linear correlation of the limits. These values for LOD and LOQ were obtained from the analysis of the different concentrations of ADR from $9.19 \times 10^{-6}\text{M}$, $7.36 \times 10^{-6}\text{M}$, $5.5 \times 10^{-6}\text{M}$, $3.67 \times 10^{-6}\text{M}$, and $1.84 \times 10^{-6}\text{M}$. Below these concentrations, it was observed that there was a loss of linearity in the peaks obtained, which is caused by poor adsorption of the ADR on the surface of electrodes. The values for standard deviation, slope, and intercept of the calibration curve are 2.38 and -0.64 respectively. Limit of detection (LOD) and limit of quantification (LOQ) was used for validation of ADR. The following equations below were used for the calculations of the LOD and LOQ using the peak currents (M. Swartz and I. S. Krull, 1997; Riley, C. M., & Rosanske, 1996).

$$\text{LOD} = 3S_a/b, \quad 4.4$$

$$\text{LOQ} = 10S_a/b, \quad 4.5$$

Where 'Sa' represents the standard deviation, 'b' is the slope of our calibration curve. The values obtained for LOD and LOQ were $1.393 \times 10^{-6}\text{M}$, $4.221 \times 10^{-6}\text{M}$, respectively.

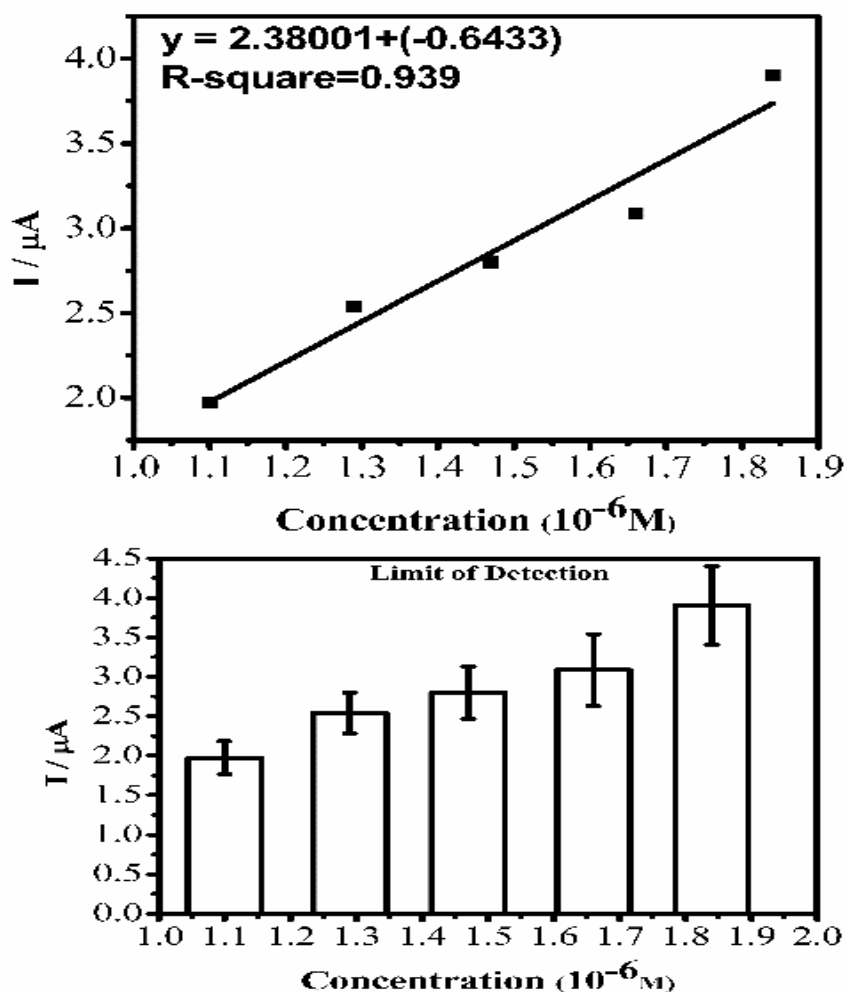


Figure 4.6. Showing the calibration curve and error bars charts of different concentrations of the ADR in the range of $9.19 \times 10^{-6}\text{M}$, $7.36 \times 10^{-6}\text{M}$, $5.5 \times 10^{-6}\text{M}$, $3.67 \times 10^{-6}\text{M}$, and $1.84 \times 10^{-6}\text{M}$ immobilized on the PGEs in 0.5M PBS pH 4.0 used for obtaining the LOD and LOQ.

4.2 Electrochemical Detection of Phenolic Compounds at CPE and MCPE

4.2.1 Electrochemical Behavior of the Phenolic Compounds at CPE and MCPE

The electrochemical behaviors of the selected phenolic compounds at the CPE and MCPE surface were studied using CV and DPV analysis. The differential pulse voltammograms (Figure 4.7) and the inset cyclic voltammograms show the electrochemical behavior of the

analytes at the surface of electrodes. The phenolic compounds show visible peak currents higher in MCPE and lower in CPE (Arduini et al., 2010; Sheng, Kai, Qian Zhang, Lantao Li, YiLun Wang, 2020; Tashkhourian & Nami-Ana, 2015). These electrochemical behaviors of the analytes observed from the peak currents, visibly shifting, could be suggested to be a result of the nanoparticles at the electrode surface increasing the current signal as a result of the catalytic effect of the nanoparticles, thus making the current signals to increase in the modified electrodes more than the unmodified electrodes (Chikere et al., 2020).

The anodic peak potentials (E_{pa}) and cathodic peak potentials (E_{pc}) observed from the CV analyses of the phenolic compounds (inset Figure 4.7) showed positions of oxidation and reduction potentials of the analytes. Sinapic acid presented positions of one E_{pa} , while syringic acid and rutin presented two positions of E_{pa} and E_{pc} ; the reduction peaks showed low current peak heights that are observed on the reverse scan. This behavior suggests that the oxidation reaction's product undergoes a further chemical reaction for syringic acid and rutin or is not reduced at the carbon paste electrode for sinapic acid (Tashkhourian & Nami-Ana, 2015). As the peak current is higher in MCPE than CPE, the shoulders of the peaks observed from MCPE are also broader than the CPE. This behavior can be suggested to be a result of increased electroactive surface area by incorporating the Fe_3O_4 nanoparticles (Chikere et al., 2020), which is similar to the results obtained from the determination of the electroactive surface area of the electrodes (Figures 4.9 and 4.10). If the modified electrode functioned as an electrocatalyst or the reaction was electro-catalyzed, there would have been a reduction in the peak potential, which suggests a reaction that is faster with a less overpotential (Chikere et al., 2020). The voltammetric behavior of the phenolic compounds is shown to agree with the chemical reaction proposed globally for phenolic group oxidation in aromatic compounds (Abdi et al., 2020; Chikere et al., 2020; Tashkhourian et al., 2013). The peak heights of the anodic peak current (I_{pa}) and cathodic peak currents (I_{pc}) of the analytes at CPE are lower compared to that of the MCPE, suggesting that the activity which occurred at the surface of the CPE is poor and less than the MCPE (Tashkhourian & Nami-Ana, 2015). The presence of Fe_3O_4 nanoparticles in the MCPE supports the transfer of electrons, enhances the current response, and can support the adsorption of the analyte and its enrichment onto the surface of the electrode, thereby promoting the oxidation process (Mirceski, Valentin, Rubin Gulaboski, Milivoj Lovric, Ivan Bogeski, Reinhard Kappl,

2013). The peaks obtained through DPV are shown to be better defined and have high sensitivity to low concentration of analytes and lower background current when compared to the results obtained using CV.

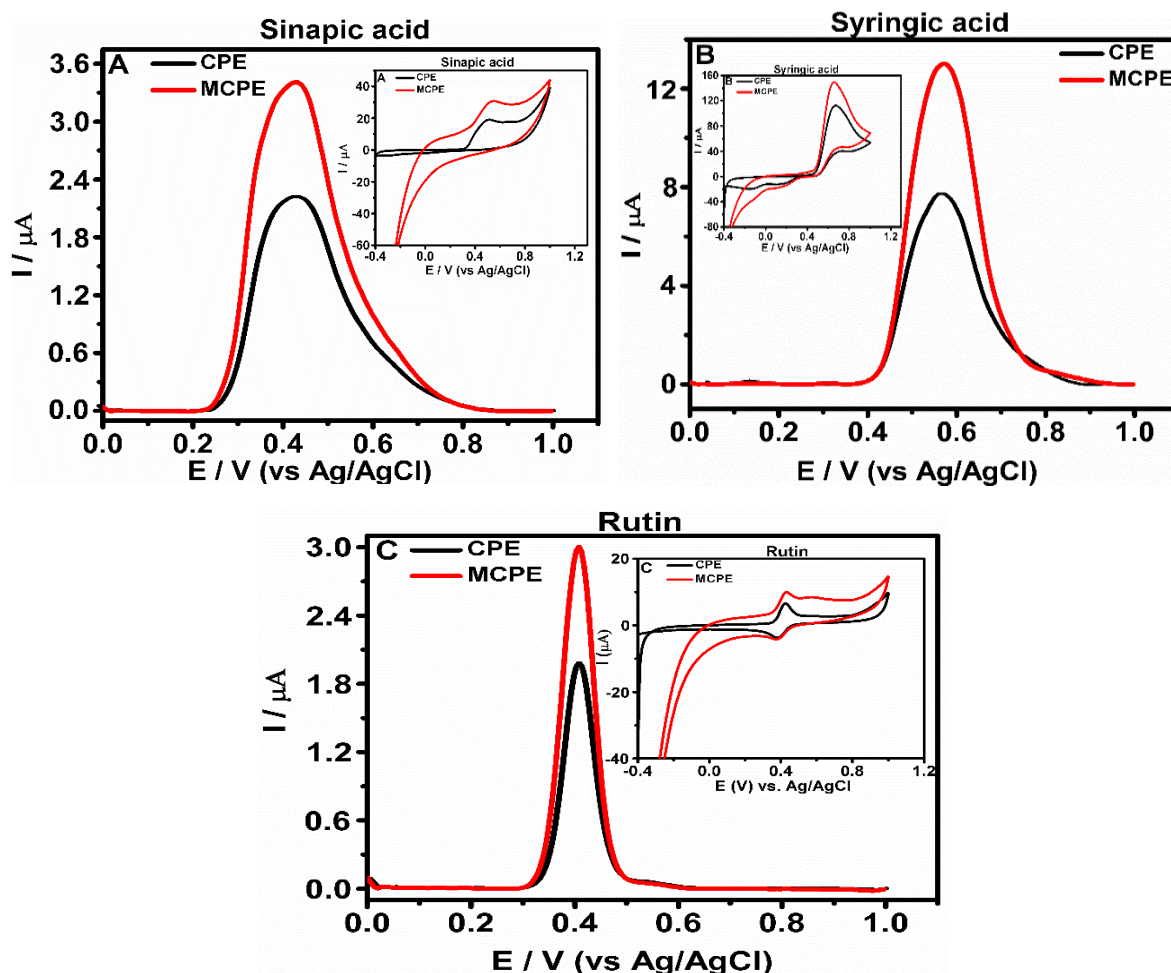


Figure 4.7. Differential pulse voltammograms (A–C) show the determination of the electrochemical behavior of the selected phenolic compounds of 0.9×10^{-3} M for sinapic, 1.0×10^{-3} M for syringic, and 0.3×10^{-3} M for rutin at carbon paste electrode (CPE) and carbon paste mixture prepared with Fe₃O₄ nanoparticles (MCPE) in 0.5 M ABS with pH 4.8, recorded at 0 V to +1.0 V. The inset cyclic voltammograms (A–C) of the selected phenolic compounds at CPE and MCPE was carried out in 0.5 M acetate buffer solutions (ABS) with pH 4.8 and recorded at a scan rate of 0.2 V s⁻¹.

The hydroxy groups of the phenols are oxidized through the transfer of two electrons, which form a quinone group after the liberation of 2H⁺. The phenolic compounds with one anodic

peak indicate an electrochemical behavior, which suggests an oxidation reaction that leads to the formation of a stable quinone group, which is reduced on the reversed scan (Figure 4.8A). This is also similar to the hydroxy group's oxidation of other phenolic compounds at their ortho position (Golabi & Zare, 1999). However, the phenolic compounds with two anodic peaks indicate the formation of a semiquinone radical in the first step. The second peak corresponds to the oxidation of the semiquinone to the quinone group. The Fe₃O₄ nanoparticles provide stability for the complete oxidation of the phenolic compounds (Souza et al., 2011; Tashkhourian & Nami-Ana, 2015) (Figure 4.8B).

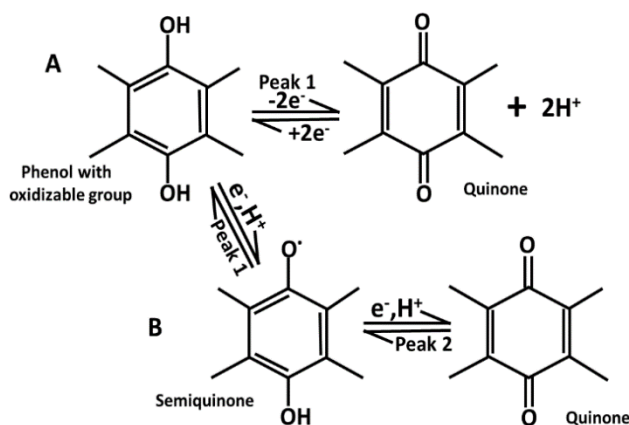


Figure 4.8. The chemical reaction process showing the oxidation of phenolic compounds having one peak in the reaction path (A) and the oxidation of phenolic compounds having two peaks in the reaction path (B).

4.2.2 Evaluation of the Electroactive Surface Area

The electroactive surface area of the electrodes CPE and MCPE were determined using CV in 1 mM K₄ [Fe (CN)₆], which was used as an electrochemical redox probe in 0.1 M KCl. MCPE displayed an enhancement of the current response (Figure 4.9), which indicates that the CPE's electrochemical active sites were increased on surface modification by the Fe₃O₄ nanoparticles. The MCPE presented a larger current response ($I_{pa} = 15.20 \mu\text{A}$) in comparison to the CPE current response ($I_{pa} = 8.64 \mu\text{A}$); this can be attributed to the electrocatalytic activity and enhancement of the modified surface area. The cyclic voltammograms of CPE (Figure 4.10A) and MCPE (Figure 4.10B) show that the oxidation and reduction potentials were shifted to more positive and more negative potentials, respectively, with a linear increase of the redox peak current as the scan rate is enhanced

from 0.1 to 0.2 V/s. The plot of I_{pa} versus $v^{1/2}$ (Figure 4.10C and D) shows linearity with an R^2 value of 0.9963 for CPE and 0.9830 for MCPE. The electrodes' electroactive surface area was estimated according to the slope of I_{pa} versus $v^{1/2}$ for a known concentration of $K_4Fe(CN)_6$ using the Randles–Sevcik equation (Monnappa et al., 2020).

$$I_{pa} = 2.69 \times 10^5 n^3/2 A C_0 D^{1/2} v^{1/2} \quad 4.6$$

I_{pa} : indicates anodic peak current (A), n : the number of electrons exchanged during the redox process, which is presumed to be equal to one, A : surface area of the electrode (cm^2), C_0 : concentration of the redox probe ($mol\ cm^{-3}$), D : diffusion coefficient assumed to be equal to $6.23 \times 10^{-6}\ cm^2\ s^{-1}$, and from the slopes of I_{pa} - $v^{1/2}$ relation, the microscopic electroactive surface area was calculated to be MCPE ($0.043\ cm^2$) in comparison with the CPE ($0.015\ cm^2$). The results show that the presence of Fe_3O_4 nanoparticles increased the active surface area of the electrode.

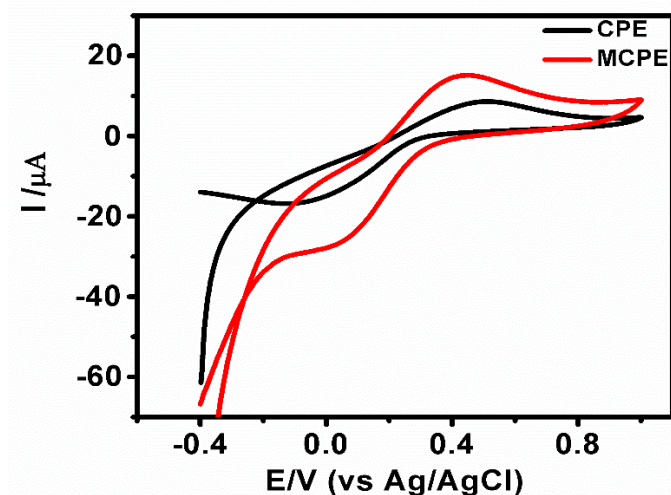


Figure 4.9. Cyclic voltammogram shows the response of 1 mM $K_4[Fe(CN)_6]$ at the CPE and MCPE at a scan rate of 0.1 V/s.

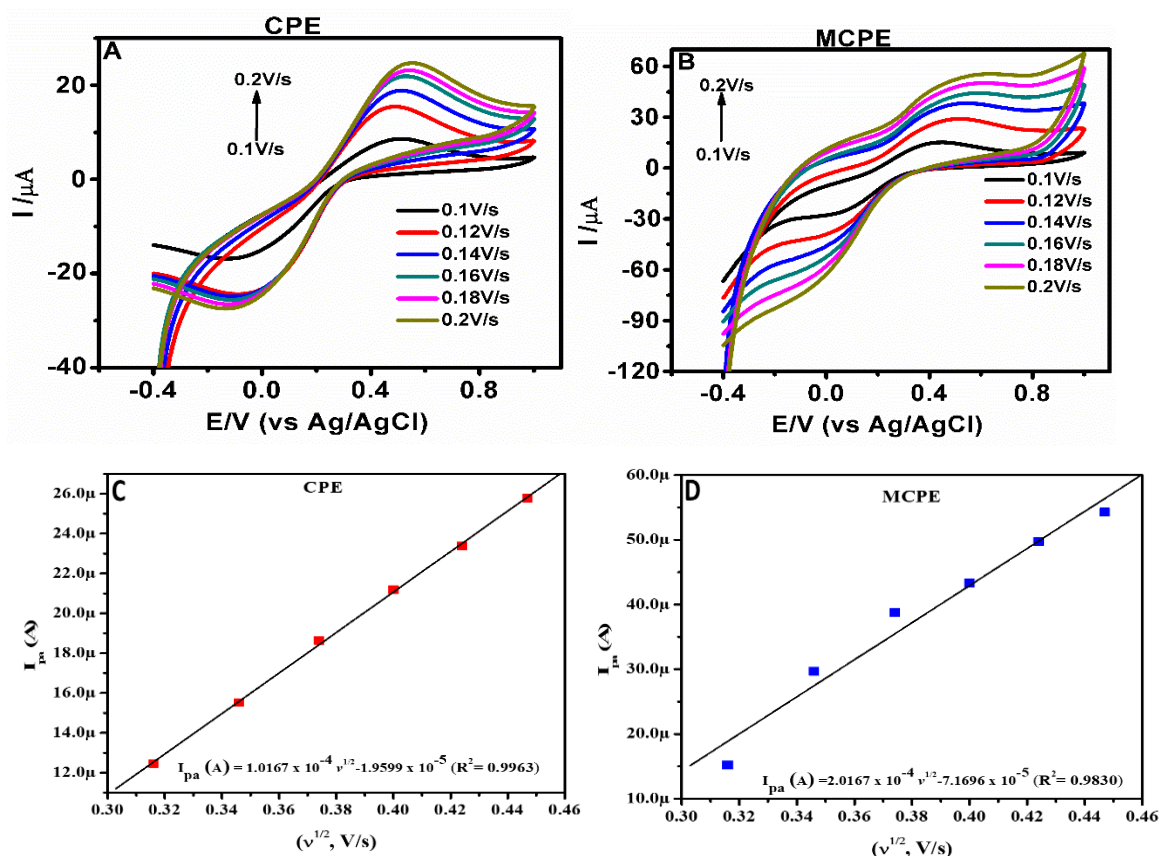


Figure 4.10. Cyclic voltammograms at (A) CPE and (B) MCPE, respectively in 1 mM $K_4[Fe(CN)_6]$ of 0.1 M KCl by varying scan rates (0.1–0.2 V/s). The corresponding Plots of I_{pa} vs $v^{1/2}$ at (C) CPE and (D) MCPE.

4.2.3. Effect of pH on the Phenolic Compounds Oxidation at CPE and MCPE

The effect of pH of the buffer solution on the current response of phenolic compounds oxidation at CPE and MCPE was studied using CV to observe their electrochemical behaviors (Figure 4.11). The pH of the different buffer solutions affected the oxidation activity of the phenolic compounds on the surface of CPE and MCPE, thereby causing changes to the electrochemical behavior of the phenolic compounds. This effect can be seen (Figure 4.11), as the anodic peak currents and potentials of the phenolic compounds on the CPE and MCPE showed a progressive decrease with increasing pH values from 2.6 to 9.2 (Compton & Banks, 2010). The cyclic voltammograms of the phenolic compounds showed

a clear pH dependence of their electrochemical behavior at the surface of the electrodes, as the increase in the pH of the ABS gradually lead to a decrease of the anodic peak current.

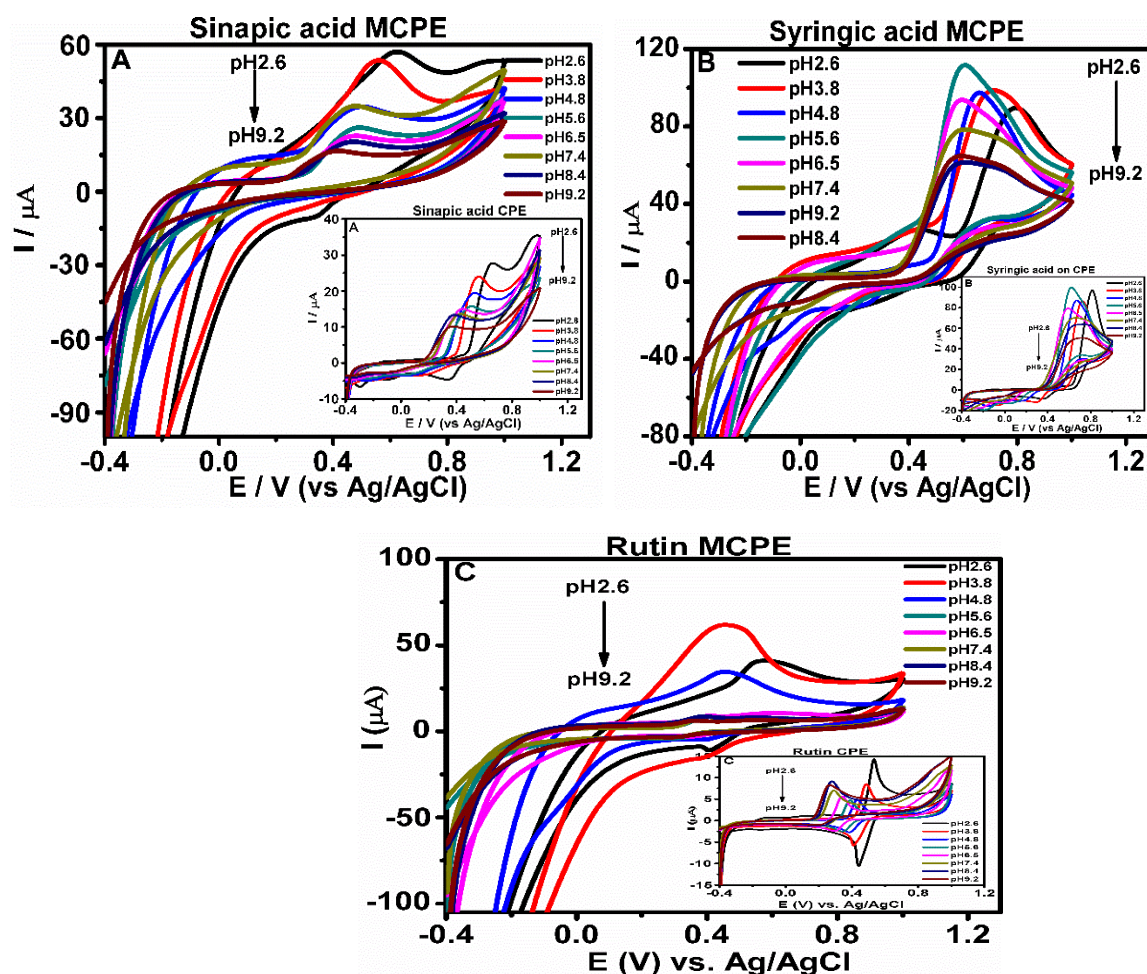


Figure 4.11. Cyclic voltammograms (A–C) show the effect of pH on the electrochemical behavior of the phenolic compounds, in 0.5 M acetate buffer of pH 2.6, 3.8, 4.8, 5.6, 6.5, 7.4, 8.4, and 9.2, at a scan rate of 0.2 V/s with a reversible scanning potential range of –0.4 to 1.0 V. The inset figures show cyclic voltammetry (CV) at CPE.

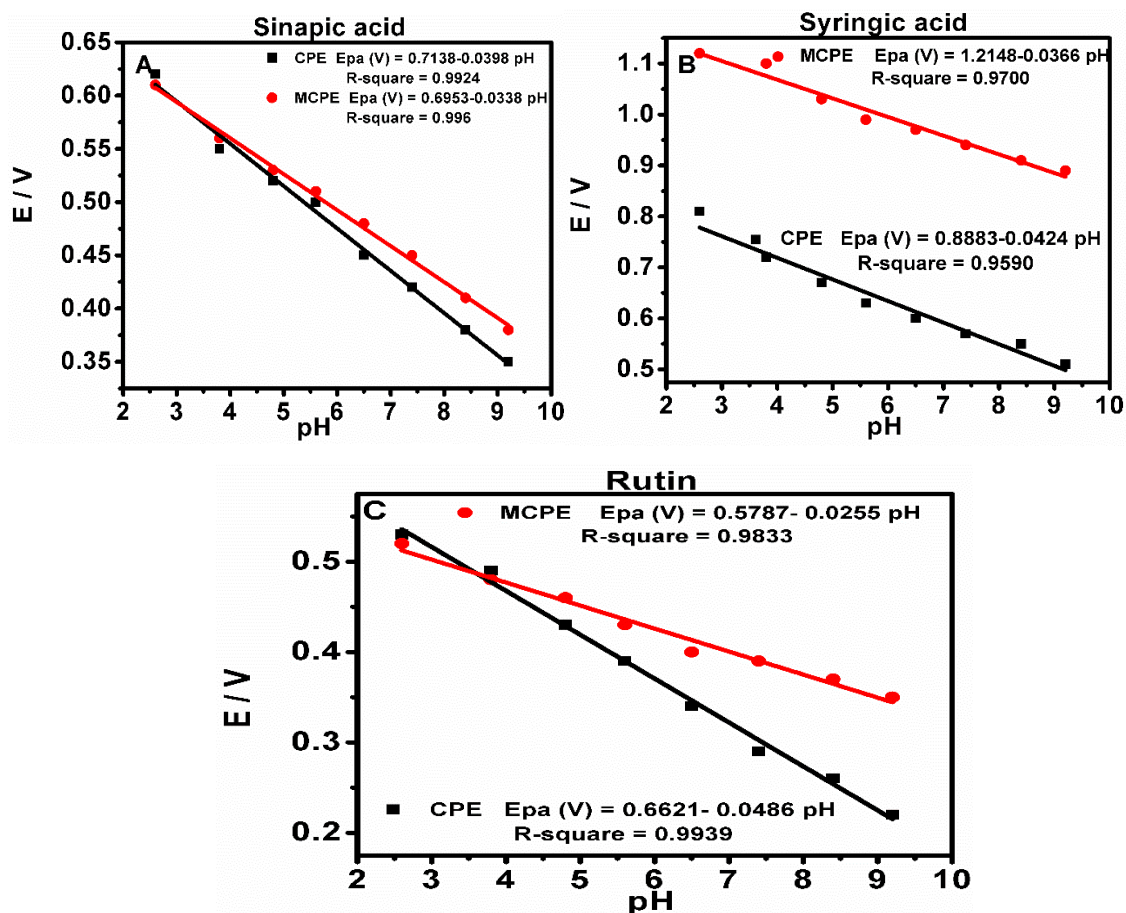


Figure 4.12. The linear regression plots for both CPE and MCPE to show the effect of pH on the electrochemical behavior of the phenolic compounds, in 0.5 M acetate buffer of pH 2.6, 3.8, 4.8, 5.6, 6.5, 7.4, 8.4 and 9.2, at a scan rate of 0.2 V/s.

As the buffer solution's pH increases, there is a gradual negative shift of the peak potentials, which shows a linear relationship between the pH values and Epa (Compton & Banks, 2010). The relationship between the anodic peak potentials Epa and the pH values were studied, and the plots produced showed a linear regression relationship with an equation having values for the phenolic compounds presented (Table 4.1 and Figure 4.12). All of the values produced from the slope of Epa/pH of the regression line are compared to the Nernstian value of 59 mV/pH and 29.5 mV/pH, which shows the number of electron and protons involved in oxidation/reduction reaction for two-electron/two-proton process and two-electron/one-proton process (Compton & Banks, 2010; Manuel M. Baizer & Henning Lund, 1972; Monnappa et al., 2020; Zare, H. R., 1999). The electrochemical behavior could further

be explained by the fact that at low pH value, the concentration of the analytes protonated form oxidized is high and increases with decreasing the pH (Giacomelli et al., 2002). This supports the ease of oxidation reaction and enhances mass transport at the surface of the electrode. When the pH is increased, the current begins to gradually decrease, which could be suggested to be a result of the decrease of the protonated form concentration (Giacomelli et al., 2002).

Table 4.1. Linear regression equation of anodic peak potentials Epa and pH of the phenolic compounds with their slopes respectively reported for cyclic voltammetry method employed in determining the pH on the electrochemical behavior of the phenolic compounds at bare CPE and MCPE.

Phenolic Compounds	Regression Equation of Anodic Peak Potentials Epa and the pH	R ² Value	Slope of Epa/pH mV/pH	Nernstian Value mV/pH
Sinapic acid (CPE)	Epa (V) = 0.7138–0.0398 pH	0.9924	40	59
Sinapic acid (MCPE)	Epa (V) = 0.6953–0.0338 pH	0.996	34	59
Syringic acid (CPE)	Epa (V) = 0.8883–0.0424 pH	0.9590	42	59
Syringic acid (MCPE)	Epa (V) = 1.2148–0.0366 pH	0.9700	37	59
Rutin (CPE)	Epa (V) = 0.6621–0.0486 pH	0.9939	49	59
Rutin (MCPE)	Epa (V) = 0.5787–0.0255 pH	0.9833	26	59

4.2.4. Effect of Scan Rate on the Phenolic Compounds Oxidation at CPE and MCPE

The influence of scan rate on the electro-oxidation behavior of the phenolic compounds at CPE and MCPE surface was demonstrated using CV (Figure 4.13). The voltammograms show an increase in the peak current signals with increased applied scan rates. The values measured for the peak current were used for plotting linear equation of peak current I_p versus square root of scan rate $\nu^{1/2}$, which indicated a typical diffusion-controlled reaction (Table 2 and Figure 4.14). Another plot of the peak currents I_p versus scan rate (ν) both for anodic and cathodic peak currents using same experimental conditions was performed and yielded

a straight line (Table 2 and Figure 4.15) which is typical for adsorption controlled. As the scan rate applied increases, the peak currents for anodic and cathodic also increase linearly, indicating a quasi-reversible oxidation reaction (Greef R, Peat R, Peter LM, Pletcher D, 1985).

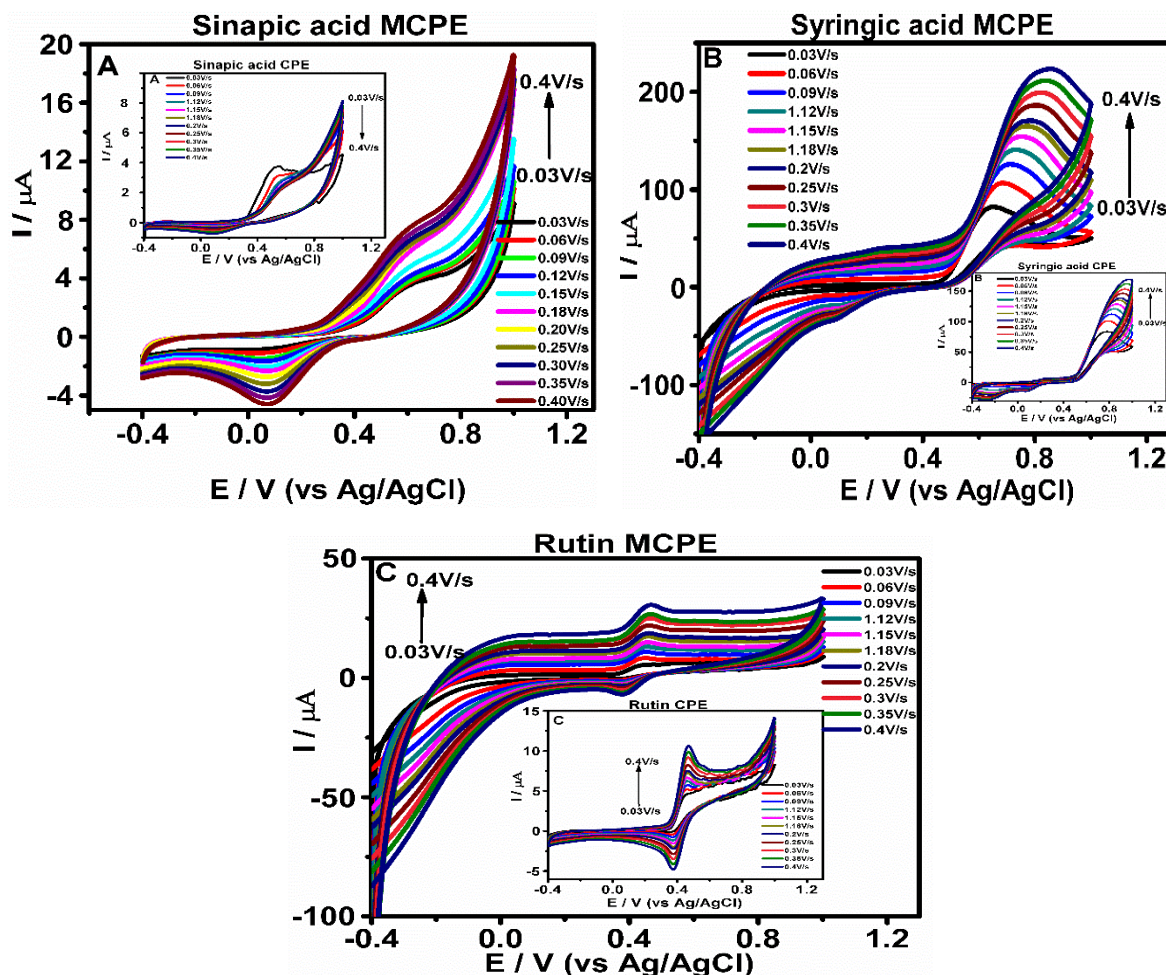


Figure 4.13. Cyclic voltammograms showing the electrochemical oxidation and reduction behavior of phenolic compounds at CPE and MCPE in 0.5 M of ABS having pH 4.8 and scan rates of 0.03, 0.06, 0.09, 0.12, 0.15, 0.18, 0.20, 0.25, 0.3, 0.35, and 0.40 V/s, respectively, with a reversible scanning potential range of -0.4 to 1.0 V.

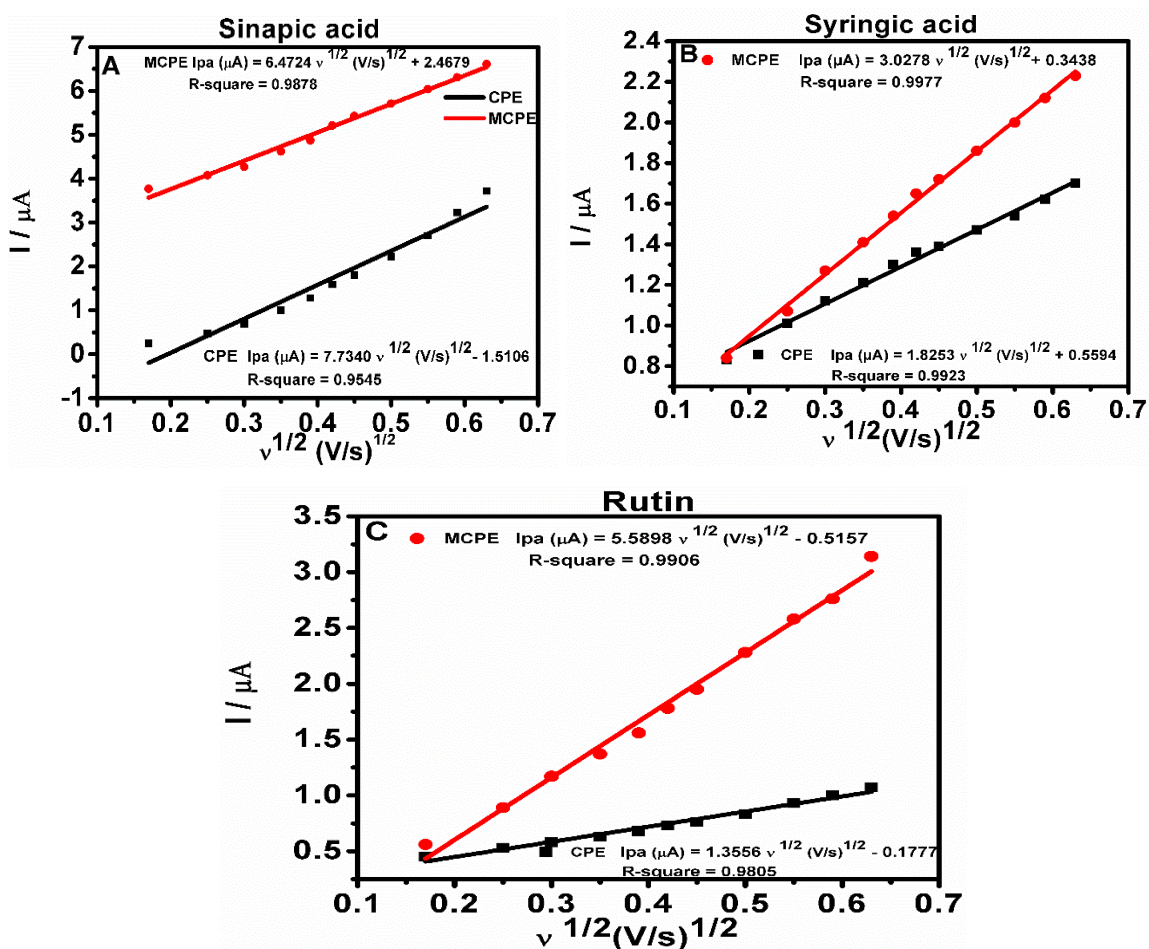


Figure 4.14. Linear regression plots of phenolic compounds showing the dependence of redox (anodic and cathodic) peak current I_p on the square root of scan rate $v^{1/2}(\text{V/s})^{1/2}$. The plots, represents controlled diffusion at CPE and MCPE in 0.5 M of ABS with pH 4.8, scan rate of 0.03, 0.06, 0.09, 0.12, 0.15, 0.18, 0.20, 0.25, 0.3, 0.35 and 0.40 V/s.

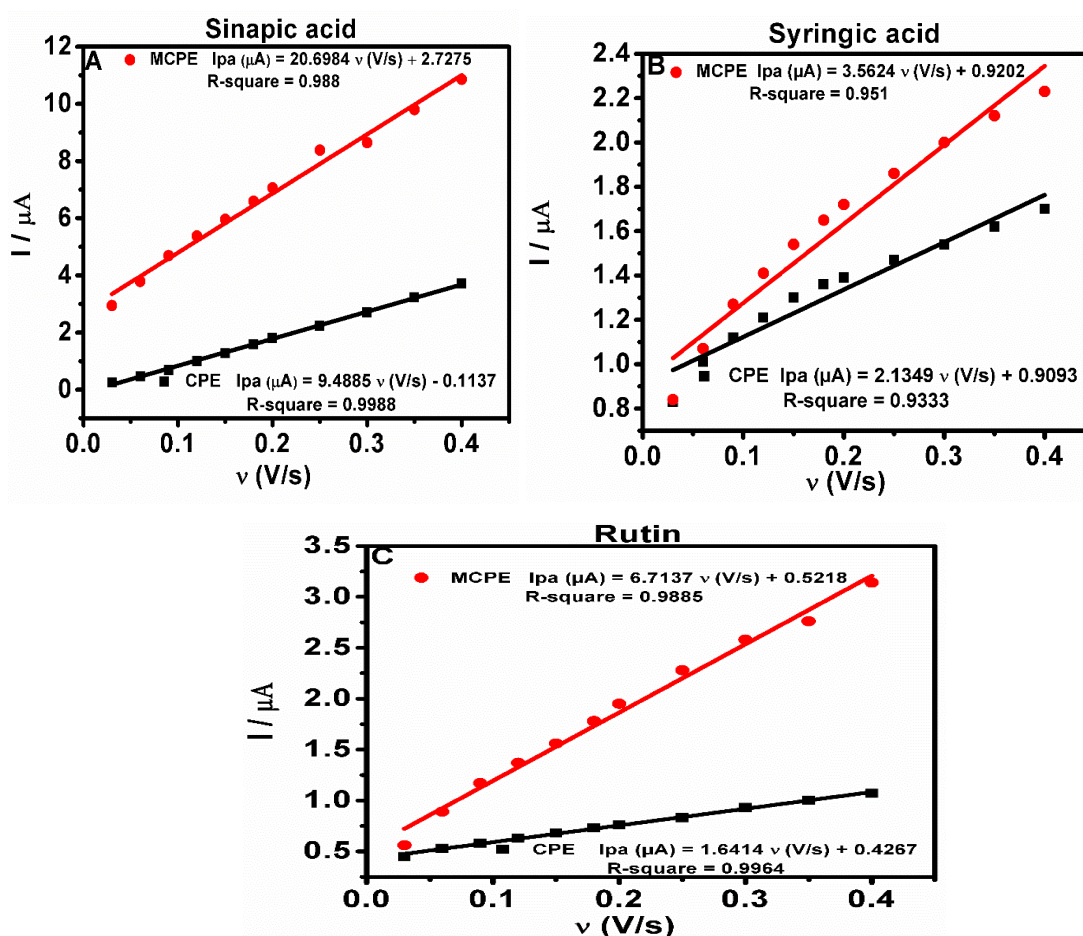


Figure 4.15. Linear regression plots showing the dependence of redox (anodic and cathodic) peak current on scan rate I_p versus scan rate v (V/s) for controlled adsorption. The plots represent controlled adsorption at CPE and MCPE in 0.5 M of ABS with pH 4.8, scan rate of 0.03, 0.06, 0.09, 0.12, 0.15, 0.18, 0.20, 0.25, 0.3, 0.35 and 0.40 V/s respectively with a reversible scanning potential range of -0.4 to 1.0 V.

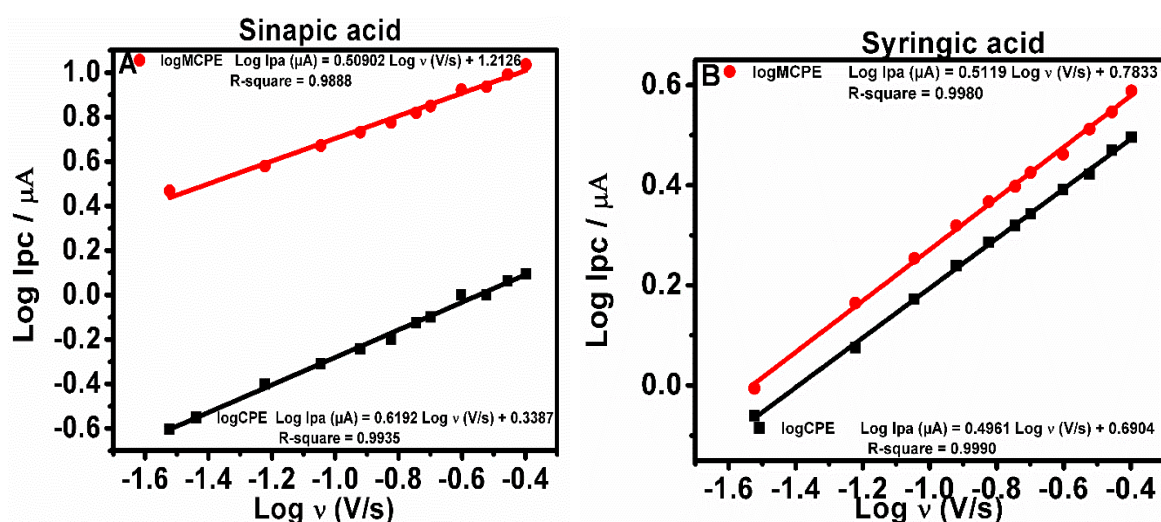
Table 4.2. Linear regression equations show the dependence of redox peak current I_p on the square root of scan rate $v^{1/2}$ (V/s) $^{1/2}$ for controlled diffusion and dependence of redox peak current I_p on scan rate v (V/s) for controlled adsorption for phenolic compounds at bare CPE and MCPE with their slopes and R-square values.

Phenolic Compounds	Regression Equation	R2 Value	Regression Equation	R2 Value
	I_p on $v^{1/2}$ (V/s) $^{1/2}$		I_p Versus Scan Rate v (V/s)	
	Controlled Diffusion		Controlled Adsorption	
Sinapic acid (CPE)	$I_p (\mu A) = 7.7340 v^{1/2} - 1.5106$	0.9545	$I_p (\mu A) = 9.4885 v - 0.1137$	0.9988

Sinapic acid MCPE)	$I_{pa} (\mu A) = 17.1927 v^{1/2} - 0.4542$	0.9848	$I_{pa} (\mu A) = 20.6984 v + 2.7275$	0.9880
Syringic acid (CPE)	$I_{pa} (\mu A) = 1.8253 v^{1/2} + 0.5594$	0.9923	$I_{pa} (\mu A) = 2.1349 v + 0.9093$	0.9333
Syringic acid (MCPE)	$I_{pa} (\mu A) = 3.0278 v^{1/2} + 0.3438$	0.9977	$I_{pa} (\mu A) = 3.5624 v + 0.9202$	0.9510
Rutin (CPE)	$I_{pa} (\mu A) = 1.3556 v^{1/2} - 0.1777$	0.9805	$I_{pa} (\mu A) = 1.6414 v + 0.4267$	0.9964
Rutin (MCPE)	$I_{pa} (\mu A) = 5.5898 v^{1/2} - 0.5157$	0.9906	$I_{pa} (\mu A) = 6.7137 v + 0.5218$	0.9885

CPE = Carbon Paste Electrode, MCPE = Iron oxide modified carbon paste electrode, I_{pa} = Anodic peak current, $v^{1/2}$ = Square root of scan rate, $(V/s)^{1/2}$ = square root of volt per second.

The logarithm of anodic peak current and logarithm of scan rate ($\log I_{pa}$ versus $\log v$) approach was used to confirm whether the electrochemical reaction at the electrode surface is diffusion or adsorption controlled (Table 3 and Figure 4.16) using linear relationship plots. The values of the slopes obtained were close to 0.5, which is attributed to electrochemical reactions that are diffusion-controlled (Chrzescijanska, Ewa, Edyta Wudarska, Elzbieta Kusmierek, 2014; P.T. Kissinger, 1996; Timbola, Ana Karina, C. D. Souza, C. Soldi, M. G. Pizzolatti, 2007).



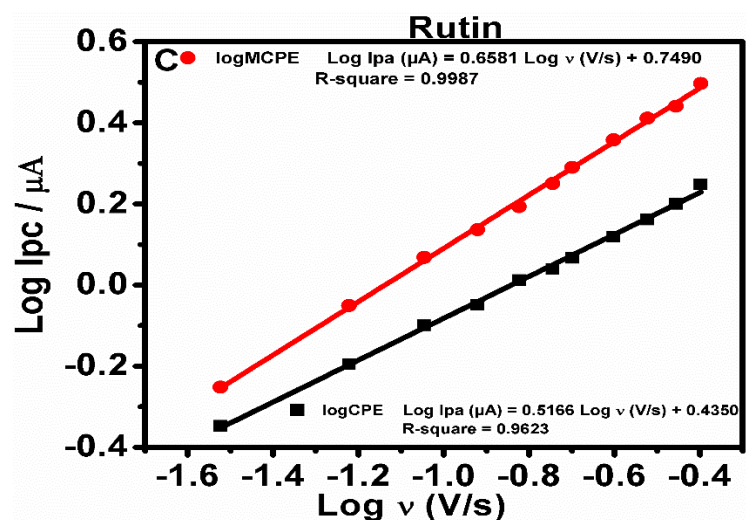


Figure 4.16. The linear relationship plots of logarithm of peak current and logarithm of scan rate ($\log I_{pa}$ versus $\log v$) for phenolic compounds. The plots, represents peak current and logarithm of scan rate at CPE and MCPE.

Table 4.3. Linear regression equation showing the logarithm of anodic peak current and logarithm of scan rate ($\log I_p$ versus $\log v$ (V/s) for the phenolic compounds at CPE and MCPE with their slopes and R-square values.

Phenolic Compounds	Regression Equation log I _{pa} Versus log v (V/s)	R ² Value
Sinapic acid (CPE)	$\text{Log } I_{pa} (\mu\text{A}) = 0.6192 \text{ Log } v + 0.3387$	0.9935
Sinapic acid (MCPE)	$\text{Log } I_{pa} (\mu\text{A}) = 0.5090 \text{ Log } v + 1.2126$	0.9888
Syringic acid (CPE)	$\text{Log } I_{pa} (\mu\text{A}) = 0.49611 \text{ Log } v + 0.6904$	0.9990
Syringic acid (MCPE)	$\text{Log } I_{pa} (\mu\text{A}) = 0.5119 \text{ Log } v + 0.7833$	0.9980
Rutin (CPE)	$\text{Log } I_{pa} (\mu\text{A}) = 0.5168 \text{ Log } v + 0.4350$	0.9976
Rutin (MCPE)	$\text{Log } I_{pa} (\mu\text{A}) = 0.6581 \text{ Log } v + 0.7490$	0.9987

4.2.5. Characterization of CPE and MCPE Using EIS

The EIS was used to study the difference in the behavior of the CPE and the MCPE. This method is an effective tool used to study the electrode/solution interface properties and how charge transfer occurs between the redox solution/electrode interface. Both electrodes were measured in the redox solution of $[\text{Fe}(\text{CN})_6]^{3-/4-}$ (5 mM) containing 1 M KNO_3 , using

the frequency range of 100 kHz–0.1 Hz, to evaluate the charge transfer resistance (R_{ct}) of electrodes which corresponds to the Randles equivalent circuit (Figure 4.17 inset). R_s represents solution resistance, R_{ct} is charge transfer resistance, C_{dl} is double-layer capacitance, and W is Warburg impedance. The Nyquist plots (Figure 4.17) demonstrate the semicircles of CPE and MCPE.

The R_{ct} values for CPE and MCPE were 15.32 k Ω and 6.84 k Ω , respectively. The R_{ct} value for CPE that is the largest, indicates a very slow electron transfer rate between the redox solution and the electrode interface. The R_{ct} value offered at MCPE implies fast charge transfer. The results suggest that the nanoparticles' presence can facilitate electron transfer between the electrode surface and the redox solution, thereby increasing electroconductibility. Hence, Fe₃O₄ nanoparticle was very efficient for developing an electrochemical sensor for the analysis of phenolic compounds (Chikere et al., 2020; Madhusudhana et al., 2020; Tashkhourian, J., SF Nami Ana, S. Hashemnia, 2013) .

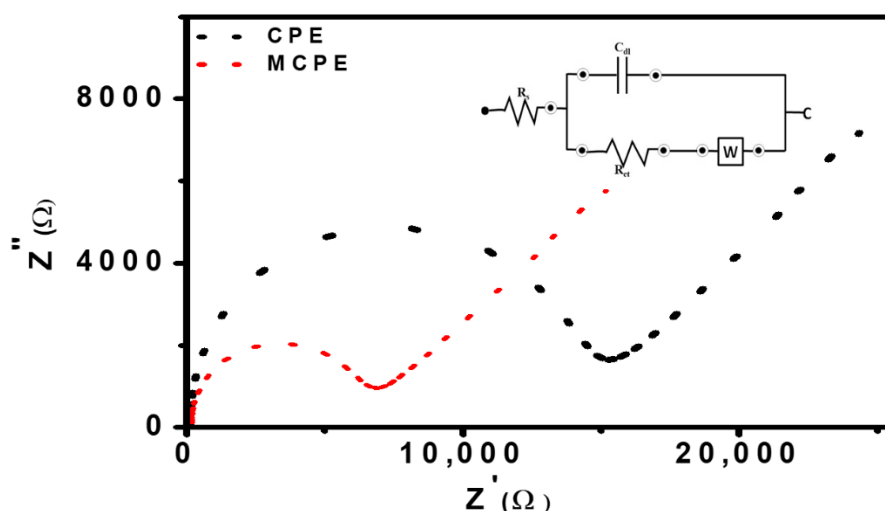


Figure 4.17. Nyquist plots represent the EIS measurement performed in the frequency range of 100 kHz–0.1 Hz, in a redox solution of 5 mM [Fe(CN)₆]^{3-/4-} containing 1 M KNO₃ using CPE and MCPE for surface characterization. The inset figure is the equivalent circuit showing resistors and capacitor (c).

4.2.6. Application of Gold Screen-Printed Electrode for Rapid Validation Test of Phenolic Compounds Using Cyclic Voltammetry

The gold screen-printed electrode was applied in the detection of rutin and sinapic acid using cyclic voltammetry technique in 0.5 mol L⁻¹ ABS with a pH value of 4.8, at a scan rate of 0.2 V/s in a reversible potential sweep range of -0.4 to +1.0 V. This analysis was performed as a rapid test for the detection of these phenolic compounds and to compare the results with the CPE and MCPE because of its reproducibility, sensitivity, accuracy, and avoidance of preparation and cleaning process. The voltammograms of the rutin and sinapic acid on the electrode surface (Figure 4.18) indicate an overlay of the gold screen-printed electrode, CPE and MCPE. The sensitivity of the gold screen-printed electrode to the concentration of the phenolic compounds is compared to CPE and MCPE used, using the current density (J) = Current Intensity (A)/Cross-sectional Area (cm²). The surface area was taken using πr^2 and divided by the value of current response for sinapic and rutin from the three electrodes used. For sinapic acid, the current density obtained is 0.1012×10^{-3} A/cm² for gold screen-printed electrode, 0.1541×10^{-3} A/cm² for CPE and 0.2466×10^{-3} A/cm² for MCPE, for rutin the current density obtained is 0.0499×10^{-3} A/cm² for gold screen-printed electrode, 0.0538×10^{-3} A/cm² for CPE, and 0.0801×10^{-3} A/cm² for MCPE. The result could also be suggested that the gold screen-printed active mass surface area is smaller than that of the CPE and MCPE. The use of the gold screen-printed electrode is important for future applications in the manufacture of electrochemical food sensor devices, which can detect different compounds present in food substances.

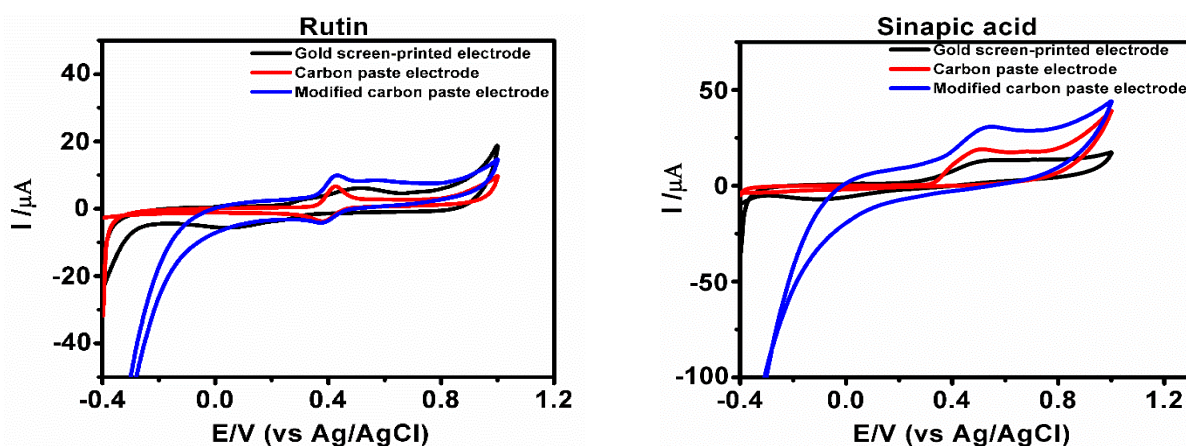


Figure 4.18. Cyclic voltammograms show an overlay of the gold screen-printed electrode with CPE and MCPE of the phenolic compounds rutin and sinapic acids in 0.5 M ABS of pH 4.8 at a scan rate of 0.2 V/s with a reversible scanning potential range of -0.4 to 1.0 V.

4.2.7. Effect of Concentration on the Phenolic Compounds Oxidation at CPE and MCPE

The effect of increasing the concentration of the phenolic compounds on their oxidation signals at MCPE was studied using DPV. The results were used to determine the limit of detection (LOD) and limit of quantification (LOQ) of the voltammetric method optimized for the quantification of the phenolic compounds on the modified carbon paste electrode surface. The phenolic compounds used in this work were investigated in a range of concentration from 0.3×10^{-6} – 13.0×10^{-6} M. The Equations (1) and (2) were used to calculate the limit of detection and limit of quantification of the phenolic compounds using the peak currents, respectively.

$$\text{LOD} = 3 * \text{Sa}/b, \quad 4.7$$

$$\text{LOQ} = 10\text{Sa}/b \quad 4.8$$

Where “b” is the slope of our calibration curve, and “Sa” represents the standard deviation.

The recorded oxidation signals of the phenolic compounds increased with a gradual increase in the concentration of the phenolic compounds ranging from 0.3×10^{-6} – 13.0×10^{-6} M. The results obtained showed a linear relationship between peak currents and the change in concentration of the phenolic compounds. The following are the linear regression equations of the phenolic compounds: $I_p = 1.3982 C + 1.2362$ (I_p : μA , C : mol L^{-1} and $R^2 = 0.9865$) for sinapic acid, $I_p = 0.1457 C + 0.7410$ (I_p : μA , C : mol L^{-1} and $R^2 = 0.9851$) for syringic acid, and $I_p = 0.7163 C + 0.6859$ (I_p : μA , C : mol L^{-1} and $R^2 = 0.9860$) for rutin. The proposed method for the phenolic compounds detection limit is compared with the maximum levels of antioxidants, within a range of 20 to 1000 ppm (20 to 1000 mg L^{-1}) that are permitted within the guidelines for food taken within the EU and North America (Parliament, 2004). The detection limits of the developed DPV method for the phenolic compounds were calculated. The values were compared with other data reported by other research groups (Table 4.4), where rutin was reported with other acids, but less or no work has been reported on sinapic acid and syringic acid, respectively.

Table 4.4. Limits of detection (LOD) and limit of quantification (LOQ) reported for the differential pulse voltammetry method employed in detecting phenolic compounds compared to other methods used.

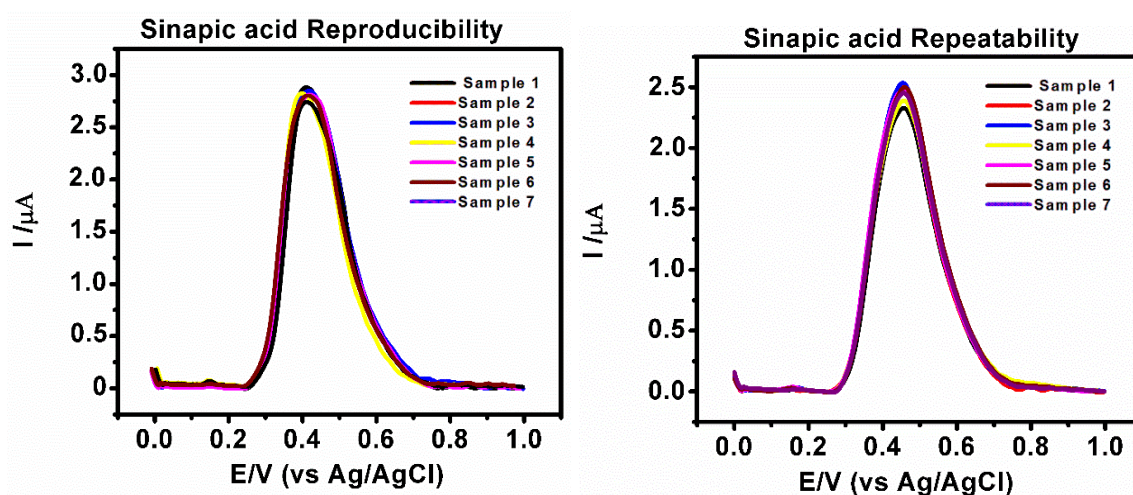
Electrode	Method	Phenolic Compounds	Linear Dynamic Range (M)	Limit of Detection (M)	Limit of Quantification (M)	Ref.
Ni-GO/GCE	SQWV	Rutin	1.1×10^{-8} to 1.0×10^{-6}	3.2×10^{-9}	--	(Karabiberoglu & Dursun, 2018)
CTAC/Gr/PdNPs	SQWV	Rutin	0.02×10^{-6} to 1.0×10^{-6}	0.005	\times --	(Sheng et al., 2020)
GCE/EAuNPs/rGO/Naf	CV, LSV, EIS	Sinapic	20×10^{-6} to 200×10^{-6}	33.43	\times --	(Kumar et al., 2020)
CPE/Fe ₃ O ₄ NPs	DPV	Rutin	0.3×10^{-6} to 3.0×10^{-6}	0.8×10^{-7}	2.5×10^{-7}	This work
CPE/Fe ₃ O ₄ NPs	DPV	Sinapic	0.9×10^{-6} to 8.0×10^{-6}	2.2×10^{-7}	6.7×10^{-7}	This work
CPE/Fe ₃ O ₄ NPs	DPV	Syringic	1.0×10^{-6} to 9.1×10^{-6}	2.6×10^{-7}	8.0×10^{-7}	This work

CPE = Carbon Paste Electrode, MCPE = Iron oxide nanoparticles modified carbon paste electrode, mol L⁻¹ = moles per liter, GCE/EAuNPs/rGO/Naf = Glassy Carbon Electrode, Electrochemically tuned gold nanoparticles and reduced graphene oxide (rGO) Ref. = References, Ni-GO/GCE = Nickel nanoparticles incorporated with graphene oxide composite-glassy carbon electrode, CTAC = cetyltrimethylammonium chloride, DPV = Differential Pulse Voltammetry, CV = Cyclic Voltammetry, SQWV = Square Wave Voltammetry.

4.2.8. Reproducibility, Repeatability, and Stability

The sensor's reproducibility was investigated by using the MCPE for the determination of 0.9×10^{-3} M for sinapic acid, 1.0×10^{-3} M for syringic acid, and 0.3×10^{-3} M for rutin, respectively, using DPV in 0.5M ABS pH 4.8. Seven independent electrodes were used to

determine each analyte. The relative standard deviations (RSD) were found to be 4.2% for sinapic acid, 3.6% for syringic acid, and 4.6% for rutin (Figure 4.19), hence showing good reproducibility. The repeatability was also investigated using seven prepared modified electrodes in seven prepared samples for each analyte, and the relative standard deviations of the peak currents were found to be 3.1% for sinapic acid, 4.2% for syringic acid, and 4.2% for rutin, hence indicating good repeatability (Figure 4.19). Three modified electrodes were prepared for the determination of the stability of the sensor. A potential of 0.6 V was applied using the chronoamperometry method for each analyte with the above concentration at the modified electrode for 30 min, respectively (Figure 4.20). These potentials are comparable to the phenolic compounds' oxidation potentials of the CV analysis results done previously from this study. The amperometric response observed remained constant throughout the experiment. The surface of the electrodes did not undergo any fouling; hence, this attests to the proposed sensor's stability (Madhusudhana et al., 2020). The stability was again analyzed using the above concentrations of the analytes using DPV on the first day using two modified electrodes, which was then stored for 10 days at room temperature in the laboratory. The electrodes were then used to determine the same concentration of the phenolic compounds after 10 days. The respective voltammograms on the 1st day and 10th day of the modified electrodes (Figure 4.20) demonstrated good stability with relative standard deviation values of 3.85% for sinapic acid, 4.54% for syringic acid, and 7.17% for rutin, respectively.



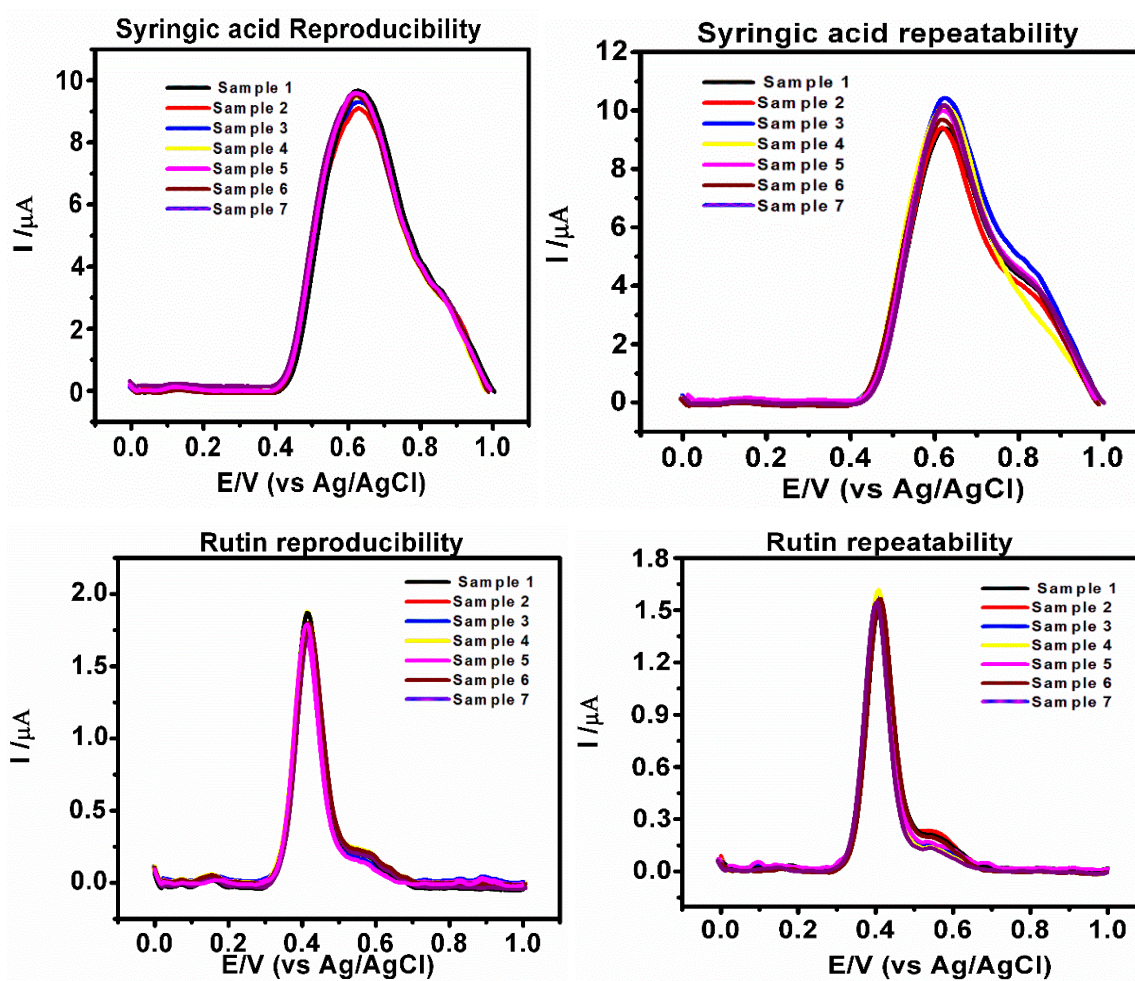
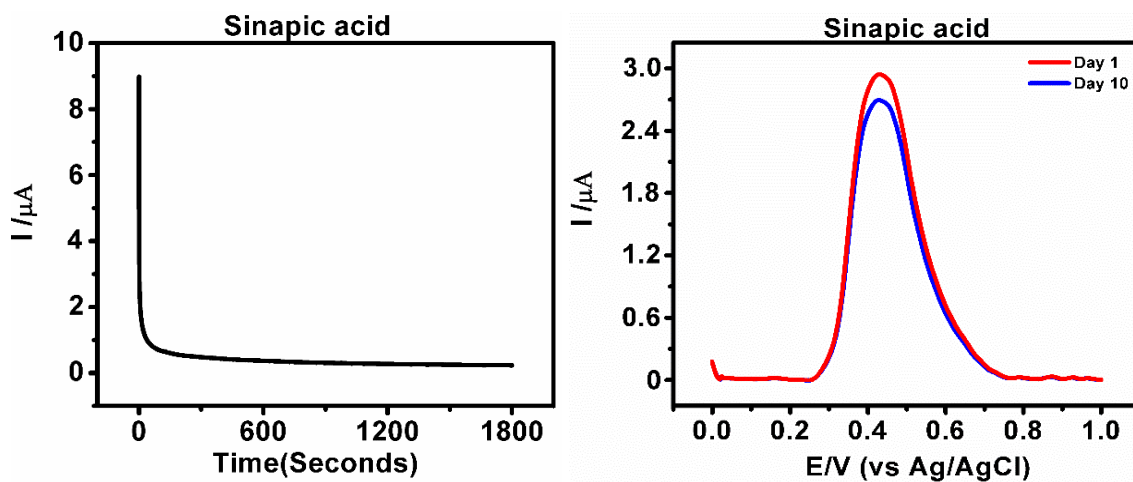


Figure 4.19. Differential voltammograms showing the reproducibility and repeatability of MCPE for the determination of the phenolic compounds respectively.



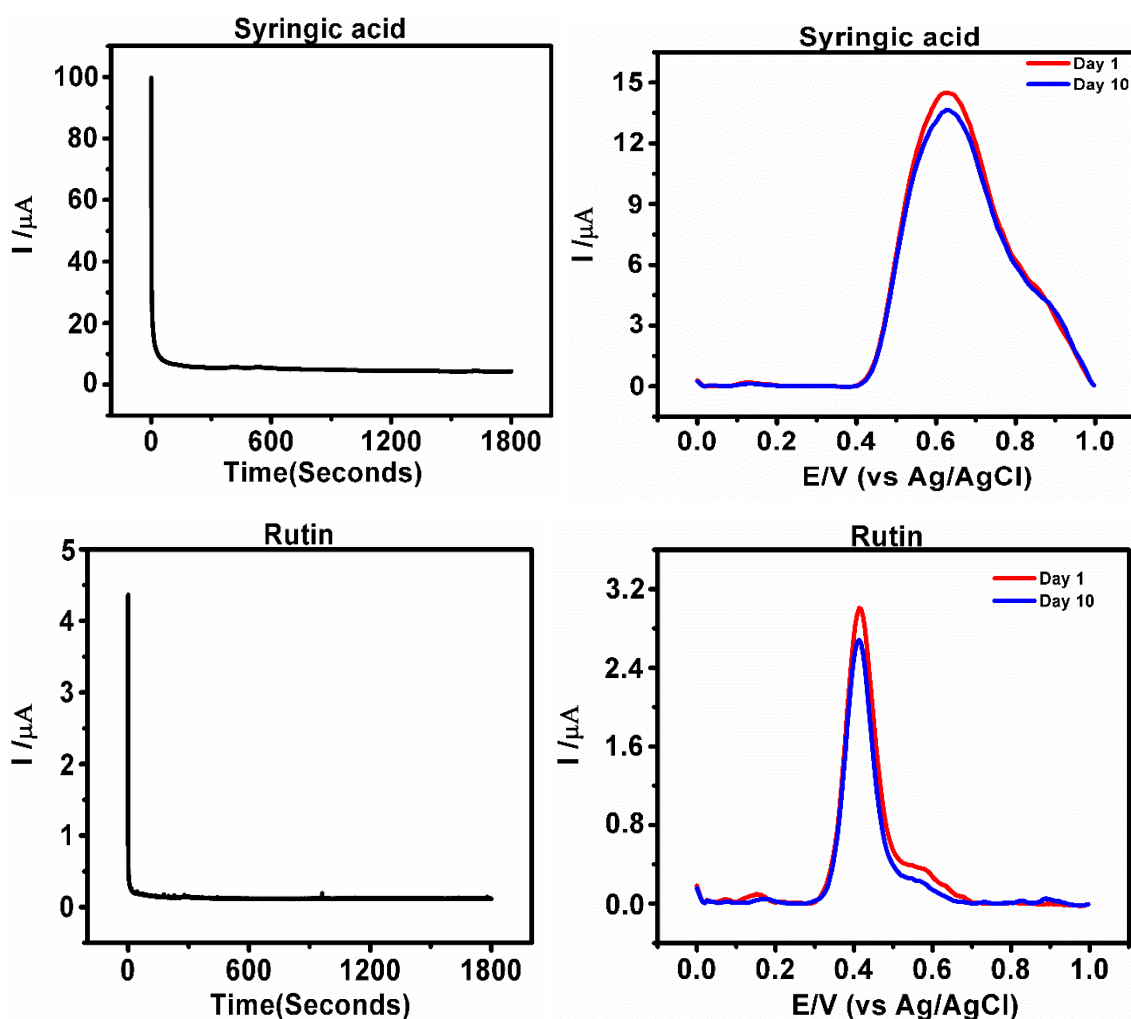


Figure 4.20. A steady amperometric current response for determination of stability of the sensor for phenolic compounds detection in (0.5 M ABS of pH 4.8), for 30 minutes, at MCPE using 0.6V potential. Differential pulse voltammograms shows the determination of 0.9×10^{-3} M for sinapic, 1.0×10^{-3} M for syringic and 0.3×10^{-3} M for rutin respectively in 0.5M ABS pH 4.8 for 1st day and 10th to show stability of the modified electrode.

4.2.9. Selectivity of the Electrode

To evaluate the selectivity of the fabricated sensor in identifying the analytes of interest, the effects of possible interferences were investigated by analyzing a standard solution of 0.9×10^{-3} M for sinapic, 1.0×10^{-3} M for syringic, and 0.3×10^{-3} M for rutin respectively in 0.5M ABS pH 4.8. Common inorganic ions such as K^+ , Cl^- , Fe^{+3} , and Ca^{+2} , had no

significant interference in determining the phenolic compounds with an RSD of the oxidation peaks obtained to be less than 5% (Table 4.5). Other potential electroactive organic interferences, such as caffeic acid and 4-hydroxybenzoic acid, which may co-exist with the analytes, were also examined. These organic interferences with their concentration increased about 500-fold excess did not meaningfully change the oxidation peak currents of the analytes of interest, and the RSD values obtained were less than 5% (Table 4.5). Therefore, MCPE can be used for the selective determination of sinapic acid, syringic acid, and rutin.

Table 4.5. Effect of various interferences on the determination of sinapic, syringic, and rutin.

Interfering Species	Sinapic (RSD%)	Acid Syringic Acid (RSD%)	Rutin (RSD%)
K ⁺	±4.99	±3.75	±4.03
Cl ⁻	±1.95	±3.00	±4.78
Fe ⁺³	±4.27	±4.76	±3.99
Ca ⁺²	±4.34	±4.26	±2.20
caffeic acid	±4.85	±3.43	±4.98
4-hydroxybenzoic acid	±3.56	±3.40	±2.74

4.2.10. Simultaneous Detection of the Phenolic Compounds at MCPE

DPV was used to study all the three phenolic compounds (sinapic acid, syringic acid, and rutin) simultaneously to observe their electro-oxidation behavior at MCPE (Figure 4.21). The analytes presented oxidation potentials similar and within the same potential with the oxidation potentials of other results in this study, where the analytes were analyzed individually. This result showed that the modified electrode has an ability to detect the presence of all the three phenolic acids simultaneously in the solution.

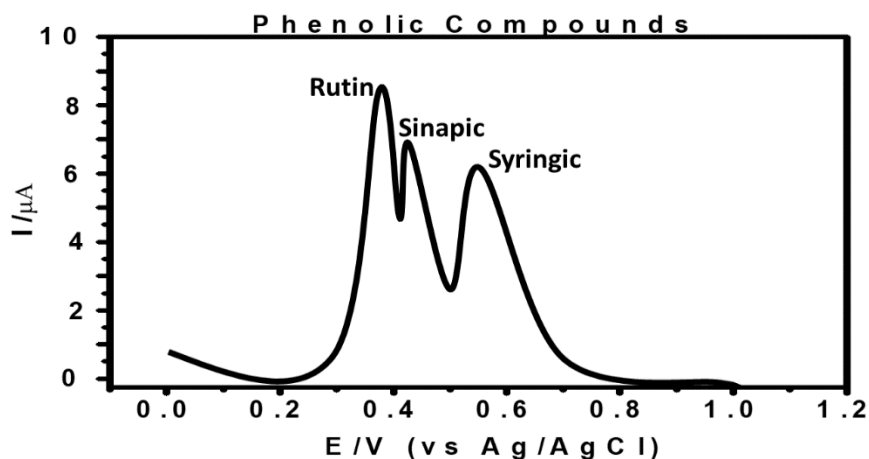


Figure 4.21. Differential pulse voltammogram showing three phenolic compounds' simultaneous determination with 4.5×10^{-3} M for sinapic acid, 5.1×10^{-3} M for syringic acid, and 1.6×10^{-3} M for rutin respectively at MCPE in 0.5 M ABS with pH 4.8, recorded at 0 V to +1.0 V.

4.2.11. Application of CPE and MCPE on Phenolic Compounds Detection in Red and White Wines

The determination of the presence of the phenolic compounds in red and white samples, respectively, was done using MCPE. This study was carried out with diluted 10 mL samples of red and white wine, which served as blanks. CV and DPV of the red and white wine samples were analyzed (Figure 4.22) using the modified electrode without the presence of the standard phenolic compounds to observe if these particular commercial wine samples that were purchased contained sinapic, syringic, and rutin. The sensor used detected that the wine samples did not contain the presence of the phenolic compounds of interest; instead, they contained other antioxidants or sulphites, indicating oxidation potentials that seem to appear as the analyte of interest. The CV of the wine samples showed little anodic peaks, while the DPV was able to indicate the presence of some other compounds, which were not the standard phenolic compounds used except sinapic acid in red wine, which has a very low concentration. Aliquots of the known concentration of phenolic compounds (sinapic, syringic, and rutin) through the standard addition method were then added to the wine samples to observe the modified electrode's detection ability. The wine samples analysis was carried out with DPV (Table 4.6), and the results of the analysis of wine samples suggest

the activity of oxidation that occurred. However, as the spiked wine concentrations were increased, there was an increase in the oxidation peaks of the phenolic compounds in the red and white wine. The modified electrode detected the presence of the added standard phenolic compounds in both white and red wine samples with recoveries at almost 100%.

Table 4.6: Results of the determination of phenolic compounds in wine samples (red and white wine) using Fe₃O₄ nanoparticles modified CPE.

Samples	Rutin				Sinapic acid			
Red Wine	$I_p = 19.1695x + 0.0045, R_2 = 0.9992$				$I_p = 10.6158x + 0.1531, R_2 = 0.9995$			
	Added (mmol L ⁻¹)	Found (mmol L ⁻¹)	Recovery (%)	Relative Error	Added (mmol L ⁻¹)	Found (mmol L ⁻¹)	Recovery (%)	Relative Error
	0	Undetected	-	-	0	0.0002	-	-
	0.03	0.0294	98	±2	0.03	0.0295	98.33	±1.67
	0.05	0.0504	100.8	±0.8	0.05	0.0503	100.6	±0.6
Syringic acid	$I_p = 9.5979x + 0.198, R_2 = 1$							
	Added (mmol L ⁻¹)	Found (mmol L ⁻¹)	Recovery (%)	Relative Error				
	0	0	-	-				
	0.03	0.03	100	±0				
	0.05	0.05	100	±0				
Samples	Rutin				Sinapic acid			
White Wine	$I_p = 26.8763x + 0.0022, R_2 = 0.9999$				$I_p = 19.2895x + 0.00995, R_2 = 0.9960$			
	Added (mmol L ⁻¹)	Found (mmol L ⁻¹)	Recovery (%)	Relative Error	Added (mmol L ⁻¹)	Found (mmol L ⁻¹)	Recovery (%)	Relative Error
	0	Undetected	-	-	0	Undetected	-	-
	0.03	0.0302	100.67	±0.67	0.03	0.0313	104.3	±4.33
	0.05	0.0499	99.8	±0.2	0.05	0.0492	98.4	±1.6

Syringic acid

$$I_p = 19.7829x + 0.0047, R^2 = 0.9992$$

Added (mmol L ⁻¹)	Found (mmol L ⁻¹)	Recovery (%)	Relative Error
0	Undetected	-	-
0.03	0.0306	102	±2
0.05	0.0496	99.2	±0.8

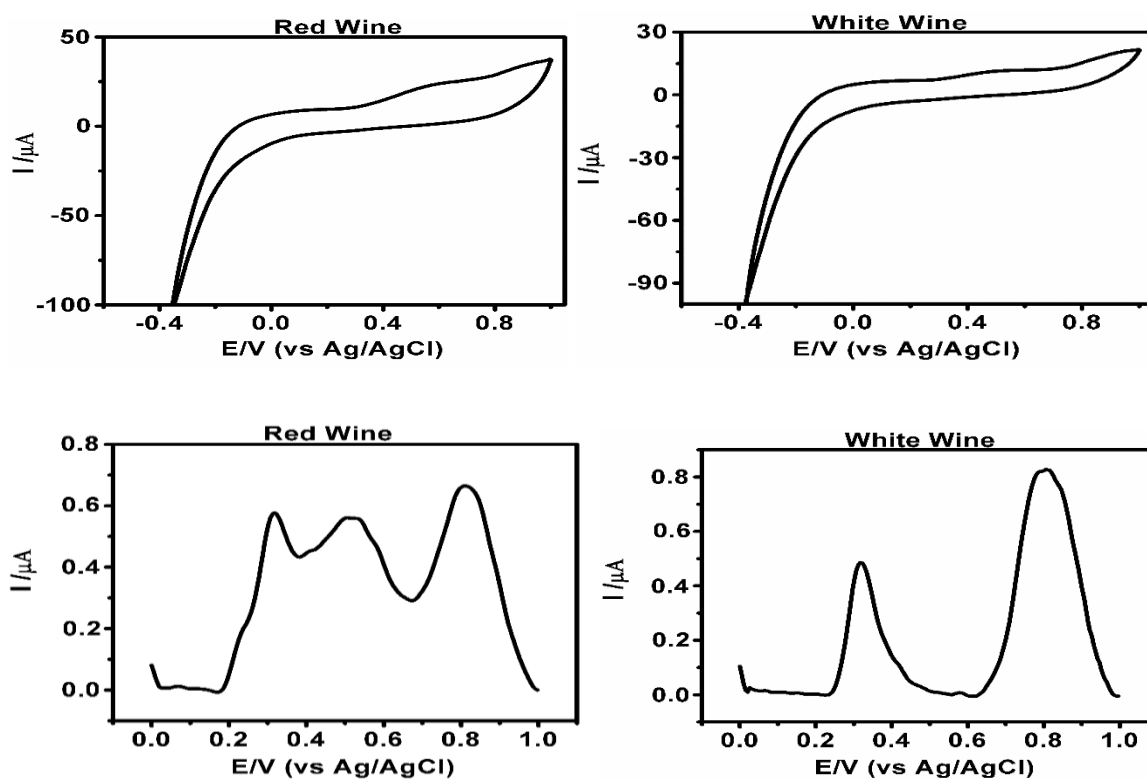


Figure 4.22. Cyclic voltammograms and Differential pulse voltammograms showing the determination of red and white wine real samples only using the modified electrode in 0.5M ABS pH 4.8 as supporting electrolyte.

CHAPTER 5

CONCLUSION

The results obtained from the DPV and EIS analysis showed that interaction between the ADR and dsDNA occurred and were adsorbed to the surface of the PGEs. This is indicated in the decrease of the guanine peak signal from the figures in the results. This work demonstrated the effect increase in the concentration of ADR on dsDNA during the interaction. There was also a correlation between the DPV results and the EIS measurements where with increase in the concentration of ADR there was decrease in charge transfer resistance, solution resistance and increase in solution conductivity. Little or no work has been done on the EIS of ADR interaction with dsDNA, and this work present an additional report on the impedimetric analysis of the interaction of dsDNA and ADR. The electrochemical behavior of ADR alone immobilized on the PGEs was observed in different pH conditions and the results confirmed that ADR is pH-dependent and the reaction is a diffusion limited process. The reaction undergoes mass transport and diffusion in the aqueous environment through the redox reaction at the electrode surface. This method for this analysis is reproducible, effective, and does not include time-consuming steps for it to be performed. The main advantages of this method employed are its simplicity, high sensitivity, high selectivity and low cost materials for analysis.

The fabrication of this electrochemical sensor for detecting the selected phenolic compounds (sinapic acid, syringic acid, and rutin) using Fe₃O₄ nanoparticles to modify CPE is first reported in this study after a careful check of other reported articles. The results obtained by CV, DPV, and EIS showed that the CPE modified with Fe₃O₄ nanoparticles increased the peak current, leading to increased sensitivity to bare CPE. EIS analysis confirmed that MCPE exhibited increased electro-conductibility, thus enhancing the electron transfer between the electrode surface and the redox solution. The MCPE showed high sensitivity, selectivity, reproducibility, repeatability, and stability towards the determination of the phenolic compounds. The CPE and MCPE were used to compare commercial gold screen-printed electrodes for rapid detection of the phenolic compounds, confirmed by their current density that the MCPE had higher current density than CPE and gold screen-printed electrodes. The fabrication of this electrochemical sensor was simple and cost- and time-

effective. The LOD and LOQ results were compared to other literature' sensors; syringic acid is first reported in this work. The electrochemical sensor was applied for real sample analysis to determine phenolic compounds in red and white wine samples. The results found are within the maximum concentrations of 20 to 1000 ppm (20 to 1000 mg L⁻¹) antioxidant levels permitted for phenolic compounds in food samples within the EU and North America.

REFERENCES

- Abdi, R., Ghorbani-HasanSaraei, A., Karimi-Maleh, H., Raeisi, S. N., & Karimi, F. (2020). Determining caffeic acid in food samples using a voltammetric sensor amplified by Fe₃O₄ nanoparticles and room temperature ionic liquid. *International Journal of Electrochemical Science*, 15(3), 2539–2548. <https://doi.org/10.20964/2020.03.30>
- Aleksić, M. M., & Kapetanović, V. (2014). An overview of the optical and electrochemical methods for detection of DNA - Drug interactions. *Acta Chimica Slovenica*, 61(3), 555–573.
- Alipour, E., Majidi, M. R., Saadatirad, A., Golabi, S. M., & Alizadeh, A. M. (2013). Simultaneous determination of dopamine and uric acid in biological samples on the pretreated pencil graphite electrode. *Electrochimica Acta*, 91, 36–42. <https://doi.org/10.1016/j.electacta.2012.12.079>
- Allen, J. B., & Larry, R. F. (2001). *Electrochemical methods fundamentals and applications*. John Wiley & Sons. <https://doi.org/10.1016/B978-0-12-381373-2.00056-9>
- Antonio, T. R. T. A., Basso, C. R., Cabra, M. F., & Pedrosa, V. A. (2013). Electrochemical studies based on local interfacial pH changes of gold nanoparticles immobilized on polystyrene brushes. *International Journal of Electrochemical Science*, 8(3), 4150–4159.
- Antuña-Jiménez, D., Díaz-Díaz, G., Blanco-López, M. C., Lobo-Castañón, M. J., Miranda-Ordieres, A. J., & Tuñón-Blanco, P. (2012). Molecularly Imprinted Electrochemical Sensors: Past, Present, and Future. In *Molecularly Imprinted Sensors*. <https://doi.org/10.1016/B978-0-444-56331-6.00001-3>
- Aoki, K., Okamoto, T., Kaneko, H., Nozaki, K., & Negishi, A. (1989). Applicability of graphite reinforcement carbon used as the lead of a mechanical pencil to voltammetric electrodes. *Journal of Electroanalytical Chemistry*, 263(2), 323–331. [https://doi.org/10.1016/0022-0728\(89\)85102-2](https://doi.org/10.1016/0022-0728(89)85102-2)
- Apetrei, I. M., & Apetrei, C. (2018). A modified nanostructured graphene-gold nanoparticle carbon screen-printed electrode for the sensitive voltammetric detection of rutin. Measurement: *Journal of the International Measurement Confederation*, 114(2017), 37–43. <https://doi.org/10.1016/j.measurement.2017.09.020>
- Arduini, F., Di Giorgio, F., Amine, A., Cataldo, F., Moscone, D., & Paleschi, G. (2010). Electroanalytical characterization of carbon black nanomaterial paste electrode: Development of highly sensitive tyrosinase biosensor for catechol detection. *Analytical Letters*, 43(10–11), 1688–1702. <https://doi.org/10.1080/00032711003653932>
- Baryeh, K., Takalkar, S., Lund, M., & Liu, G. (2017). *Introduction to medical biosensors for point of care applications*. In *Medical Biosensors for Point of Care (POC) Applications*. Elsevier Ltd. <https://doi.org/10.1016/B978-0-08-100072-4.00001-0>

Berg, H., Horn, G., Luthardt, U., & Ihn, W. (1981). Interaction of anthracycline antibiotics with biopolymers: Part V. Polarographic behavior and complexes with DNA. *Bioelectrochemistry and Bioenergetics.*, 8(5), 537–553. [https://doi.org/10.1016/S0022-0728\(81\)80246-X](https://doi.org/10.1016/S0022-0728(81)80246-X)

Bhalla, N., Jolly, P., Formisano, N., & Estrela, P. (2016). Introduction to biosensors. *Essays in Biochemistry*, 60(1), 1–8. <https://doi.org/10.1042/EBC20150001>

Brett, C. M. A., & Oliveira-Brett, A. M. (2011). Electrochemical sensing in solution-origins, applications and future perspectives. *Journal of Solid State Electrochemistry*, 15(7–8), 1487–1494. <https://doi.org/10.1007/s10008-011-1447-z>

Cagnin, S., Caraballo, M., Guiducci, C., Martini, P., Ross, M., Santaana, M., Danley, D., West, T., & Lanfranchi, G. (2009). Overview of electrochemical DNA biosensors: New approaches to detect the expression of life. *Sensors*, 9(4), 3122–3148. <https://doi.org/10.3390/s90403122>

Canavar, E., Kuralay, F., & Erdem, A. (2011). Interaction of Mitomycin C with DNA Immobilized onto Single-walled Carbon Nanotube/Polymer Modified Pencil Graphite Electrode. *Electroanalysis*, 23(10), 2343–2349. <https://doi.org/10.1002/elan.201100149>

Cao, Y. H., Wang, Y., & Yuan, Q. (2004). Analysis of Flavonoids and Phenolic Acid in Propolis by Capillary Electrophoresis. *Chromatographia*, 59(1–2), 135–140. <https://doi.org/10.1365/s10337-003-0138-z>

Chehreh Chelgani, S., Rudolph, M., Kratzsch, R., Sandmann, D., & Gutzmer, J. (2016). A Review of Graphite Beneficiation Techniques. *Mineral Processing and Extractive Metallurgy Review*, 37(1), 58–68. <https://doi.org/10.1080/08827508.2015.1115992>

Chikere, C. O., Faisal, N. H., Kong-Thoo-Lin, P., & Fernandez, C. (2020). Interaction between amorphous zirconia nanoparticles and graphite: Electrochemical applications for gallic acid sensing using carbon paste electrodes in wine. *Nanomaterials*, 10(3). <https://doi.org/10.3390/nano10030537>

Chiorcea-Paquim, A. M., Enache, T. A., De Souza Gil, E., & Oliveira-Brett, A. M. (2020). Natural phenolic antioxidants electrochemistry: Towards a new food science methodology. *Comprehensive Reviews in Food Science and Food Safety*, 19(4), 1680–1726. <https://doi.org/10.1111/1541-4337.12566>

Chrzescijanska, Ewa, Edyta Wudarska, Elzbieta Kusmierk, and J. R. (2014). Study of acetylsalicylic acid electroreduction behavior at platinum electrode. *Journal of Electroanalytical Chemistry*, 713, 17-21.

Chu, X., Shen, G., Jiang, J., & Yu, R. (1999). Intercalation of pharomorubicin anticancer drug to DNA studied by cyclic voltammetry with analytical applications. *Analytical Letters*, 717–727.

Compton, R., & Banks, C. (2010). *Understanding Voltammetry* (2nd Editio). Imperial College Press.

Cullinane, C., & Phillips, D. R. (1990). Induction of Stable Transcriptional Blockage Sites by Adriamycin: GpC Specificity of Apparent Adriamycin-DNA Adducts and Dependence on Iron(III) Ions. *Biochemistry*, 29(23), 5638–5646. <https://doi.org/10.1021/bi00475a032>

D'Souza, O. J., Mascarenhas, R. J., Satpati, A. K., & Basavaraja, B. M. (2019). A novel ZnO/reduced graphene oxide and Prussian blue modified carbon paste electrode for the sensitive determination of Rutin. *Science China Chemistry*, 62(2), 262–270. <https://doi.org/10.1007/s11426-018-9353-x>

da Silva, D. M., & da Cunha Areias, M. C. (2020). Rutin as an Electrochemical Mediator in the Determination of Captopril using a Graphite Paste Electrode. *Electroanalysis*, 32(2), 301–307. <https://doi.org/10.1002/elan.201900145>

David, I. G., Buleandră, M., Popa, D. E., Bîzgan, A. M. C., Moldovan, Z., Badea, I. A., Iorgulescu, E. E., Tekiner, T. A., & Basaga, H. (2016). Voltammetric determination of polyphenolic content as rosmarinic acid equivalent in tea samples using pencil graphite electrodes. *Journal of Food Science and Technology*, 53(6), 2589–2596. <https://doi.org/10.1007/s13197-016-2223-y>

David, I. G., Popa, D. E., & Buleandra, M. (2017). Pencil graphite electrodes: A versatile tool in electroanalysis. *Journal of Analytical Methods in Chemistry*, 2017(Cv). <https://doi.org/10.1155/2017/1905968>

David, S. S., & Williams, S. D. (1998). Chemistry of glycosylases and endonucleases involved in base-excision repair. *Chemical Reviews*, 98(3), 1221–1261. <https://doi.org/10.1021/cr980321h>

Di, A. M., Gaetani, M., & Scarpinato, B. (1969). Adriamycin (NSC-123,127): a new antibiotic with antitumor activity. *Cancer Chemotherapy Reports*, 53(1), 33-37.

Dobes, J., Zitka, O., Sochor, J., Ruttkay-Nedecky, B., Babula, P., Beklova, M., Kynicky, J., Hubalek, J., Klejdus, B., Kizek, R., & Adam, V. (2013). Electrochemical tools for determination of phenolic compounds in plants. A review. *International Journal of Electrochemical Science*, 8(4), 4520–4542.

Dudok de Wit, C. (1987). Medische informatie voor verpleegkundigen. Autologe bloedtransfusie. *Tijdschrift Voor Ziekenverpleging*, 41(20), 655–657.

Eksin, E., Karadeniz, H., & Erdem, A. (2015). Voltammetric and Impidimetric Detection of Anticancer Drug Mitomycin C and DNA Interaction by Using Carbon Nanotubes Modified Electrodes. *Current Bionanotechnology*, 1(1), 32–36.

Eksin, E., Muti, M., & Erdem, A. (2013). Chitosan/ionic liquid composite electrode for electrochemical monitoring of the surface-confined interaction between mitomycin C and DNA. *Electroanalysis*, 25(10), 2321–2329. <https://doi.org/10.1002/elan.201300188>

Erdem, A., Karadeniz, H., & Caliskan, A. (2009). Single-walled carbon nanotubes modified graphite electrodes for electrochemical monitoring of nucleic acids and biomolecular interactions. *An International Journal Devoted to Fundamental and Practical Aspects of Electroanalysis*, 21(3-5), 464–471. <https://doi.org/10.1002/elan.200804422>

Erdem, A., Meric, B., Kerman, K., Dalbasti, T., & Ozsoz, M. (1999). Detection of interaction between metal complex indicator and DNA by using electrochemical biosensor. *Electroanalysis: An International Journal Devoted to Fundamental and Practical Aspects of Electroanalysis*, 11(18), 1372–1376. [https://doi.org/10.1002/\(SICI\)1521-4109\(199912\)11:18<1372::AID-ELAN1372>3.0.CO;2-4](https://doi.org/10.1002/(SICI)1521-4109(199912)11:18<1372::AID-ELAN1372>3.0.CO;2-4)

Erdem, A., Muti, M., Papakonstantinou, P., Canavar, E., Karadeniz, H., Congur, G., & Sharma, S. (2012). Graphene oxide integrated sensor for electrochemical monitoring of mitomycin C-DNA interaction. *Analyst*, 137(9), 2129–2135. <https://doi.org/10.1039/c2an16011k>

Evtugyn, G. (2014). *Biosensors : Essentials*. Springer.

Fojta, M., Doffková, R., & Paleček, E. (1996). Determination of Traces of RNA in Submicrogram Amounts of Single- or Double-Stranded DNAs by Means of Nucleic Acid-Modified Electrodes. *Electroanalysis*, 8(5), 420–426. <https://doi.org/10.1002/elan.1140080504>

Frederick, C. A., Williams, L. D., Ughetto, G., van der Marel, G. A., van Boom, H. J., Rich, A., & Wang, A. H. J. (1990). Structural Comparison of Anticancer Drug-DNA Complexes: Adriamycin and Daunomycin. *Biochemistry*, 29(10), 2538–2549. <https://doi.org/10.1021/bi00462a016>

Fritzsche, H., Akhebat, A., Taillandier, E., Rippe, K., & Jovin, T. M. (1993). Structure and drug interaction of parallel-stranded DNA studies by infrared spectroscopy and fluorescence. *Nucleic Acids Research*, 21(22), 5085–5091. <https://doi.org/10.1093/nar/21.22.5085>

Fukuji, T. S., Tonin, F. G., & Tavares, M. F. M. (2010). Optimization of a method for determination of phenolic acids in exotic fruits by capillary electrophoresis. *Journal of Pharmaceutical and Biomedical Analysis*, 51(2), 430–438. <https://doi.org/10.1016/j.jpba.2009.05.014>

Gabriella, S., Veronica, A., Virginia, C., Leontin, D., & Zaharie, M. (2012). Determination of phenolic compounds from wine samples by GC/MS system. *Revista de Chimie*, 63(9), 855–858.

Gan, T., Shi, Z., Sun, J., & Liu, Y. (2014). Simple and novel electrochemical sensor for the determination of tetracycline based on iron/zinc cations-exchanged montmorillonite catalyst. *Talanta*, 121(March), 187–193. <https://doi.org/10.1016/j.talanta.2014.01.002>

Giacomelli, C., Ckless, K., Galato, D., Miranda, F. S., & Spinelli, A. (2002). Electrochemistry of caffeic acid aqueous solutions with pH 2.0 to 8.5. *Journal of the*

Brazilian Chemical Society, 13(3), 332–338. <https://doi.org/10.1590/S0103-50532002000300007>

Golabi, S. M., & Zare, H. R. (1999). Electrocatalytic oxidation of hydrazine at glassy carbon electrode modified with electrodeposited film derived from caffeic acid. *Electroanalysis*, 11(17), 1293–1300.

Greif R, Peat R, Peter LM, Pletcher D, R. J. (1985). *Instrumental Methods in Electrochemistry*. Woodhead Publishing Ltd.

Gutiérrez-Grijalva, E. P., Picos-Salas, M. A., Leyva-López, N., Criollo-Mendoza, M. S., Vazquez-Olivo, G., & Heredia, J. B. (2018). Flavonoids and phenolic acids from Oregano: Occurrence, biological activity and health benefits. *Plants*, 7(1), 1–23. <https://doi.org/10.3390/plants7010002>

Hedborg, E., Windquist, F., Lundström, I., Andersson, L. I., & Mosbach, K. (1993). Some studies of molecularly-imprinted polymer membranes in combination with field-effect devices. *Sensors and Actuators A: Physical*, 37, 796–799.

Janata, J. (2009). Introduction to sensors. In *Principles of Chemical Sensors*. Springer,.

Janeiro, P., Novak, I., Seruga, M., & Oliveira-Brett, A. M. (2007). Electroanalytical oxidation of p-coumaric acid. *Analytical Letters*, 40(17), 3309–3321. <https://doi.org/10.1080/00032710701672822>

Karabiberoglu, Ş. U., & Dursun, Z. (2018). Fabrication of nickel coated graphene oxide composite electrode for sensitive determination of Rutin. *Journal of Electroanalytical Chemistry*, 815(2017), 76–85. <https://doi.org/10.1016/j.jelechem.2018.02.049>

Kiyomiya, K. I., Matsuo, S., & Kurebe, M. (2001). Differences in intracellular sites of action of Adriamycin in neoplastic and normal differentiated cells. *Cancer Chemotherapy and Pharmacology*, 47(1), 51–56. <https://doi.org/10.1007/s002800000201>

Kostoryz, E. L., & Yourtee, D. M. (2001). Oxidative mutagenesis of doxorubicin-Fe(III) complex. *Mutation Research - Genetic Toxicology and Environmental Mutagenesis*, 490(2), 131–139. [https://doi.org/10.1016/S1383-5718\(00\)00158-3](https://doi.org/10.1016/S1383-5718(00)00158-3)

Kumar, A., Purohit, B., Mahato, K., Roy, S., Srivastava, A., & Chandra, P. (2020). Design and Development of Ultrafast Sinapic Acid Sensor Based on Electrochemically Nanotuned Gold Nanoparticles and Solvothermally Reduced Graphene Oxide. *Electroanalysis*, 32(1), 59–69. <https://doi.org/10.1002/elan.201900406>

Kurucsev, T., & Kubista, M. (1992). Linear dichroism spectroscopy of nucleic acids. *Quarterly Reviews of Biophysics*, 25(1), 51–170. <https://doi.org/10.1017/S0033583500004728>

Labuda, J. (2012). *Terminology Related to Electrochemical DNA-Based Biosensors*. Pan Stanford Publishing.

Lipscomb, L. A., Peek, M. E., Zhou, F. X., Bertrand, J. A., VanDerveer, D., & Williams, L. D. (1994). Water Ring Structure at DNA Interfaces: Hydration and Dynamics of DNA-Anthracycline Complexes. *Biochemistry*, 33(12), 3649–3659. <https://doi.org/10.1021/bi00178a023>

Lowe, C. R. (1984). Trends in biotechnology. *Biosensors*, 2((3)), 59–65.

Lown, J. W., Hanstock, C. C., Bradley, B. D., & Scraba, D. G. (1984). Interactions of the antitumor agents mitoxantrone and bisantrene with deoxyribonucleic acids studied by electron microscopy. *Molecular Pharmacology*, 25(1), 178–184.

M. Swartz and I. S. Krull. (1997). *Analytical Method Development and Validation*. Marcel Dekker.

Maalouf, R., Chebib, H., Saikali, Y., Vittori, O., Sigaud, M., & Jaffrezic-Renault, N. (2007). Amperometric and impedimetric characterization of a glutamate biosensor based on Nafion® and a methyl viologen modified glassy carbon electrode. *Biosensors and Bioelectronics*, 22(11), 2682–2688. <https://doi.org/10.1016/j.bios.2006.11.003>

Madhusudhana, Manasa, G., Bhakta, A. K., Mekhalif, Z., & Mascarenhas, R. J. (2020). Bismuth-nanoparticles decorated multi-wall-carbon-nanotubes cast-coated on carbon paste electrode; an electrochemical sensor for sensitive determination of Gallic Acid at neutral pH. *Materials Science for Energy Technologies*, 3, 174–182. <https://doi.org/10.1016/j.mset.2019.10.001>

Manuel M. Baizer, & Henning Lund. (1972). *Organic Electrochemistry*. Harper and Row.

McGown, L. B., Joseph, M. J., Pitner, J. B., Vonk, G. P., & Linn, C. P. (1995). The Nucleic Acid Ligand. A New Tool for Molecular Recognition. *Analytical Chemistry*, 67(21), 663A-8A. <https://doi.org/10.1021/ac00117a002>

Minotti, G. (1999). Erratum: Role of iron in anthracycline cardiotoxicity: New tunes for an old song? (FASEB Journal (199-212)). *FASEB Journal*, 13(3), 594. <https://doi.org/10.1096/fasebj.13.3.594>

Mirceski, Valentin, Rubin Gulaboski, Milivoj Lovric, Ivan Bogeski, Reinhard Kappl, and M. H. (2013). Square-wave voltammetry: A review on the recent progress. *Electroanalysis*, 25(11), 2411-2422.

Monnappa, A. B., Manjunatha, J. G., & Bhatt, A. S. (2020). Design of a sensitive and selective voltammetric sensor based on a cationic surfactant-modified carbon paste electrode for the determination of alloxan. *ACS Omega*, 5(36), 23481–23490. <https://doi.org/10.1021/acsomega.0c03517>

Nandibewoor, S. M. P. and S. T. (2015). Electrochemical Behavior of Antiemetic Drug Metoclopramide at Electrochemically Pre-treated Pencil Graphite Electrode. *Anal. Bioanal. Electrochem*, 7(4), 387–400.

Nunn, C. M., Van Meervelt, L., Zhang, S., Moore, M. H., & Kennard, O. (1991). DNA-drug interactions. The crystal structures of d(TGTACA) and d(TGATCA) complexed with daunomycin. *Journal of Molecular Biology*, 222(2), 167–177. [https://doi.org/10.1016/0022-2836\(91\)90203-I](https://doi.org/10.1016/0022-2836(91)90203-I)

Oliveira-Brett, A. M., Vivan, M., Fernandes, I. R., & Piedade, J. A. P. (2002). Electrochemical detection of in situ adriamycin oxidative damage to DNA. *Talanta*, 56(5), 959–970. [https://doi.org/10.1016/S0039-9140\(01\)00656-7](https://doi.org/10.1016/S0039-9140(01)00656-7)

Ozkan-Ariksoysal, D., Kara, P., & Ozsoz, M. (2012). *Electrochemical DNA biosensors for detection of compound-DNA interactions*. In *Electrochemical DNA Biosensors*. Pan Stanford Publishing.

Ozkan, D., Karadeniz, H., Erdem, A., Mascini, M., & Ozsoz, M. (2004). Electrochemical genosensor for Mitomycin C-DNA interaction based on guanine signal. *Journal of Pharmaceutical and Biomedical Analysis*, 35(4), 905–912. <https://doi.org/10.1016/j.jpba.2004.03.001>

P.T. Kissinger, W. H. H. (1996). *Laboratory Techniques in Electroanalytical Chemistry* (Second Edi). Marcel Dekker.

Parliament, E. (2004). *Regulation (EC) No 1333/2008 OF The European Parliament and of the council of 16 December 2008 on Food Additives*. In: Euratom.

Perry, C. M. (1996). *The Chemotherapy Source Book*. In William & Wilkins. Awaverly Company, USA (Issues 19-20.).

Pigram, W. J., W. Fuller, and L. D. H. (1972). Stereochemistry of intercalation: interaction of daunomycin with DNA. *Nature New Biology*, 235(53), 17-19.

Plambeck, J. A., & William Lown, J. (1984). Electrochemical Studies of Antitumor Antibiotics V. An Electrochemical Method of Measurement of the Binding of Doxorubicin and Daunorubicin Derivatives to DNA. *Journal of the Electrochemical Society*, 131(11), 2556. <https://doi.org/10.1149/1.2115358>

Purushothama, H. T., Nayaka, Y. A., Vinay, M. M., Manjunatha, P., Yathisha, R. O., & Basavarajappa, K. V. (2018). Pencil graphite electrode as an electrochemical sensor for the voltammetric determination of chlorpromazine. *Journal of Science: Advanced Materials and Devices*, 3(2), 161–166. <https://doi.org/10.1016/j.jsamd.2018.03.007>

Ramirez-Lopez, L. M., McGlynn, W., Goad, C. L., & Mireles DeWitt, C. A. (2014). Simultaneous determination of phenolic compounds in Cynthiana grape (*Vitis aestivalis*) by high performance liquid chromatography-electrospray ionisation-mass spectrometry. *Food Chemistry*, 149, 15–24. <https://doi.org/10.1016/j.foodchem.2013.10.078>

Rauf, S., Gooding, J. J., Akhtar, K., Ghauri, M. A., Rahman, M., Anwar, M. A., & Khalid, A. M. (2005). Electrochemical approach of anticancer drugs-DNA interaction. *Journal of*

Pharmaceutical and Biomedical Analysis, 37(2), 205–217.
<https://doi.org/10.1016/j.jpba.2004.10.037>

Riley, C. M., & Rosanske, T. W. (1996). *Development and validation of analytical methods*. Elsevier.

Robbins, R. J. (2003). Phenolic acids in foods: An overview of analytical methodology. *Journal of Agricultural and Food Chemistry*, 51(10), 2866–2887.
<https://doi.org/10.1021/jf026182t>

Rountree, K. J., Mccarthy, B. D., Rountree, E. S., Eisenhart, T. T., & Dempsey, J. L. (2018). A Practical Beginner ' s Guide to Cyclic Voltammetry. *Journal of Chemical Education*., 95(2), 197–206. <https://doi.org/10.1021/acs.jchemed.7b00361>

Sanchayanukun, P., & Muncharoen, S. (2020). Chitosan coated magnetite nanoparticle as a working electrode for determination of Cr(VI) using square wave adsorptive cathodic stripping voltammetry. *Talanta*, 217(Vi), 121027.
<https://doi.org/10.1016/j.talanta.2020.121027>

Serra, P. A. (2010). *Biosensors*.

Sheng, Kai, Qian Zhang, Lantao Li, YiLun Wang, and B. Y. (2020). A new voltammetric sensor and its application in pharmaceutical analysis for rutin. *Journal of Environmental Science and Health, Part A*, 1-10.

Sheng, K., Zhang, Q., Li, L., Wang, Y. L., & Ye, B. (2020). A new voltammetric sensor and its application in pharmaceutical analysis for rutin. *Journal of Environmental Science and Health - Part A Toxic/Hazardous Substances and Environmental Engineering*, 0(0), 1–10.
<https://doi.org/10.1080/10934529.2020.1747892>

Smith, T. J., & Stevenson, K. J. (2007). *Reference electrodes*. *Handbook of Electrochemistry*, 73–110. <https://doi.org/10.1016/B978-044451958-0.50005-7>

Sousa, W. R., da Rocha, C., Cardoso, C. L., Silva, D. H. S., & Zanoni, M. V. B. (2004). Determination of the relative contribution of phenolic antioxidants in orange juice by voltammetric methods. *Journal of Food Composition and Analysis*, 17(5), 619–633.
<https://doi.org/10.1016/j.jfca.2003.09.013>

Souza, L. P., Calegari, F., Zarbin, A. J. G., Marcolino-Júnior, L. H., & Bergamini, M. F. (2011). Voltammetric determination of the antioxidant capacity in wine samples using a carbon nanotube modified electrode. *Journal of Agricultural and Food Chemistry*, 59(14), 7620–7625. <https://doi.org/10.1021/jf2005589>

Tashkhourian, J., SF Nami Ana, S. Hashemnia, and M. R. H.-N. (2013). Construction of a modified carbon paste electrode based on TiO₂ nanoparticles for the determination of gallic acid. *Journal of Solid State Electrochemistry*, 17(1), 157-165.

Tashkhourian, J., Ana, S. F. N., Hashemnia, S., & Hormozi-Nezhad, M. R. (2013). Construction of a modified carbon paste electrode based on TiO₂ nanoparticles for the determination of gallic acid. *Journal of Solid State Electrochemistry*, *17*(1), 157–165. <https://doi.org/10.1007/s10008-012-1860-y>

Tashkhourian, J., & Nami-Ana, S. F. (2015). A sensitive electrochemical sensor for determination of gallic acid based on SiO₂ nanoparticle modified carbon paste electrode. *Materials Science and Engineering C*, *52*, 103–110. <https://doi.org/10.1016/j.msec.2015.03.017>

Teijeiro, C., Perez, P., Marín, D., & Paleček, E. (1995). Cyclic voltammetry of mitomycin C and DNA. *Bioelectrochemistry and Bioenergetics*, *38*(1), 77–83. [https://doi.org/10.1016/0302-4598\(95\)01791-C](https://doi.org/10.1016/0302-4598(95)01791-C)

Tian, R. R., Pan, Q. H., Zhan, J. C., Li, J. M., Wan, S. B., Zhang, Q. H., & Huang, W. D. (2009). Comparison of phenolic acids and flavan-3-ols during wine fermentation of grapes with different harvest times. *Molecules*, *14*(2), 827–838. <https://doi.org/10.3390/molecules14020827>

Timbola, Ana Karina, C. D. Souza, C. Soldi, M. G. Pizzolatti, and A. S. (2007). Electro-oxidation of rutin in the presence of p-toluenesulfinic acid. *Journal of Applied Electrochemistry*, *37*(5), 617–624.

Tomac, I., Šeruga, M., & Labuda, J. (2020). Evaluation of antioxidant activity of chlorogenic acids and coffee extracts by an electrochemical DNA-based biosensor. *Food Chemistry*, 126787. <https://doi.org/10.1016/j.foodchem.2020.126787>

Topkaya, S. N., & Cetin, A. E. (2019). Determination of Electrochemical Interaction between 2-(1H-benzimidazol-2-yl) Phenol and DNA Sequences. *Electroanalysis*, *31*(8), 1571–1578. <https://doi.org/10.1002/elan.201900199>

Topkaya, S. N., Ozyurt, V. H., Cetin, A. E., & Otles, S. (2018). Nitration of tyrosine and its effect on DNA hybridization. *Biosensors and Bioelectronics*, *102*, 464–469. <https://doi.org/10.1016/j.bios.2017.11.061>

Wang, J. (2001). *Analytical electrochemistry*. WILEY-VCH. <https://doi.org/10.5860/choice.38-5590>

Wang, J. (2006). *Analytical electrochemistry (Third edit)*. A John Wiley & sons, inc. <https://onlinelibrary.wiley.com/doi/book/10.1002/0471790303>

Wang, J., Ozsoz, M., Cai, X., Rivas, G., Shiraishi, H., Grant, D. H., Chicharro, M., Fernandes, J., & Paleček, E. (1998). Interactions of antitumor drug daunomycin with DNA in solution and at the surface. *Bioelectrochemistry and Bioenergetics*, *45*(1), 33–40. [https://doi.org/10.1016/S0302-4598\(98\)00075-0](https://doi.org/10.1016/S0302-4598(98)00075-0)

Westbroek, P. (2005). *Fundamentals of electrochemistry. Analytical Electrochemistry in Textiles*, 3–36. <https://doi.org/10.1533/9781845690878.1.1>

Wong, E. L. S., & Gooding, J. J. (2007). The Electrochemical Monitoring of the Perturbation of Charge Transfer through DNA by Cisplatin. *Journal of the American Chemical Society*, *129*(29), 8950–8951.

Xu, J. K., Zhang, F. F., Sun, J. J., Sheng, J., Wang, F., & Sun, M. (2014). Bio and nanomaterials based on Fe₃O₄. *Molecules*, *19*(12), 21506–21528. <https://doi.org/10.3390/molecules191221506>

Yan, L., Niu, X., Wang, W., Li, X., Sun, X., Zheng, C., Wang, J., & Sun, W. (2016). Electrochemical sensor for rutin detection with graphene oxide and multi-walled carbon nanotube nanocomposite modified electrode. *International Journal of Electrochemical Science*, *11*(2), 1738–1750.

Yıldırım, S., Kadioğlu, A., Sağlam, A., & Yaşar, A. (2017). Determination of phenolic acids and rutin in *Heliotropium thermophilum* by high-performance liquid chromatography with photodiode array detection. *Instrumentation Science and Technology*, *45*(1), 35–48. <https://doi.org/10.1080/10739149.2016.1191020>

Yuan, X. Z., Song, C., Wang, H., & Zhang, J. (2009). Electrochemical impedance spectroscopy in PEM fuel cells: Fundamentals and applications. In *Electrochemical Impedance Spectroscopy in PEM Fuel Cells: Fundamentals and Applications*. Springer Science & Business Media. <https://doi.org/10.1007/978-1-84882-846-9>

Zare, H. R., and S. M. G. (1999). Electrocatalytic oxidation of reduced nicotinamide adenine dinucleotide (NADH) at a chlorogenic acid modified glassy carbon electrode. *Journal of Electroanalytical Chemistry*, *464*(1), 14–23.

Zeng, L., & Xiao, Z. (2017). A lateral flow biosensor for the detection of single nucleotide polymorphisms. In *Methods in Molecular Biology*. 1572. https://doi.org/10.1007/978-1-4939-6911-1_27

Zhao, J., Hu, G. Z., Yang, Z. S., & Zhou, Y. Y. (2007). Determination of 1-naphthol with denatured DNA-modified pretreated glassy carbon electrode. *Analytical Letters*, *40*(3), 459–470. <https://doi.org/10.1080/00032710600964759>

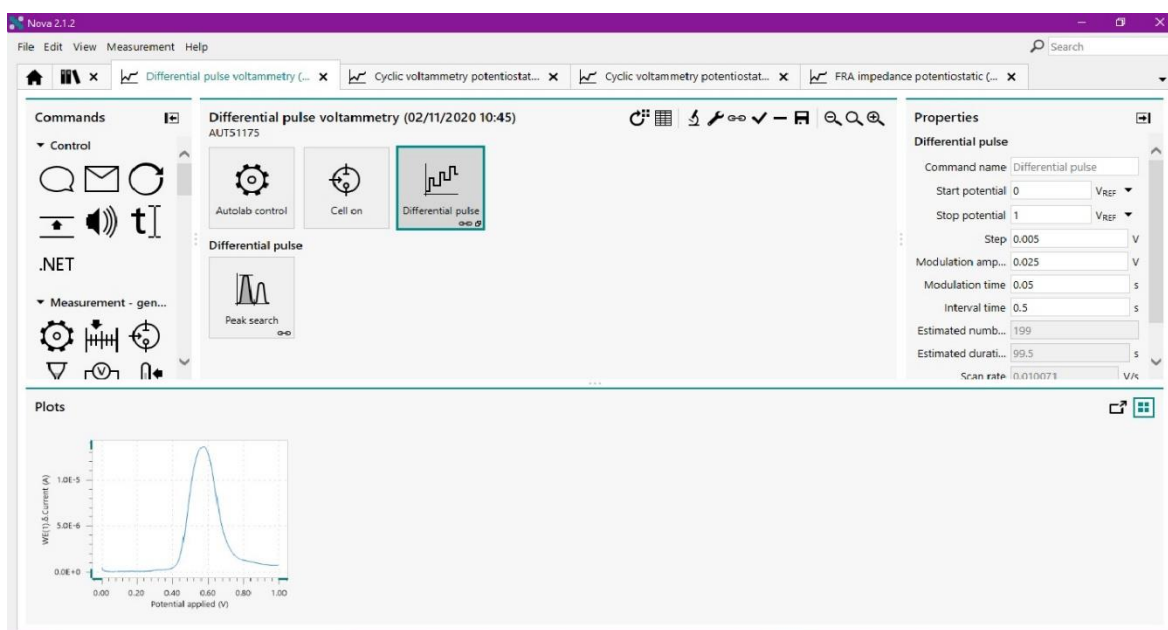
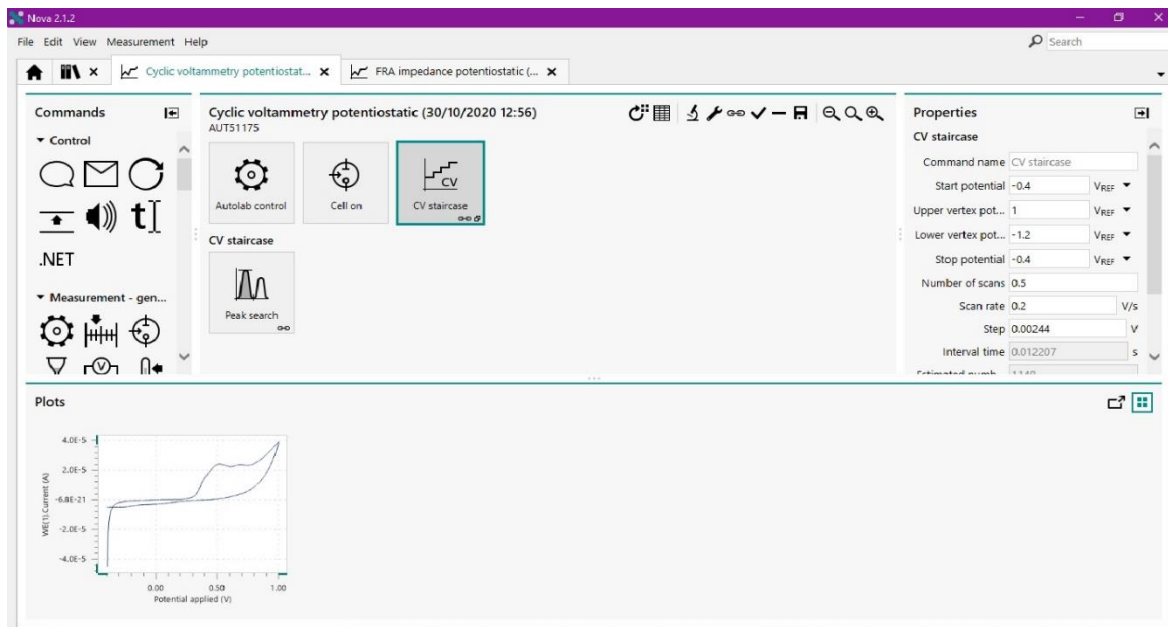
Zhou, S., Starkov, A., Froberg, M. K., Leino, R. L., & Wallace, K. B. (2001). Cumulative and irreversible cardiac mitochondrial dysfunction induced by doxorubicin. *Cancer Research*, *61*(2), 771–777.

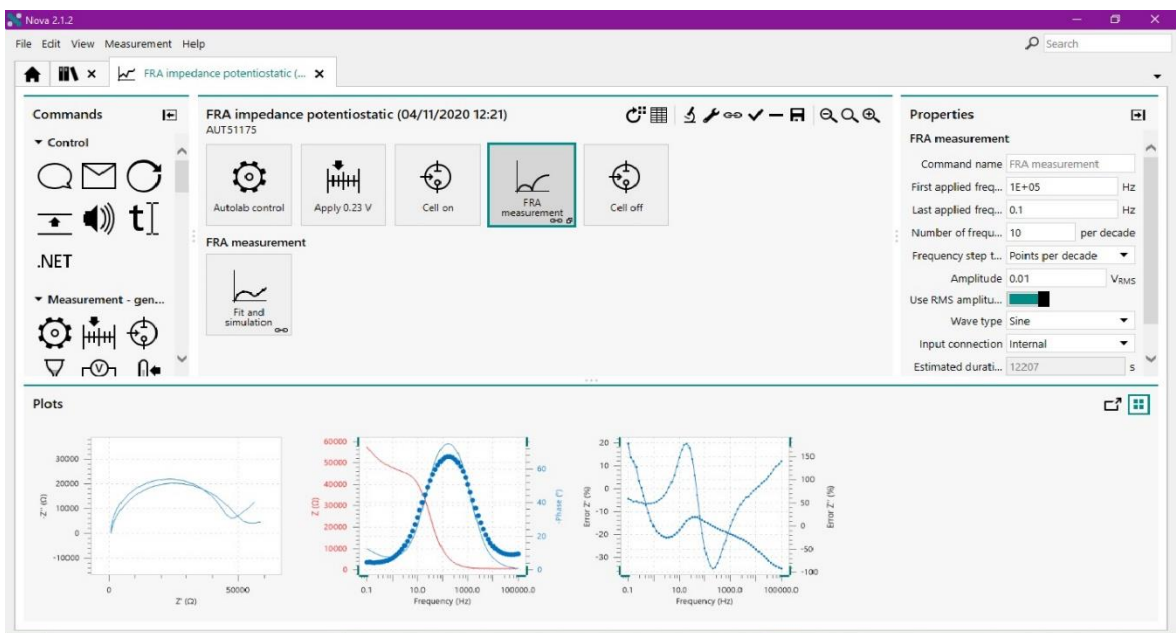
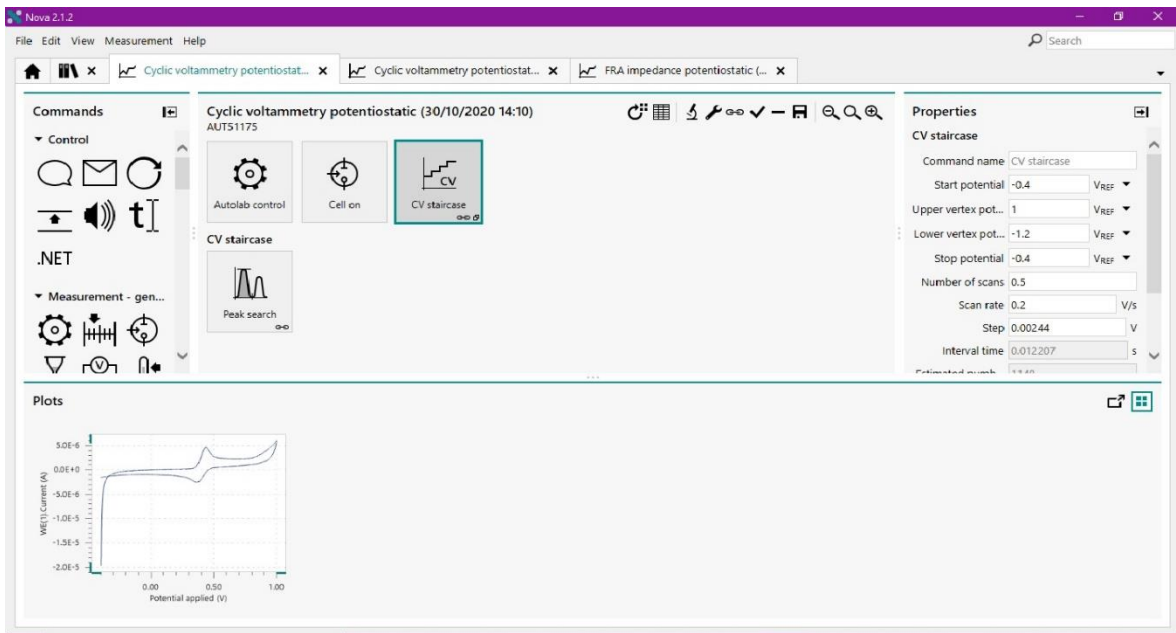
Zunino, F., Gambetta, R., Di Marco, A., Velcich, A., Zaccara, A., Quadrifoglio, F., & Crescenzi, V. (1977). The interaction of adriamycin and its beta anomer with DNA. *Biochimica et Biophysica Acta*, *476*(1), 38–46. <http://www.ncbi.nlm.nih.gov/pubmed/856282>

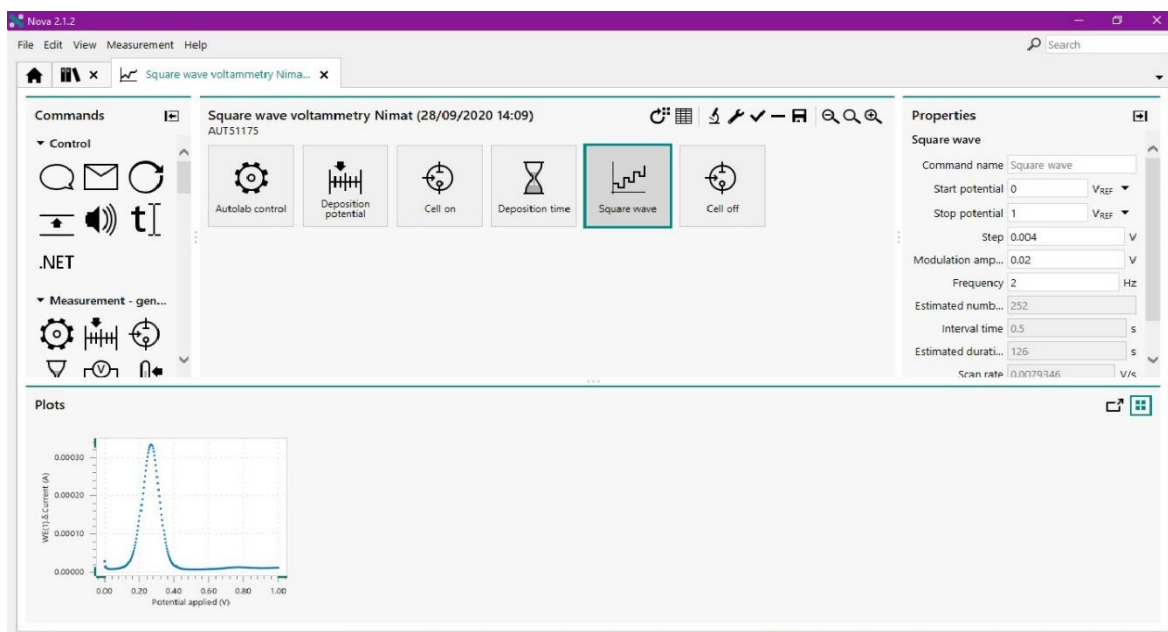
APPENDICES

APPENDIX 1

Voltammetric Procedures using NOVA 2.1.2







APPENDIX II: ETHICAL APPROVAL DOCUMENT



NEAR EAST UNIVERSITY

Date: 22/04/2021

To the Institute of Graduate Studies

For the thesis project entitled as “Electrochemical detection of DNA and their Interaction with chemical compounds.”, the researchers declare that they did not collect any data from human/animal or any subjects. Therefore, this project does not need to go through the ethics committee evaluation.

Title: Electrochemical detection of DNA and their Interaction with chemical compounds

Name/Surname: Prof. Dr. Mehmet Ozsoz Name/Surname: Assist. Prof. Dr. Suleyman Asir

Signature:

Signature:

Role in the Research Project: Supervisor

Role in the Research Project: Co-Supervisor

Appendix III

CURRICULUM VITAE



PERSONAL INFORMATION

Surname, Name : Pwadubashi Coston Pwavodi
Nationality : Nigerian
Date and Place of Birth : 25 January 1989, Adamawa State.
Marital Status : Single

EDUCATION

a. Schools Attended with Dates

- ❖ Near East University 2017-Present
- ❖ Near East University 2014-2016
- ❖ Ahmadu Bello University, Zaria 2008-2012
- ❖ Walter Gowans Memorial College, Gombe 2001-2007
- ❖ Bright Future International School 1992-2000

b. Qualifications Obtained with Dates

- ❖ PhD Biomedical Engineering in view 2017-
- ❖ Masters in Biomedical Engineering 2017
- ❖ National Youth Service corps 2014
- ❖ Bachelor of Science Human Anatomy 2012
- ❖ National Examination Council (NECO), 2007
- ❖ West African Examination Council (WAEC), 2007
- ❖ First School Leaving Certificate (FSLC) 2000

c. TEACHING EXPERIENCE (Lecturer Assistant and Student Advisor)

NEAR EAST UNIVERSITY, NICOSIA, TRNC, NORTH CYPRUS. 2017-Present

- ❖ Planned and Taught core modules in these courses : Introduction to Biomedical Engineering, Anatomy and Physiology, Biomechanics, Cardiac biomechanics, Introduction to Tissue engineering, System Design on bioengineering, Modeling of biological systems, Introduction to Nanotechnology. Introduction to biostatistics, Genetics, Bioenergy Sources, Principles and Applications of Ecology (539 students enrolled for the courses from year one to four and gave the courses either in spring, summer and fall semesters)
- ❖ Student Course Advisor from year one to four (103 students). 2019-Present

- ❖ Biosensors and Bioinstrumentation equipment instructor in the department of biomedical engineering.

Other Teaching Experience

Government Day Secondary School, Birnin-Kebbi, Nigeria (NYSC) 2013-2014

- ❖ Planned and Taught Biology subject to senior class students (SS2 and SS3)
- ❖ Planned and taught Integrated Science subject to junior class students (JSS2)

d. RESEARCH EXPERIENCE

Doctoral Research 2017-Present

- ❖ Presently carrying out experiments on fabrications of DNA biosensors, Electrochemical Sensors for determination of DNA interaction with drugs, food analysis, using potentiostat-galvanostat AUTOLAB-PGSTAT204, Metrohm, Utrecht, Netherlands, operated with Nova 2.1.2 software.
- ❖ Application of electrochemical techniques (Cyclic voltammetry, Differential Pulse voltammetry, Electrochemical Impedance Spectroscopy, Chrono amperometry and Chrono potentiometry, Square wave voltammetry.
- ❖ Modifications of electrodes with Nanoparticles and exploring candidate materials that can be used for the modification of the electrodes.
- ❖ Have theoretical knowledge on Crispr Technology and current trends in Crispr

Masters Research 2014-2016

Department of Biomedical Engineering, Near East University, TRNC, Lefkosa, Turkey

- ❖ Carried out research on biomaterials (Chitosan and Silk fibroin) against antimicrobial organisms and its potentials in wound healing.

Undergraduate Research 2011-2012

- ❖ Researched on wistar rats, we compared the hepatoprotective effect of standard drug (Sylimarin) and methanolic extracts of cashew leaves on CCl4 induced liver toxicity on the wistar rats.

e. RESEARCH AND TEACHING INTERESTS

- ❖ Biomedical Engineering
- ❖ Biomedical Sciences.
- ❖ Biomaterials and Nanomaterials
- ❖ Tissue Engineering, Regenerative Medicine.
- ❖ Artificial Organs, Neuroscience
- ❖ Electrochemical sensors for food analysis, pollutants in water, DNA biosensors, Nanobiosensors, Biosensors and Bioelectronics

f. CURRENT RESEARCH WORKS

- ❖ Electrochemical determination of antibiotics (cephalexin hydrate, Sulfamethoxazole, amoxicillin) using sulfamethaxole imprinted magnetite nanoparticles.

- ❖ Electrochemical determination of the interaction between DNA and phenolic acids using pencil graphite electrodes.
- ❖ Electrochemical sensors for detection of various pollutants in water.
- ❖ Voltammetric and Impedimetric Detection of Double Stranded DNA and Adriamycin interaction using Pencil Graphite Electrodes.

g. PUBLICATIONS

- ❖ Pwavodi PC, Ozyurt VH, Asir S, Ozsoz M. Electrochemical Sensor for Determination of Various Phenolic Compounds in Wine Samples Using Fe₃O₄ Nanoparticles Modified Carbon Paste Electrode. *Micromachines*. 2021 Mar;12 (3):312. <https://doi.org/10.3390/mi12030312>
- ❖ Ilker Ozsahin, Boran Sekeroglu, Pwadubashiyi Coston Pwavodi and Greta S. P. Mok, “High-Accuracy Automated Diagnosis of Parkinson's Disease”, *Current Medical Imaging* (2019) 15: 1. <https://doi.org/10.2174/1573405615666190620113607>
- ❖ Ozsoz M, Ibrahim AU, Coston PP (2019) Analysis Tocopherol Using Chromatographic and Electrochemical Techniques. *Vitam Miner* 8:186.
- ❖ Ozsoz M, Ibrahim AU, Coston PP (2019) Application of Crispr Technology for the Generation of Biofuels: A Review. *J Fundam Renewable Energy Appl* 9: 278.
- ❖ T. Adali, P. C. Pwavodi, E. Guler, and K. Suer. 2017. Antimicrobial Activity Of Chitosan Coated Silk Fibroin Micro-Fibers. *Journal of biotechnology*. Volume 256, Supplement, 30 August 2017, Page S114 <https://doi.org/10.1016/j.jbiotec.2017.06.1190>
- ❖ Ikyembe, D., Pwavodi, C. P., and Agbon, A.N. 2014, Hepatoprotective effect of methanolic leaf extract of anacardium occidentale (cashew) on carbon-tetrachloride-induced liver toxicity in wistar rats. *Sub-Saharan African Journal of Medicine*. 1(124),2384-5147

h. POSTER PRESENTATION /CONFERENCES ATTENDED

- ❖ 10th annual conference and AGM of anatomical society of Nigeria (ASN) University of Portharcourt 7th-10th, November 2012. **Hepatoprotective effect of methanolic leaf extract of anacardium occidentale (cashew) on carbon-tetrachloride-induced liver toxicity in wistar rats.**
- ❖ International Biomedical Engineering Congress 12th-14th March 2015, Near East University, Nicosia, TRNC, North Cyprus.
- ❖ International Biomedical Engineering Congress 24th-27th May 2018, Near East University, Nicosia, TRNC, North Cyprus. **Antimicrobial Activity Of Chitosan Coated Silk Fibroin Micro-Fibers.**

- ❖ Research Centre of experimental health sciences, Nicosia, Cyprus. ASK AN EXPERT: Things to consider while writing article. 24 October 2019. Near East University.
- ❖ Organized and one of the keynote speakers, Seminar for Graduates; Life after School- How to get the best of life 19th-20th June, 2020.

i. SCHOLARSHIPS/AWARDS

- ❖ Total Upstream Nigeria Limited Scholarship Award 2009-2012
- ❖ Adamawa State Student Scholarship 2009-2012
- ❖ Near East University Doctoral Scholarship 2017-Present
- ❖ Near East University Scientific Research Project (Project No: FEN-2019-1-007). 2019

j. COMMUNITY INVOLVEMENT/MEMBERSHIP

- ❖ Founder and Member Soteria Globals 2011-Present
- ❖ Anatomical Students Society of Nigeria (ASSON) 2012
- ❖ State Outreach Coordinator, Nigeria Christian Corpers' Fellowship, (NYSC), Birnin-Kebbi State, Nigeria
2013-2014
- ❖ MDGS society (NYSC) Birnin-Kebbi, Kebbi State, Nigeria. 2013-2014
- ❖ Worked and Trained with the Prisoners 2013-2014
- ❖ Near East Christian Fellowship 2014-Present
- ❖ Soteria Widows and orphans of God Mission 2015-present
- ❖ Founder Think Global ideas 2016-Present
- ❖ Life Coach and Mentor of Youths 2016-Present
- ❖ Executive Secretary to the president and later General Secretary, National Association of Nigerian Students (NANS) Turkish Zone 2018-2020

k. ENTREPRENEURSHIP TRAININGS AND SKILLS

- ❖ Skill Acquisition and Entrepreneurship training on Poultry Production 2013
- ❖ Youth Enterprise With Innovation in Nigeria (YouWIN) 2014
- ❖ Founder Soteria Transports 2014
- ❖ Co-Founder Soteria Flight Agency 2018
- ❖ Trainer on writing Business proposals 2014-present

l. COMPUTER SKILLS

- ❖ Proficient in Computer fundamentals such as Microsoft Office Word, Excel, PowerPoint, Editing, Software Installations and use, Computer hardware repairs and maintenance, Computer designs, Internet applications.

- ❖ Expert in using Potentiostat-galvanostat AUTOLAB-PGSTAT204, Metrohm, Utrecht, Netherlands, operated with Nova 2.1.2 software
- ❖ Proficient in Origin software to report analysis

m. PERSONAL QUALITIES

- ❖ Excellent Interpersonal Relationship and communication skills, Positive Team playing, Strong leadership skill, High strength of character and integrity, Dedicated to tasks and duties, Result oriented, flexible and punctual to duties and responsibilities.
- ❖ Love Researching new information, enthusiastic about inventions that will help people, Reading, Listening to music/singing/playing guitar/piano, meeting new people, public speaking, travelling and playing badminton.

n. LANGUAGES SPOKEN

- ❖ Fluent in English Language, Fluent in Hausa, Average in Bachama, Average in Jukun, Average in Turkish.

REFEREES

Prof. Dr Mehmet Ozsoz
 Department of Biomedical Engineering.
 Near East University / Near East Boulevard
 ZIP: 99138 Nicosia / TRNC
 Mersin 10 – Turkey
mehmet.Ozsoz@neu.edu.tr ozsozsg@gmail.com

Prof. Dr. Ayse Gunay Kibarar
 Head of Department
 Department of Biomedical Engineering.
 Near East University / Near East Boulevard
 ZIP: 99138 Nicosia / TRNC
 Mersin 10 – Turkey
aysegunay.kibarar@neu.edu.tr

Assist. Prof. Dr. Suleyman Asir
 Head of Department
 Department Materials Science and Nanotechnology Engineering,
 Near East University / Near East Boulevard
 ZIP: 99138 Nicosia / TRNC
 Mersin 10 – Turkey
suleyman.asir@neu.edu.tr

Appendix IV

Future Works

- ❖ Electrochemical determination of antibiotics (cephalexin hydrate, Sulfamethoxazole, amoxicillin) using sulfamethaxole imprinted magnetite nanoparticles.
- ❖ Electrochemical determination of the interaction between DNA and phenolic acids using pencil graphite electrodes.
- ❖ Electrochemical sensors for detection of various pollutants in water, food and environment
- ❖ Voltammetric and Impedimetric Detection of Double Stranded DNA and candidate Compounds interaction using Pencil Graphite Electrodes.
- ❖ Integration of Machine learning and electrochemistry
- ❖ Fabrication of devices such as paper biosensors and other biosensor devices
- ❖ The use of nanoparticles to modify electrodes for biosensor detection of compounds-DNA interaction.

APPENDIX V: SIMILARITY REPORT DOCUMENT



SIMILARITY REPORT DOCUMENT

Pwadubashiyi C. Pwavodi - Prof. Dr. Mehmet Ozsoz, Assist. Prof. Dr. Suleyman Asir

NOW VIEWING: HOME > ELECTROCHEMICAL DNA BIOSENSORS- PWADUBASHIYI COSTON PWAVODI > ELECTROCHEMICAL DNA BIOSENSORS- PWADUBASHIYI COSTON PWAVODI

About this page

This is your assignment inbox. To view a paper, select the paper's title. To view a Similarity Report, select the paper's Similarity Report icon in the similarity column. A ghosted icon indicates that the Similarity Report has not yet been generated.

Electrochemical DNA Biosensors- Pwadubashiyi Costo...

INBOX | NOW VIEWING: NEW PAPERS ▾

Submit File		Online Grading Report Edit assignment settings Email non-submitters							
<input type="checkbox"/>	AUTHOR	TITLE	SIMILARITY	GRADE	RESPONSE	FILE	PAPER ID	DATE	
<input type="checkbox"/>	Pwadubashiyi Coston ...	ABSTRACT	0% 	--	--		1573175926	29-Apr-2021	
<input type="checkbox"/>	Pwadubashiyi Coston ...	CHAPTER FIVE	0% 	--	--		1573178675	29-Apr-2021	
<input type="checkbox"/>	Pwadubashiyi Coston ...	CHAPTER ONE	7% 	--	--		1573176435	29-Apr-2021	
<input type="checkbox"/>	Pwadubashiyi Coston ...	CHAPTER FOUR	10% 	--	--		1573178333	29-Apr-2021	
<input type="checkbox"/>	Pwadubashiyi Coston ...	CHAPTER THREE	12% 	--	--		1573177678	29-Apr-2021	
<input type="checkbox"/>	Pwadubashiyi Coston ...	CHAPTER TWO	13% 	--	--		1573177179	29-Apr-2021	
<input type="checkbox"/>	Pwadubashiyi Coston ...	ALL THESIS	14% 	--	--		1573179508	29-Apr-2021	



[Download Similarity Report](#)

Prof.Dr.Mehmet Özsoz



Yrd. doç. dr. Suleyman Asir